AD ______________ Accession Number ______________

Surface Communications Systems Laboratory
Radio Corporation of America, 75 Varick Street, New York 13, New York

MICROWAVE RADIO RELAY STUDY
by R. Gardner and J. Rabinowitz

Final Report Task III-4 1 May 1963 vii + 191 p. incl. illus. Signal Corps Contract DA-36-039-sc-87240 Unclassified Report

Task III-4 entailed a study to determine the relative merits of Single Sideband transmission as against Frequency Modulation transmission of multi-channel (e.g. 12-channel) PCM signals, for tactical radio relay equipment in the lower portion of the UHF range, and to recommend immediate and long range development plans.

Unclassified

An Analysis of PCM Transmission Via Single Sideband

- I. Introduction
- II. Discussion of Results
- III. The SSB Signal
- IV. The Filter Method For Generating a SSB Signal
- V. Error Rate
- VI. AFC For SSB Reception
- VII. APC Design For PCM-SSB Reception

Appendices - A, B, C, D, E

Bibliography
Supplemental Report

AD ______________ Accession Number ______________

Surface Communications Systems Laboratory
Radio Corporation of America, 75 Varick Street, New York 13, New York

MICROWAVE RADIO RELAY STUDY
by R. Gardner and J. Rabinowitz

Final Report Task III-4 1 May 1963 vii + 191 p. incl. illus. Signal Corps Contract DA-36-039-sc-87240 Unclassified Report

Task III-4 entailed a study to determine the relative merits of Single Sideband transmission as against Frequency Modulation transmission of multi-channel (e.g. 12-channel) PCM signals, for tactical radio relay equipment in the lower portion of the UHF range, and to recommend immediate and long range development plans.

Unclassified

An Analysis of PCM Transmission Via Single Sideband

- I. Introduction
- II. Discussion of Results
- III. The SSB Signal
- IV. The Filter Method For Generating a SSB Signal
- V. Error Rate
- VI. AFC For SSB Reception
- VII. APC Design For PCM-SSB Reception

Appendices - A, B, C, D, E

Bibliography
Supplemental Report

AD ______________ Accession Number ______________

Surface Communications Systems Laboratory
Radio Corporation of America, 75 Varick Street, New York 13, New York

MICROWAVE RADIO RELAY STUDY
by R. Gardner and J. Rabinowitz

Final Report Task III-4 1 May 1963 vii + 191 p. incl. illus. Signal Corps Contract DA-36-039-sc-87240 Unclassified Report

Task III-4 entailed a study to determine the relative merits of Single Sideband transmission as against Frequency Modulation transmission of multi-channel (e.g. 12-channel) PCM signals, for tactical radio relay equipment in the lower portion of the UHF range, and to recommend immediate and long range development plans.

Unclassified

An Analysis of PCM Transmission Via Single Sideband

- I. Introduction
- II. Discussion of Results
- III. The SSB Signal
- IV. The Filter Method For Generating a SSB Signal
- V. Error Rate
- VI. AFC For SSB Reception
- VII. APC Design For PCM-SSB Reception

Appendices - A, B, C, D, E

Bibliography
Supplemental Report

AD ______________ Accession Number ______________

Surface Communications Systems Laboratory
Radio Corporation of America, 75 Varick Street, New York 13, New York

MICROWAVE RADIO RELAY STUDY
by R. Gardner and J. Rabinowitz

Final Report Task III-4 1 May 1963 vii + 191 p. incl. illus. Signal Corps Contract DA-36-039-sc-87240 Unclassified Report

Task III-4 entailed a study to determine the relative merits of Single Sideband transmission as against Frequency Modulation transmission of multi-channel (e.g. 12-channel) PCM signals, for tactical radio relay equipment in the lower portion of the UHF range, and to recommend immediate and long range development plans.

Unclassified

An Analysis of PCM Transmission Via Single Sideband

- I. Introduction
- II. Discussion of Results
- III. The SSB Signal
- IV. The Filter Method For Generating a SSB Signal
- V. Error Rate
- VI. AFC For SSB Reception
- VII. APC Design For PCM-SSB Reception

Appendices - A, B, C, D, E

Bibliography
Supplemental Report

CR-63-419-2

AN ANALYSIS OF PCM TRANSMISSION VIA SINGLE SIDEBAND

R. Gardner
J. Rabinowitz

1 May 1963

Work done for USASRDL on Microwave Radio Relay Study

Contract No. DA-36-039-sc-87240
by
Surface Communications Systems Laboratory
Defense Electronic Products
Radio Corporation of America
75 Varick Street
New York 13, New York

SUBJECT: AN ANALYSIS OF PCM TRANSMISSION VIA SINGLE SIDEBAND

OBJECT: To determine the relative merits of Single Sideband transmission as against Frequency Modulation transmission of multichannel (e. g. 12-channel) PCM signals, for tactical radio relay equipment in the lower portion of the UHF range, and to recommend immediate and long range development plans

CONCLUSIONS: The results, conclusions and recommendations of this analysis are contained in pages 7 through 10.

WORK DONE BY:

M. Feldman
R. Gardner
M. Landis
J. Rabinowitz
A. Schmidt
R. Sommer
S. Weber

REPORT PREPARED BY:

R. Gardner
J. Rabinowitz

REPORT APPROVED BY:

J. Rabinowitz, Project Director

ACTIVITY ISSUING REPORT:

Surface Communications Systems Laboratory
New York, N. Y.
Defense Electronic Products

DEP. NUMBER CR-63-419-2

WORK DONE UNDER: Microwave Radio Relay Study
Contract No. DA-36-039-sc-87240
Task III-4

GENERAL DISTRIBUTION LIST

Vice President, Research
RCA Laboratories, Princeton, New Jersey

Patent Department
Princeton, New Jersey

Chief Defense Engineer, DEP

Surface Communications Systems Laboratory Library
New York City, New York (1 copy)

DEP Central Engineering Library
Camden, New Jersey (1 copy)

Surface Communications Systems Laboratory Library
Tucson, Arizona

New York Engineering Publications (10 copies)

SPECIAL DISTRIBUTION LIST

J. Acunis	RCA, New York
E. Bradburd	RCA, New York
S. W. Cochran	RCA, Camden
O. B. Cunningham	RCA, Camden
J. Dutka	RCA, New York
M. Feldman	RCA, New York
R. Guenther	RCA, New York
I. Guttmann	RCA, New York
J. Holshouser	RCA, New York
M. Landis	RCA, New York
A. Mack	RCA, New York
M. Masonson	RCA, New York
S. Mehlman	RCA, New York
S. Metzger	RCA, New York
A. Schmidt	RCA, New York
R. Sommer	RCA, New York
S. Weber	RCA, New York
Signal Corps (5 copies)	Attn: L. G. Fobes, USAERDL Ft. Monmouth, N. J.

Signal Corps Distribution (50 copies)

REFERENCES

1. "The Compatibility Problem in Single-Sideband Transmission" - K. H. Powers, Proceedings of the IRE pgs. 1431-1435, Vol. 48, No. 8, August 1960.

2. "Envelopes and Pre-envelopes of Real Waveforms" - J. Dugundji, IRE Trans. on Information Theory, Vo. IT-4 pgs. 53-57, March 1958.

3. "Introduction to Statistical Communication Theory" - David Middleton, McGraw-Hill, 1960.

4. "Nonlinear Transformations of Random Processes" - R. Deutsch, Prentice-Hall 1962.

5. "Information Transmission, Modulation and Noise" - Mischa Schwartz, McGraw-Hill 1959.

6. "Tables of the Bivariate Normal Distribution Function and Related Functions" - National Bureau of Standards, Applied Mathematics Series, No. 50, 1959.

7. "Summation of Series" - L. B. W. Jolley, 2nd Edition, Dover Publications, 1961.

8. "The Analytic Signal Representation of Modulated Waveforms" - Edward Bedrosian, Proceedings of the IRE pgs. 2071-2076, Vol. 50, No. 10, October 1962.

9. Richman, Proceedings of the IRE, Color TV Issue, Jan. 1954, pgs. 106-1

10. "The Fourier Integral and its Applications" - A. Papoulis, Mc-Graw Hill 1962.

11. "Error Probabilities for Binary Symmetric Ideal Reception Through Nonselective Slow Fading and Noise" - G. L. Turin, Proc. IRE, Vol. 46, No. 9 pgs. 1603-1619, Sept. 1958.

12. "Minimum Error Rate Reception of PCM-FM Using A Discriminator" - A. Meyerhoff, W. Mazer - Final Report Task II, 31 August 1959 - Microwave Radio Relay Systems Study DA-36-039-sc-78045.

REFERENCES (Continued)

13. "Poisson, Shannon, and the Radio Amateur" - J. P. Costas, Proc. IRE, Dec. 1959.

14. "Poisson, Shannon, and the Ham" - Easly/Costas, Proc. IRE Aug 1960, Corresp.

15. "Traffic Efficiencies in Congested Band Radio Systems" - Weber-Costas, Proc. IRE, Nov. 1960, Corresp.

16. "Can SSB Provide More Usable Channels in the Land Mobile Service?" - Korelenko/Shepherd, Trans. PGVC, Aug. 1960.

17. "A Third Method of Generation and Detection of SSB Signals" - D. K. Weaver, Proc. IRE, Dec. 1956.

18. "The Phase Shift Method of Single-Sideband Signal Generation" - D. E. Norgaard, Proc. IRE, Dec. 1956.

19. "Normalized Design of 90° Phase-Difference Networks" - S. D. Bedrosian, PGST June 1960, pg. 128-136.

20. "Network Analysis and Feedback Amplifier Design" - H. W. Bode/ D. VanNostrand, New York 1945.

21. "On the Design of Filters by Synthesis" - R. Saal, E. Ulbrich, Trans. PGCT Dec.1958

22. "Der Entwurf von Filtern mit Hilfe des Kalaloges normierter Tielpasse" - Von R. Saal, Telefunken.

ANALYSIS OF PCM TRANSMISSION VIA SINGLE SIDEBAND

R. Gardner
J. Rabinowitz

LIST OF FIGURES

LIST OF FIGURES (Continued)

LIST OF FIGURES (Continued)

ACKNOWLEDGEMENTS

1.	Dr. J. Dutka	For mathematical help on many problems, and particularly for developing the method used to calculate the distribution of the quadrature distribution.
2.	M. Feldman	For the design and tests of the SSB filter and equalizer.
3.	M. Landis	For the computation of the error rate curves (Figure 2) from equation (22).
4.	M. Masonson	For supervision and assistance with the error rate analysis in Supplementa' Report.
5.	A. Schmidt	For the study of APC performance, Section VII, and assistance with the experimental work.
6.	R. Sommer	For the study of centroid controlled AFC systems, in Section VI.
7.	S. Weber	For the error rate analysis in Supplemental Report.
8.	M. S. Corrington and T. C. Hilinsky	For the computer calculations of the quadrature distribution.

RESULTS, CONCLUSIONS, RECOMMENDATIONS

RESULTS

For Task III-4 certain critical problems of generation, transmission, and detection of PCM-SSB signals were analyzed to determine what levels of performance are attainable with equipment suitable for tactical radio relay applications. In the performance of this analysis, answers to the following questions were obtained.

- o What methods of generation are suitable for PCM-SSB signals?
- o For the filter method of generation: How well can the undesired sideband be suppressed? How well can phase and amplitude be controlled in the desired sideband, and what is the effect of distortion?
- o How well do APC loops perform in extraction, at the receiver, of a phase reference, and what are the requirements in the way of transmitter and receiver frequency stability, and pilot carrier power?
- o What amount of error rate can be expected as a function of thermal noise and phase-reference jitter.
- o What is the distribution of amplitudes of the envelope of the PCM-SSB signal, and what requirements does this place on power sources and power amplifier?

CONCLUSIONS

It is possible to realize a reduction of spectrum occupancy of up to 30 percent utilizing SSB as opposed to FM transmission i.e., with SSB an equal number of channels may be accommodated in 70 percent of the FM bandwidth. This reduction would be obtained at the cost of a considerable increase in equipment complexity (with attendant increases in size, weight, cost, and reliability) and an increase of primary power in order to maintain equivalent performance.

The results indicate approximately equal average radiated power is required for FM and SSB for an equal error rate. However, the lower efficiency of the linear power amplifiers of SSB results in two things. The first, and most obvious, is the requirement for higher primary power to obtain the same radiated power. This can become very important in high-power installations such as troposcatter and in high-efficiency transistorized radio communications sets. Secondly, where power amplifier operation is limited by peak envelope power requirements, or by allowable electron tube or transistor power dissipation, a given electron tube or transistor, and associated cooling apparatus, will yield less average radiated power in SSB than in FM operation. The ratio of FM as opposed to SSB average radiated power might be as high as 6:1.

Some of the additional equipment needed in SSB, such as higher-stability frequency synthesizers, and SSB generation circuitry, have not yet been proven feasible in tactical UHF communications systems. A major problem remaining unsolved involves the generation of PCM-SSB signals without introduction of excessive phase and amplitude distortion while maintaining a satisfactory amount of undesired sideband rejection. It is believed that a satisfactory solution will leave a significant amount of power in the undesired sideband, thus reducing the spectrum occupancy savings below the 30 percent previously mentioned.

Another important question that has not yet been adequately answered is the relative immunity of SSB to interference and jamming. The relative immunity of SSB to interference determines the width of guard bands that are required and is thus a factor in the determination of spectrum occupancy. A satisfactory determination of interference immunity must await construction of a PCM-SSB radio so that experiments can be made.

Because of these unresolved and serious problems it is considered inadvisable to proceed with development of a PCM-SSB radio until an experimental feasibility study has been accomplished. An experimental study would furnish answers to the question of feasibility and yield an accurate estimate of actual spectrum savings that can be obtained. A decision can then be made as to whether the increase in equipment cost and complexity is justified by the spectrum savings.

Considering the necessity of making an experimental feasibility study (having an uncertain outcome) and then entering upon the development of a rather complex equipment, it is our belief that a time period of at least five years will elapse before a service test model of a PCM-SSB radio will be available. An equivalent FM radio, with proven capability, could be developed in a considerably shorter time-span with considerably less effort. Therefore, a project for new equipment for immediate use, such as the AN/GRC-103, should continue with FM.

RECOMMENDATIONS

As previously stated, it has not yet been demonstrated that PCM-SSB is either a practical or desirable alternative to PCM-FM. However, if determination is made that the spectrum savings that tentatively appear possible are desirable, despite probable equipment penalties, it is recommended that:

- An experimental feasibility study be initiated of PCM-SSB generation methods to determine what performance levels (signal distortion, emitted spectrum) can be attained in practical application and with what degree of equipment complexity and size.

- An experimental feasibility study be initiated of a high-stability (10^{-5} to 10^{-6}) frequency synthesizer suitable for tactical applications.
- An experimental feasibility study be initiated of an AFC/APC system for a PCM-SSB receiver.
- Utilizing the feasibility models constructed for the studies, an experimental comparative study be made of the interference and jamming vulnerability of PCM-SSB and PCM-FM.
- Double-sideband suppressed-carrier modulation of quadrature carriers with half-rate PCM trains should also be studied. This method promises greater spectrum savings than SSB with less increase in equipment complexity and primary power requirements. The penalty for utilization of this method would be the need to modify PCM multiplex equipment in order to provide parallel half-rate pulse trains.
- Finally, it is recommended that immediate development programs for new equipments should rely on FM.

SECTION I

INTRODUCTION

The continually increasing quantity of communications and other equipment which emit electromagnetic energy is placing a premium on the economy of spectrum utilization. In view of a potential 50 percent reduction in the occupancy of the frequency spectrum by the utilization of SSB as opposed to low-deviation FM it has become necessary to consider the former mode for possible future use.

As might have been expected, the reduction in spectrum occupancy that can actually be realized in practice is less than the potential and is dependent upon what we are willing to pay for it. The cost is reckoned in the following:

- Amount of additional equipment complexity.
- Increase in power.

Increased complexity means greater size, weight, and cost; higher breakdown rates; and a need for more highly skilled maintenance personnel. In tactical use, there is a limit, though not well-defined, beyond which the equipment becomes too unwieldy or too delicate. It is therefore necessary to determine the nature of the equipment that is needed for the generation and reception of PCM-SSB, and, keeping it within acceptable limits for tactical use, to determine the resulting level of performance and spectrum occupancy. In accomplishing this we first examined the many methods that have been proposed for the generation and detection of SSB or SSB-like signals, and selected the most promising method. The final choice was the filter method of generation, and homodyne detection. We then proceeded to determine design parameters for the critical elements of the system which could be satisfied within (what was judged to be) the limits of tactical equipment use. An estimate of system performance was then made.

Our study resulted in a PCM-SSB system which compared unfavorably with existing PCM-FM systems. The result of the study must be regarded with caution, however, as it is based on a number of engineering judgements as to what is, or is not, feasible for tactical equipment use. As such, the decision must be revised as the state of the art advances. For example, one decision concerned the permissible size and complexity of the SSB filter and phase equalizer. Within the limits which were placed on these equipments, we were unable to obtain a sufficiently linear phase response. The result was an entirely unacceptable level of distortion of the signal with consequent high error rates. Even so, the undesired sideband suppression of this filter was only approximately 30 db. To obtain greater suppression would have further aggravated the phase equalization problem. An additional example is the estimate of 10^{-4} as a practical limit for tactical frequency synthesizer stability in the UHF range of interest. This limit leads to a requirement for a strong pilot carrier and increased sideband power.

The results of the analysis must also be recognized as pertaining to the specific implementation that was studied in detail (filter generation and homodyne) detection. There are other possibilities for "true" SSB systems, a number of "compatible" SSB methods, and there is also the possibility of a vestigal sideband (VSB) system. The selection of the filter-homodyne method from among the "true" and "compatible" SSB methods was made on the basis of the known state-of-the-art and with an obviously incomplete array of facts. It is possible that improved technology, or further study, would present a better candidate. The VSB system was set aside as settling for too little too soon. A promising double sideband, quadrature modulation scheme using half-rate PCM trains was set aside as being outside of our contract to investigate SSB.

SECTION II

DISCUSSION OF RESULTS

2.1 DESCRIPTION OF ILLUSTRATIVE SYSTEM

Figure 1 shows a block diagram of an illustrative 12-channel PCM-SSB system that might be used in the UHF range.

The transmitter would contain a Baseband Amplifier, a High-Pass Filter (with cutoff frequency in the range 500 cps to 2000 cps), and a Gaussian Filter to shape the PCM pulses coming from the PCM. The shaped baseband signal is then applied to a Double-Balanced Modulator followed by an SSB Filter-Equalizer to produce the SSB signal at as low a carrier frequency as possible. In general, the lower the frequency of this first conversion, the simpler will be the SSB Filter-Equalizer design. In our experimental and analytical work a low-pass type was considered for the SSB Filter-Equalizer. Following this is a summing circuit in which the desired level of carrier pilot, at the proper phase, is added to the SSB signal. The SSB signal is then heterodyned twice more to reach the desired RF frequency, power amplified, and fed to the antenna. In most instances the transmitter and receiver will be duplexed to a common antenna.

At the front end of the receiver, is an RF Preselector filter to suppress the image frequency and exclude other unwanted signals from the RF Amplifier and Mixer. The center frequency of the first IF Amplifier is chosen subject to the usual requirements, i.e., the frequency must be high enough to permit adequate image rejection with an RF Preselector of reasonable design, and as low as possible to achieve a satisfactory noise figure.

At the second Mixer the received signal is heterodyned down to a frequency convenient for high-stability AFC/APC and homodyne detection

operations. If AFC is to be used, a crystal discriminator would be desirable and available in the indicated range. The local oscillator signal for the second Mixer is obtained by mixing a high-stability, high-frequency signal from the Frequency Synthesizer with the lower frequency output from the Voltage-Controlled Oscillator (VCO). The frequency and phase of the VCO are controlled by the output of the AFC/APC detectors. The phase detector compares the phase of the incoming (IF) carrier pilot with the phase of a high-stability 5 mc Reference Oscillator (part of the Frequency Synthesizer) and through the action of the VCO causes the carrier pilot phase to be made equal to that of the 5 mc Reference Oscillator. It appears to be more desirable to adjust the frequency and phase of the IF (received) signal rather than that of the reference signal. Done in either manner, it is still necessary to separate the carrier pilot by means of a very narrow Bandpass Filter ahead of the phase detector. If the IF signal is permitted to lay anywhere within this band (as it would if it were merely AFC'd) it would, in some cases, fall near the edge of the band where the phase variation of the filter is large. If the demodulating carrier (phase reference oscillator) was then locked to the IF signal, the phase relative to the sidebands would be in error and severe distortion could result. This distortion can be avoided by locking the (IF) carrier pilot to the center of the filter by phase locking the (IF) carrier pilot to the 5 mc Reference Oscillator.

The 5 mc Reference Oscillator signal is then mixed with the received signal in the Homodyne Detector, thus recovering the PCM baseband signal. After gaussian filtering and amplification the received PCM signal is ready for the multiplex (PCM out). Since SSB does not exhibit any appreciable threshold effects, as in the case of FM, there is no reason to go to the extra trouble of putting the Gaussian Filter in the IF section rather than at baseband.

The Frequency Synthesizer, as shown, is common to both the receive and transmit functions, in the expectation that economies could be effected.

However, no attempt has here been made to select frequencies that could accomplish this dual purpose.

2.2 INTERRELATIONSHIP OF PARAMETERS

In a comparison of PCM-SSB with PCM-FM the most significant items of comparison are:

a. Spectrum occupancy.

b. Required frequency stability.

c. Total radiated power.

d. Primary power requirements.

e. Equipment complexity.

f. Equipment size.

g. Equipment weight.

For comparison purposes it is understood that the above listed characteristics are measured for systems having an equal error rate.

Assuming proper operation of the multiplex (decision) circuitry, errors are caused by the following disturbing influences:

a. Thermal noise, added to the desired sideband signal by the transmission medium and the receiver.

b. Intersymbol interference in the PCM train.

c. Reduction of received PCM pulse amplitude due to demodulating carrier phase error.

d. Fluctuation of the amplitude of the received PCM pulse due to introduction of the quadrature component caused by demodulating carrier phase error.

In an "ideal" SSB system the only disturbing influence would be thermal noise, all of the other influences being "avoidable" as they are due to

implementation problems. Such an "ideal" SSB system has an error rate performance of the ideal coherent system described by Turin (Ref. 11). In a practical system application it is impossible to avoid entirely the additional disturbing influences. In fact, measures taken to reduce one effect usually result in an increase in another undesirable effect. Proper design necessitates a proper balance of these factors in order to achieve the desired performance at the least cost - cost being measured in the terms of the items of comparison previously listed.

In order to reduce the effect of thermal noise (and minimize spectrum occupancy), gaussian filtering is used at both the transmitter and receiver. However, this introduces intersymbol interference. The Gaussian Filter parameters used are those, recommended by Meyerhoff and Mazer (Ref. 12), for which intersymbol interference results in a fractional -db loss of performance.

A more serious source of intersymbol interference is the SSB Filter. In the attempt to eliminate as much of the undesired sideband as possible, non-linear phase shift and non-uniform attenuation are introduced into the desired passband. In our attempt to design a filter and equalizer, of tactical equipment proportions, the resulting distortion was totally unacceptable. It is assumed, however, that if the requirements are relaxed for the rate of cutoff of the filter and/or a larger size of filter-equalizer is permitted and/or an improved design and construction techniques are found, that the resultant distortion can be brought under control, to the extent that only a fractional -db penalty is paid. In addition, a penalty will doubtless be paid in spectrum occupancy.

An additional source of intersymbol interference is the requirement for a baseband high-pass filter to eliminate low-frequency energy of the PCM train. This low-frequency energy, appearing as it does in the immediate

vicinity of the carrier pilot, would seriously increase the phase jitter of the regenerated demodulating carrier at the receiver. For present purposes, it should be noted that, for a 12-channel PCM system a cutoff frequency of about 1 KC can be tolerated. A 6-channel PCM system probably would not tolerate a cutoff frequency of this magnitude.

The two remaining causes of received bit errors are the direct result of demodulating carrier phase jitter and static phase-error. It is believed that the static phase error can be made sufficiently minute so that it may be neglected. The amount of phase jitter obtained is a function of the following:

a. Ratio of carrier-to-sideband power.
b. Ratio of carrier-to-thermal noise power.
c. Required APC capture range.
d. Required APC pull-in time.
e. Cutoff frequency of baseband high-pass filter.

In order to obtain a given error rate, and having made allowance for the effects of intersymbol interference, the best balance must be found between the effects of thermal noise (video signal-to-noise ratio) and the effects of phase jitter. Video signal-to-noise ratio is directly related to the sideband-to-noise power ratio, and as phase jitter is a function of the carrier-to-sideband power ratio and the carrier-to-thermal noise ratio, it may be seen that there is an intimate relationship between carrier, sideband, and thermal noise power. When items c, d, and e, above, are specified it is possible to obtain a least total signal power-(carrier-plus-sideband)-to-noise ratio required for a given error rate. This optimum does not necessarily coincide with a low carrier-to-sideband power ratio. If carrier-to-sideband ratio is reduced below that specified for optimum condition, phase jitter increases, and an increase in sideband power is called for in order to maintain the desired error rate. If the carrier-to-sideband power ratio is increased, phase

jitter is decreased, and sideband power can be reduced accordingly. In both cases, however, there is a net increase in total power.

The optimum (least) total power level is always greater than that required for an "ideal" system. The amount by which it is greater is determined by items c, d, and e. Item c, required APC capture range, is determined by frequency stability of the transmitter and receiver, and by whether or not an AFC loop is used. In any case, the poorer the stability, the greater must be the capture range, and the greater must be the total power requirement.

Item d, required APC pull-in time, is determined by the need of the customer, and by such requirements as required pull-in time following loss-of-lock due to deep fades, etc. The shorter the required pull-in time, the greater must be the total power requirement.

Item e has been discussed previously, we need only to add that the lower the cut-off frequency, the higher must be the total power requirement.

Optimum parameters of a typical 12-channel PCM-SSB system and a detailed description of the design procedure is given in paragraph 2.3.

2.3 SYSTEM DESIGN

In this paragraph we will use the results of the analyses described in succeeding sections to explain a near-optimum system design for satisfying a particular set of customer requirements. The procedures will be given in sufficient detail to permit a designer to follow the procedural steps for any other given set of assumed design conditions. While the method is general the results are specific. It is believed that the hypothetical design will prove to be typical of the performance that can be expected from a PCM-SSB system. The basic illustrative system block diagram configuration is shown in Figure 1, and explained in paragraph 2.1.

Basic assumptions made, are as follows:

a. 12-channel, 6-bit binary PCM signal, 576 Kb/s.

b. Full-baud, gaussian-shaped pulses

c. Error rate = 10^{-5}

d. Frequency stability of transmitter and receiver oscillators is between 10^{-4} and 10^{-5} each.

e. Operating frequency is 220-700 mc.

f. Total transmitted power (carrier plus sideband) is to be a minimum.

The first step in a system design is to examine the curve of the bit error as a function of pulse amplitude with rms phase error as a parameter. (See Figure 2.) For convenience, an interpolation curve has been constructed (see Figure 3) to show the power increase required for a constant error rate as a function of rms phase error. This figure shows that as phase error increases beyond 3 degrees, a sharp increase in required signal power is necessary to maintain a constant error rate. The phase error is dependent on the strength of the pilot carrier, however, it seems clear, intuitively, that an optimum value of pilot carrier will be such as to keep rms phase error near the knee of the power versus phase error curve. This brings us to the second step in the design.

It is shown in Section VII (APC Design for PCM-SSB Reception) equation (78), that the product of $\varphi_{2\,rms}$ (rms phase error) and Q (pilot carrier amplitude) is dependent on parameters in the APC loop and, for fixed parameters, this product is a constant. Consequently, as pilot amplitude is varied, $\varphi_{2\,rms}$ must vary in an inverse manner. For a given pilot carrier amplitude (or equivalently, a given ratio of carrier-to-sideband power R) there is still a finite phase error which requires an increase in sideband power (over the ideal) by an amount P_{si}. The total power increase over ideal,

$P_{Ti} = P_C + P_{si}$, can thus be plotted as a function of R, under the assumption of a fixed error rate and a fixed value for the product $\varphi_{rms}\sqrt{R}$. An example of such a plot is shown in Figure 4. This figure shows the expected result that for an optimum value of R there is a minimum increase in total power. One can repeat the plotting procedure described above for different values of $\varphi_{rms}\sqrt{R}$ and find the optimum value of R as a function of the APC loop constant $C = \varphi_{rms}\sqrt{R}$. Such a plot is shown in Figure 5. Also shown on this figure are curves for error rates of 3×10^{-6} and 10^{-6}. These are obtained as previously described. It is of interest that the locus of minimum power increase shown on Figure 4 is apparently identical for any error rate between 10^{-5} and 10^{-6}.

The next procedural step in the general design procedure involves the effects of frequency uncertainty in the received carrier. If the received carrier can be anywhere in a band ± W cycles/second, we can introduce AFC and reduce the uncertainty to f_e cycles per second. The APC capture range must then be $\pm f_e$ (in order that the received carrier at lock-up is in the center of the range of the APC filter). The magnitude of frequency correction obtainable with AFC is dependent on the strength of the pilot carrier, structure of the sideband spectrum, initial frequency uncertainty, and the particular type of AFC system chosen. The structure of the sideband is important because of the possibility of locking on-line components in the sideband. These problems would require detailed study before a final design could be specified. We will assume that the AFC analysis given in Section VI is applicable. Using Figure 21, derived in Section VI, AFC for SSB Reception, we obtain Table I which shows the resultant frequency error, f_e, as a function of initial frequency uncertainty, and strength of carrier.

TABLE I

Stability	Total Frequency Instability at 700 Mc	AFC Error, f_e		
		R = 1	R = 0.5	R = 0.25
10^{-4}	± 140,000	34,500	57,600	74,000
3×10^{-5}	± 42,000	3,910	7,480	13,800
10^{-5}	± 14,000	460	875	1,730

NOTE

If no AFC is used, the capture range of the APC loop must equal the full frequency instability given in the second column.

The results tabulated are used to plot curves showing APC capture range (equal ± f_e) as a function of R, for specified frequency instability and pull-in time. Specific curves of this type are shown in Figure 6. The other curves on this figure are described in the following paragraphs.

The final step in the design procedure is to determine specific values for APC loop parameters, and an optimum value of R which will be satisfactory with a specified degree of frequency instability. As shown by equation (79) in Section VII, APC Design for PCM-SSB Reception, the capture range, pull-in time, and low-frequency cutoff of the modulating signal will determine $c = \varphi_{rms}\sqrt{R}$. The capture range must be sufficient to lock the carrier despite allowed drift in carrier frequency, after AFC. Pull-in time can be reasonably long, e.g., 1 second, if the designer can be certain that the system will rarely lose synchronism caused by deep signal fades. This problem has not been analyzed and would require study prior to completion of an actual design. We have assumed that pull-in times of between 0.1 and 0.01

2.3.1 Illustrative System Designs

2.3.1.1 Stability = 10^{-5}

	No AFC	AFC
Error rate	10^{-5}	10^{-5}
Pull-in time	T_F = 0.1 sec.	T_F = 0.1 sec.
Carrier-to-sideband power ratio	R = 0.25	R = 0.09
Required power increase over ideal	P_i = 1.5 db	P_i = 0.57 db
	T_F = 0.01 sec.	T_F = 0.01 sec.
	R = 1.2	R = 0.2
	P_i = 4.5 db	P_i = 1.25 db

2.3.1.2 Stability = 3×10^{-5}

	No AFC	AFC
Error rate	10^{-5}	10^{-5}
Pull-in time	T_F = 0.1 sec.	T_F = 0.1 sec.
Carrier-to-sideband power ratio	R = .55	R = .25
Required power increase over ideal	P_i = 2.7 db	P_i = 1.5 db
	T_F = 0.01 sec.	T_F = 0.01 sec.
	R = 3.17	R = .6
	P_i = 8 db	P_i = 2.9 db

2.3.1.3 Stability = 10^{-4}, Using AFC

Error rate 10^{-5}

$T_F = 0.1$ sec.

$R = 0.63$

$P_i = 3$ db

An examination of the possible system designs indicate that some combination of synthesizer stability, pull-in time, and use, or non-use, of AFC can be arranged that will result in a power requirement 1 to 3 db greater than that for an "ideal" system. Since the present FM systems require about 2 db more power than the ideal, there is no significant advantage of one system over the other on the basis of transmitted signal power.

It is estimated that the power amplifiers for such systems will have efficiencies of about 40 percent for FM and 10 percent for SSB. Since equal average radiated power is required, the SSB amplifier will require approximately 4 times as much primary power. If the radios are transistorized power amplifier requirements will be a large fraction of the total power required, and the overall increase may exceed 50 percent, even for low-power sets. For high-power sets, such as for troposcatter, the overall increase would be even greater. Further, where the power amplifier is limited by the dissipation limits of the output device (particularly so in the case of low-power tactical sets), the given output device will deliver as much as 6 times greater radiated power in FM operation than in SSB operation, for the above-stated efficiencies.

2.4 SPECTRUM OCCUPANCY

Users of communications equipment are aware that in some parts of the frequency spectrum, there is a major congestion problem. However, the precise statement of the problem and how to quantify it varies with the specific application and is often not clear. In the operation of communications equipment interference from other communication equipment and from a wide miscellany of electromagnetic radiators is encountered. At the same time, the communications equipment user is interfering with the interferors. Thus there are two problems:

a. Construction and design of equipment as immune as possible to interference.

b. Contruction and design of equipment which generates as little interference as possible.

In considering both of these problems it is useful to make a distinction between internal interference in a system and external interference between coexistent, disparate systems. The individual components of a system (e.g., a vehicular communication system) may be able to coexist with each other (for example through orderly channelizing) but be a distinct nuisance to the electromagnetic community at large. It is argued that the external nuisance value of a system can be reduced by a reduction in the amount of spectrum occupied. This argument is based on the assumption that the less conspicious the interference the less nuisance the interference will be. It is difficult to take issue with this idea (although J. P. Costas does in Refs. 13, 14, 15) but to avoid pitfalls in its application recognition must be given to the fact that conspicuousness is measured in several dimensions:

a. Spectrum occupancy

b. Spectral power density

c. Time

d. Physical space

Two narrow-band systems (e.g., two pairs of HF communicators) will be inconspicuous to each other if they simply remain far apart in frequency. If they overlap each other, or are too close in frequency, the systems will become mutually intolerable, if they have the same spectral power density (equal total power in this case). In contrast, a wideband (spread-spectrum) system of a given total power may overlap the channel of a narrow-band system of equal power without harming it, because the wideband system is smaller in power density. Depending upon its structure, the wideband system may in fact suffer from the presence of the narrow-band signal rather than vice versa.

The dimension of time (except in its implications with respect to bandwidth) is not pertinent to the present discussion since both PCM-FM and PCM-SSB emit continuously.

Concerning the dimension of physical space, the greater distance a signal travels the more equipment operation it will interfere with. All else being equal (same frequency, same antennas, heights, etc.) a stronger signal will carry the farthest distance, therefore a system that must radiate more power will have a greater interference potential.

How does this apply to the specific cases of PCM-FM and PCM-SSB? in the case of internal interference, neither of these systems permit co-channel operation of units that are within interference range of each other. It is necessary in either case to separate the frequencies of radios which are in range of each other. The amount of frequency separation needed will be determined by the "bandwidth" of the emitted signal, the reaction of the system

to interference, and the range. No known system has a strictly limited bandwidth but, depending upon the context, the "bandwidth" will be defined as the 3-db, 6-db, 30-db, 60-db, etc., bandwidth. An interfering signal, comparable in field strength to the desired signal, may have an "interference" bandwidth defined perhaps as its 10-db bandwidth. The same signal, originating at a transmitter that is relatively close to the receiver in question, may have a field strength 60 db stronger than that of the desired signal. The interference bandwidth here might be perhaps the 70-db bandwidth.

As regards internal interference in either the SSB or FM case, an idealized version of the situation is shown in Figure 7. It is assumed in each case that the baseband power spectrum is gaussian with $\sigma = 1$. For the SSB case, infinite rejection of the unwanted sideband is assumed. For the FM case, small deviation is assumed and the further assumption is made that the spectrum is therefore essentially the same as at baseband, i.e., gaussian. It is also assumed that, in each case, equal shaping takes place in the transmitter and the receiver. For the SSB case, then, the total interference falling into the desired channel, due to the presence of signals in the two adjacent channels, is given by:

$$I_{ssb}(\alpha) = \int_0^\infty A_1 e^{-\frac{1}{2}x^2} e^{-\frac{1}{2}(x+\alpha)^2} dx + \int_\alpha^\infty A_2 e^{-\frac{1}{2}x^2} e^{-\frac{1}{2}(x-\alpha)^2} dx \quad (1)$$

This is easily reduced to:

$$I_{ssb}(\alpha) = (A_1 + A_2) e^{-\frac{\alpha^2}{4}} \int_{\frac{\alpha}{2}}^\infty e^{-v^2} dv \quad (2)$$

The total desired signal power is given by:

$$S_{ssb} = \int_0^\infty e^{-x^2} dx = \frac{\sqrt{\pi}}{2} \quad (3)$$

For the SSB case, therefore, the ratio of interference to signal power is:

$$\frac{I_{ssb}(\alpha)}{S_{ssb}} = \frac{2(A_1+A_2)}{\sqrt{\pi}} e^{-\frac{\alpha^2}{4}} \int_{\frac{\alpha}{2}}^{\infty} e^{-v^2} dv \tag{4}$$

For the FM case the total interference power falling into the desired signal channel is given by:

$$I_{FM}(\beta) = \int_{-\infty}^{\infty} A_1 e^{-\frac{1}{2}x^2} e^{-\frac{1}{2}(x+\beta)^2} dx + \int_{-\infty}^{\infty} A_2 e^{-\frac{1}{2}x^2} e^{-\frac{1}{2}(x-\beta)^2} dx \tag{5}$$

Which reduces to:

$$I_{FM}(\beta) = (A_1+A_2) e^{-\frac{\beta^2}{4}} \int_{-\infty}^{\infty} e^{-z^2} dz = \sqrt{\pi}(A_1+A_2) e^{-\frac{\beta^2}{4}} \tag{6}$$

The total desired signal power for the FM case is:

$$S_{FM} = \int_{-\infty}^{\infty} e^{-x^2} dx = \sqrt{\pi} \tag{7}$$

Hence, for the FM case, the ratio of interference to signal power is:

$$\frac{I_{FM}(\beta)}{S_{FM}} = (A_1+A_2) e^{-\frac{\beta^2}{4}} \tag{8}$$

In order to have equal interference-to-signal ratios we find:

$$\frac{2(A_1+A_2)}{\sqrt{\pi}} e^{-\frac{\alpha^2}{4}} \int_{\frac{\alpha}{2}}^{\infty} e^{-v^2} dv = (A_1+A_2) e^{-\frac{\beta^2}{4}} \tag{9}$$

$$\frac{2}{\sqrt{\pi}} e^{-\frac{\alpha^2}{4}} \int_{\frac{\alpha}{2}}^{\infty} e^{-v^2} dv = e^{-\frac{\beta^2}{4}}$$

This can be cast into the following form:

$$e^{-\frac{\alpha^2}{4}} \left[1 - P\left(\frac{\alpha}{\sqrt{2}}\right)\right] = e^{-\frac{\beta^2}{4}} \tag{10}$$

Where: $P\left(\frac{\alpha}{\sqrt{2}}\right) = \frac{1}{\sqrt{2\pi}} \int_{-\frac{\alpha}{2}}^{\frac{\alpha}{2}} e^{-\frac{1}{2}y^2} dy$

By assuming values of α one can readily solve for β thus obtaining Table II. (The values of α and β are, of course, the required channel spacings given in multiples of σ.) The table also shows the signal-to-interference power ratio, S/I for the given channel spacing assuming that $A_1 = A_2 = 1$, i.e., the desired signal strength and the interfering signal strengths are all equal. (For A_1, A_2 other than unity, subtract 10 log $\frac{(A_1 + A_2)}{2}$ from the tabulated values of S/I.)

TABLE II

RATIO OF CHANNEL SPACINGS FOR SSB AS COMPARED WITH FM FOR EQUAL SIGNAL-TO-INTERFERENCE RATIO

α	β	α/β	S/I (db)
1.0	1.98	.505	1.3
1.5	2.62	.573	4.5
2.0	3.38	.592	9.4
2.5	4.06	.617	14.9
3.0	4.74	.632	21.4
3.5	5.42	.647	29.0
4.0	6.13	.653	37.7
4.5	6.82	.66	47.3
large	large	.707	large

The conclusions to be drawn from Table II are dependent upon the nature of the interference situation. If, in a situation where interfering signals (in adjacent channels) are likely to be of the same order of magnitude as the desired signal, and if the S/I must be greater than 15 db, then the spectrum saving will be about 38 percent. That is to say, SSB channels can be spaced 38 percent closer than FM channels.

If the interfering signals are appreciably greater than the desired signal, as when interfering transmitters are located close to the receiver (a number of radio sets at the same terminal or repeater), then the saving is less. For example, if the interfering signals are 35 db stronger, and the required S/I is 15 db, this is the same as a requirement for spacing that gives 50 db for equal strengths. In this case the spectrum saving is about 35 percent. For greater S/I ratios the spectrum saving approaches a minimum limiting value of about 30 percent. At the other extreme, when interfering signals are small, savings in spectrum occupancy can approach 50 percent. Based on this analysis expected spectrum savings are in the range 30-50 percent. However, we have not accounted for a number of other pertinent facts:

a. Incomplete suppression of the undesired sideband.

b. Spectrum splatter due to power amplifier saturation on SSB peaks.

c. Frequency drift.

d. Transmitter (oscillator) noise.

e. Relative sensitivity to interfering (and jamming) signals.

When these facts are considered, the spectrum savings for the moderate and strong interference cases will become less than 30 percent. Special notice should be taken of item (e). Due to the necessity for homodyne detection of PCM-SSB signals, the reception process is especially sensitive to interference in the vicinity of the carrier pilot, - precisely where the adjacent channel interference is strongest. (Experimental work dealing with this problem is described in Ref. 16. Unfortunately the requirements for the referenced experiments were less critical as the experiments dealt with voice transmission and heterodyne reception.)

The above discussion applies to the problem of "internal" interference, that is, the interference among signals which are arranged in an orderly fashion in a set of channels. When considering "external" interference two cases must be considered:

a. How much spectrum must be allocated on an "exclusive" basis for X channels of such a system?

b. What are the interfering effects on other services which for one reason or another, lie within the allocated band of channels?

If a system is allocated a block of spectrum on an exclusive basis, interference with the system will be almost entirely internal and therefore is under the control of the system designers and operators. (We do not consider here the separate problem of spurious out-of-band emissions of equipments which are nominally operating in another block.) Under these conditions it is desirable that the system require the smallest possible block of spectrum in order to leave more room for other users. Any spectrum savings that can be gained, as through the use of SSB, would be extremely desirable.

If, however, system members must coexist with other users, either on a cochannel or adjacent channel basis, the situation is no longer clear, and more work must be done before determination can be made as to how much, if any, benefit can be derived from SSB as compared with FM. For example, SSB signals will interfere more with cochannel and adjacent channel narrow-band signals than will FM signals since the latter has one-half the spectral power density for the same total emitted power.

From our incomplete study of these problems, we have reached the tentative conclusion that, on the whole, there will probably be a spectrum occupancy saving, in the use of SSB as opposed to FM, of up to 30 percent.

This is an appreciable economy but, if it can or should be effected depends upon the shortage of the spectrum occupancy space relative to the equipment penalties of SSB. The remainder of this study was devoted to discovering what these penalties might be.

2.5 EXPERIMENTAL WORK

Early in the study program it was decided that a working model of the basic PCM-SSB System should be constructed. This would allow experimental work to test and supplement our theoretical conclusions. A block diagram of the experimental system is shown in Figure 8.

The Random Pulse Train Generator was constructed by RCA for the Signal Corps under an earlier task. It supplies a full baud rectangular pulse output which is filtered and used to modulate a carrier, as shown. The SSB filter and equalizer are described in Section IV. The SSB "receiver" consisted of a balanced phase shift circuit for the carrier, a ring demodulator, and a Difference Amplifier. No attempt was made to construct the AFC and APC circuits which are an essential part of a full SSB receiver. Instead the carrier was obtained in the ideal manner - directly from the transmitter. The circuits indicated on the block diagram were all conventional vacuum tube circuits.

Because of the severe amplitude and phase distortion in the filter-equalizer, as described in Section IV, the recovered pulse signal was badly distorted. In fact, the output signal resembled noise more than it did a random binary pulse train. Very little use could be made of the experimental circuits for this reason. Nevertheless, the output signal was compared with the input pulse train in an error detector and with careful adjustment of carrier phase an error rate of one in ten pulses was observed.

SECTION III

THE SSB SIGNAL

3.1 VARIETIES OF SSB SIGNALS

When it is desirable to use the smallest possible bandwidth for carrier transmission of a signal, some form of single-sideband transmission is necessary. (Note that in the case of PCM it is possible to divide the pulse train into two or more (parallel) trains of lower repetition rate. It would be relatively simple to convert the PCM train into a pair of half-rate trains, each occupying half the bandwidth of the parent train, and to double sideband (DSB) modulate a pair of orthogonal carriers ($\cos \omega_c t$ and $\sin \omega_c t$) one each with these trains. The resulting RF spectrum would be half the width of the present PCM-FM signal, and because of its symmetry, present fewer problems in carrier regeneration at the receiver.) The most general band-pass signal can be represented as the sum of two amplitude-modulated orthogonal carriers, thus:

$$s(t) = a(t) \cos \omega_0 t + b(t) \sin \omega_0 t \tag{11}$$

If the desired signal is to have frequency components on only one side of the carrier frequency, (i.e., SSB) then a(t) and b(t) must be related as Hilbert transform pairs, which simply means that b(t) is the 90° phase-shifted version of a(t). This is developed by Dugundji in Ref. 2. In conventional SSB, a(t) is the message signal, and the result is that neither the envelope nor the phase is simply related to the message signal.

An alternative point of view is obtained by considering the envelope and phase of the band-pass signal. From this point of view, Powers in Ref. 1 has shown that the phase angle and the logarithm of the envelope must be Hilbert

transform pairs if the signal is to be single-sideband. Powers has suggested amplitude modulating a carrier with the square root of the message signal, and simultaneously modulating phase with a related function, yielding an envelope-detectable signal. Bedrosian in Ref. 8 suggests conventional phase modulation accompanied by amplitude modulation with a related function yielding a discriminator-detectable signal. Other methods of modulation which result in simultaneous envelope and phase modulation are also discussed by Bedrosian. Apparently, all of the methods discussed for SSB modulation are intended for transmitting analog speech signals. Each method has certain features which may be useful in specific cases, but no attempt has been made to fully assess the individual potentialities for pulse transmission.

For this report we have assumed a conventional SSB signal will be used to convey binary modulation. Two reasons support this choice: First, it is easily shown that conventional SSB transmission can, with "ideal" homodyne reception, achieve the theoretical limit of power economy, although this is probably not true for the methods suggested by Powers and Bedrosian. Secondly, the spectrum of the transmitted signal has the same shape as that of the baseband modulating signal. In general, pulse train spectra are constrained as nearly as possible rectangular, which, as far as spectrum occupancy is concerned, must be considered an ideal shape. This advantage is not enjoyed by Powers' method, where a rectangular transmitted spectrum requires a triangular modulating spectrum. Similar considerations apply to Bedrosian's SSB-FM. Both of these methods, however, apparently result in an appreciable carrier component.

It can be stated, that on theoretical grounds, conventional SSB is at least good as alternative SSB methods, however, there may be practical reasons for considering the alternative methods. This is especially true in light of the difficulties which attend the generation and reception of conventional SSB signals conveying binary information. Nevertheless, it appears

that the other known methods are equally difficult for generating SSB signals. Each method is bound by the required Hilbert transform relation between components in order to generate the 90° phase shifted version of the modulating signal. However, even if this can be accomplished, a conventional SSB signal can be equally well generated.

Much simpler detection methods can be used, which do not require generation at the receiver of phase-locked demodulating carrier, utilizing the compatible methods suggested by Powers and Bedrosian. Powers' envelope detection method is possible, and a discriminator can be used in Bedrosian's method.

Finally, it is necessary to consider the distinction we have drawn between single sideband (SSB) and vestigial sideband (VSB). In actual practice an SSB signal cannot be made to have a completely suppressed, and undesired, sideband. In this sense every SSB signal is essentially a VSB signal albeit with a very small vestige. In the present context however, it has been found convenient to draw a distinction based upon an important problem. In a VSB system a relatively broad transition region between the desired and undesired sidebands is used, and the amplitude and phase response in this region is very carefully controlled in order to have constructive combination of the two sidebands at the receiver. To obtain the utmost in spectrum economy (SSB) the transition region must be made as narrow as possible, and the out-of-band attenuation must be made as great as possible. In accomplishing this, hope must ultimately abandoned of controlling amplitude and phase response in the transition region, and instead concentration placed on the maintenance of satisfactory response as close to the edge as possible, and the removal of everything else as efficiently as possible. If the filter method of generation is used, the filter-equalizer problem is quite different for each of the two cases. The following differences arise due to different treatments of the transition region:

a. A baseband high-pass filter is required for SSB but not necessarily for VSB. This introduces additional intersymbol interference into the PCM pulse train.

b. Carrier regeneration, at the receiver, is more difficult in the SSB case.

c. The shape of the spectrum on the suppressed sideband side is different and will therefore have different interference characteristics.

3.2 GENERATION OF SSB SIGNALS

There are essentially two methods of generating SSB signals:

a. Use a filter with a sharp cutoff.

b. Use the modulating signal, and a 90° phase-shifted version of the modulating signal to separately modulate an in-phase and a quadrature carrier.

In principle, the same result can be achieved with either method.

3.2.1 Filter Method

The filter method of generating an SSB signal is quite simple in principle, see the block diagram of the illustrative system, Figure 1. The Double Balanced Modulator (DBM) is, ideally, a multiplier for the desired modulation, a(t), and the first carrier, $2 \cos w_1 t$. The low-pass SSB Filter has a frequency response H (w) which eliminates the upper sideband of the modulator output. To obtain a high carrier frequency the process is repeated several times.

In the SSB issue of the Proceedings of the IRE, Weaver proposed a so-called "Third Method of Generation and Detection of SSB Signals," Ref. 17. A simplified block diagram of this method is shown in Figure 9.

The characteristics of the low-pass filter influence the received signal in a mathematically identical fashion. Weaver's method has a slight advantage in that the cutoff frequency of his low-pass filter can be lower than in a more conventional filter of an SSB system, however, this advantage may be more than offset by the greater degree of balance required in the first balanced modulator. Because of the great similarity of Weaver's method and the conventional method of SSB generation, no additional discussion is required. Discussions of filter requirements for the conventional method will be applicable to both methods.

A detailed discussion of filter requirements and work accomplished on the realization of a filter, suitable for SSB-PCM, is given in Section IV.

3.2.2 Phase Shift Methods

Norgaard has given an excellent description, Ref. 18, of the phase shift method of SSB generation. A simplified block diagram of such a method is shown in Figure 10. Design of the two networks, each with a 90° phase difference, appears to be a relatively easy task using the procedure described by Bedrosion, Ref. 19, which is based on work by Darlington. It is shown that with a seven section all-pass network, a 40-db rejection of the unwanted sideband can be achieved, with a desired sideband having a ratio of upper and lower cutoff frequencies of 200. This approaches a satisfactory solution to the problem of generating an SSB signal for up to 12 channels, except, as pointed out by Norgaard, the networks introduce severe phase distortion in the received signal. For voice transmission this phase distortion is tolerable but pulses signals will be badly distorted.

Another, more promising, method for obtaining a 90° phase shift is described by Powers, Ref. 1. This method utilizes a tapped delay line to develop two signals which have an exact 90° phase shift between each of the respective frequency components, and no phase distortion. In general, the amplitude of corresponding frequency components will not be equal, however, using a sufficient number of delay sections any desired degree of approximation can be achieved.

A block diagram of a Delay Line Phase Shifter is shown in Figure 11. The delay line consisting of six delay sections D_1 through D6 is symmetrical about the center point from which the delayed original modulation is obtained. A portion of the delayed signal is taken from each tap on the delay line, attenuated an amount α_n, and added to form a 90° phase shifted signal. A variety of characteristics can be obtained with this system depending on the amount of delay, number of sections, and value of the attenuation coefficients.

Providing the attenuation coefficients to the left of the center point are taken as negative (indicated on the diagram by summation and then polarity inversion), a pure 90° phase shift is obtained for all frequencies up to some maximum frequency. This can be shown as follows: suppose the signal, a(t), has a Fourier spectrum A(w), and passes through two equal delay sections. The spectrum of the signal taken from the tap between sections is: $A(w)\, e^{-jw\tau}$, where τ is the delay time for each section. Now, adding the output from the second delay section to the negative of the input results in a signal having a spectrum:

$$A(\omega)e^{-j\omega 2\tau_0} - A(\omega) = A(\omega)e^{-j\omega\tau_0}\left[e^{-j\omega\tau_0} - e^{+j\omega\tau_0}\right] \qquad (12)$$

$$= -2j \sin\omega\tau_0\, A(\omega)e^{-j\omega\tau_0}$$

The factor -j indicates a pure 90° phase shift for frequencies from zero to the frequency where the factor, sin $w\tau_o$ changes sign, that is, where $w\tau_o > \pi$, or $f > \frac{1}{2\tau_o}$. For frequencies for which the factor $\sin\omega\tau_o$ is of opposite sign, the output spectrum falls on the side of the undesired sideband. When a number of delay sections are used in a symmetrical arrangement as shown in the block diagram, the output $b(t - \tau_c)$ has a spectrum:

$$B(\omega)e^{-j\omega\tau_c} = jA(\omega)e^{-j\omega\tau_c} \sum_{n=1}^{N} 2\alpha_n \sin\omega\tau_n \; ; \; \tau_c = \sum_{1}^{N} \tau_n \qquad (13)$$

In order to make the amplitudes of the components of B(w) equal to those of A(w) the delays and coefficients can be chosen so that the sum represents the Fourier series for a square wave in terms of the variable w. Thus:

$$\alpha_n = \frac{2}{\pi(2n-1)}$$

$$\tau_n = \tau_o[2n-1] \qquad (14)$$

With this choice of parameters, the summation is the usual approximation to a square wave given by the first N terms of a Fourier series. Other approximations are possible, some of which may be more suitable in the band of interest.

A system for obtaining an SSB signal using the delay line phase shifter (Figure 11) is shown in Figure 12. The Fourier spectrum of the SSB signal is easily shown to be (neglecting the delay):

$$\begin{aligned} S(\omega) &= A(\omega-\omega_o) + A(\omega+\omega_o) \\ &\quad - jA(\omega-\omega_o)e^{-j\frac{\pi}{2}} \sum_{1}^{N} 2\alpha_n \sin(\omega-\omega_o)\tau \\ &\quad - jA(\omega+\omega_o)e^{+j\frac{\pi}{2}} \sum_{1}^{N} 2\alpha_n \sin(\omega+\omega_o)\tau \end{aligned} \qquad (15)$$

$$\begin{aligned} S(\omega) &= A(\omega-\omega_o)\left[1 - \sum_{1}^{N} 2\alpha_n \sin(\omega-\omega_o)\tau_n\right] \\ &\quad + A(\omega+\omega_o)\left[1 + \sum_{1}^{N} 2\alpha_n \sin(\omega+\omega_o)\tau_n\right] \end{aligned}$$

Using this expression, an estimate of the relative amount of signal energy which appears in the unwanted sideband, as a function of the number of delay sections which are used, can be developed as shown in Appendix C, An Estimate of the Amount, etc. Computed in this manner, Table III shows that a total of 80 delay sections are required to ensure that the energy in the unwanted sideband is 30 db down. The total delay in this case is 40 times the bit interval. For systems in which a 30 db sideband rejection is acceptable delay line phase shifts may be useful but it appears impractical to achieve much greater sideband rejection utilizing this method alone. This method could, however, be combined with an SSB filter to provide additional attenuation of the unwanted sideband.

TABLE III

SIDEBAND REJECTION VS. NUMBER OF DELAY SECTIONS

Number of Delay Sections (2N)	Ratio of Power In Unwanted Sideband To Total Power (Db)
20	-25.8
40	-27.0
60	-28.7
80	-29.9
100	-30.8
120	-31.6
140	-32.3
160	-32.8

SECTION IV

THE FILTER METHOD FOR GENERATING A SSB SIGNAL

The most direct approach to generation of a SSB signal is to use a filter having a sharp cutoff characteristic for attenuating one sideband of an AM signal. Filters can be designed with extremely sharp cutoff characteristics, and this method is widely used for SSB transmission of voice signals. Conventional SSB filters have a severe phase distortion, which, while not troublesome for voice signals, is disastrous for pulse transmission. For this reason conventional SSB filter designs are unsuited to PCM-SSB applications. We are assuming that the usual quasi-gaussian pulses are to be transmitted in random sequence. More complicated pulse shapes and special coding methods (such as dicode) may allow a relaxation of SSB filter requirements (but may also shift the spectrum in a manner unfavorable for spectrum conservation.

Although a designer can choose from many classes of filters such as image parameter, modern networks, active filters, crystal or electromechanical filters, etc., fundamental limitations exist. These limitations are summarized by Bode, Ref. 20, in a number of theorems applicable to finite, lumped constant, linear networks. Two of these theorems are as follows:

a. "A general transfer immittance function can always be represented by a passive circuit and an ideal flat amplifier in tandem." (Ref. 20, page 245.)

In a theoretical manner, this theorem disposes of active filters in the sense that such filters have no special characteristics which are not found in equivalent passive filters, although they may aid in attaining desirable impedance matches, Q's, and buffering.

b. "Any physically realizable transfer impedance can be represented, to within a constant loss, by a combination of passive constant resistance lattice sections in tandem, each of the constituent sections being of at most the second degree." (Ref. 20, page 251.)

This theorem is of great theoretical interest for it specifies an electrical circuit corresponding to any realizable transfer function whose pole and zero locations are specified. In practice, because a lattice structure is balanced with respect to ground, filter networks are usually designed with some other configuration to allow a ground connection between input and output. Implicit in this theorem is the fact that phase response can be controlled independently of amplitude response by the addition of all-pass sections. The all-pass sections can be realized as bridged "T" networks, usually without mutual inductances. Because of theorem b., the basic theoretical problem of filter design is to specify the location of poles and zeroes of the transfer function so as to best realize some desired amplitude, and/or phase response. No general solution to the problem exists.

The earliest systematic filter design methods, based on the concept of image impedance, approximated a desired characteristic by the cascading of simple structures of known behavior. While these methods are widely used and lead to practical designs, they are best applied by experienced specialists. It is generally impossible to ensure the performance of such a design without resort to test or computer computations. Modern network designs based on the insertion loss principle, are exact, and lead to filters with a minimum number of elements with explicit performance characteristics. These designs involve very intricate computation but, with the advent of computers, extensive tables of standard design have been published. These standard designs are accompanied by exact performance characteristics, and

can be used with confidence by non-specialists. An example of the calculations and tables obtained in this manner is given by R. Saal and E. Ulbrich, Ref. 21.

For the present application it is not clear that the classes of filters which have been solved by modern methods are entirely suitable. The question of suitability arises because these filters have been designed on the basis of amplitude characteristics only. Phase characteristics for SSB filters must obey the relations described by Bode for minimum phase networks. In principle it is possible to equalize phase response with the addition of all-pass phase correctors, however, the final combination of filter and equalizer may contain a great number of elements. It is possible that a design method based on both amplitude and phase response would lead to much better performance for a given number of filter elements. The outlook for such methods is discouraging, as the following quote from Saal and Ulbrich (Pg. 314) indicates:

> "With this method, however, fewer circuit elements are usually required, and less difficulty in the physical realization is involved, since in most cases only ladder networks without mutual inductances would be used. For cases in which the smallest possible attenuation ripple in the pass-band and a sharp cutoff are required, the method mentioned above can no longer be used. Solution is only possible by means of an alternative method, with which a subsequent correction to the group delay of the filter - - is made by means of additional all-pass networks. Such requirements are encountered, for instance, in carrier frequency systems, which have to transmit pulse modulation in addition."

It will become apparent, in the following paragraphs, that the design of a sharp cutoff SSB filter with satisfactory phase response, close to the edge of the band, is very difficult. This is not surprising as we are attempting to

approximate an "ideal" filter. As indicated by Saal and Ulbrich, we approximate the amplitude characteristics by a minimum phase network (any ladder network is minimum phase) and then rely on all-pass phase correction sections. However, as developed in Bode's classic work, a minimum phase network function must be an analytic function for which the real and imaginary parts are Hilbert pairs. In this case, the desired attenuation curve has a rectangular shape, therefore the phase function has a logarithmic singularity at the band edge. If the attenuation curve is permitted to have a finite slope, the total phase shift becomes bounded and, in principle, can be equalized.

In order to gain experience with the SSB-PCM filters, a filter and equalizer was designed, constructed and tested. The primary aim of this task was to select the most complicated filter equalizer combination that seemed compatible with size and weight restrictions on tactical radios, and to design for true SSB operation. That is, where the unwanted sideband is attenuated as much as possible and the transition region is not controlled so as to usefully contribute to the signal reception.

The filter design was based on the normalized Cauer filter design given by Von R. Saal (Ref. 22). The design chosen is shown in Figure 13. This theoretical design does not allow for losses in the components. For assumed coil Q's of 314 (about the upper limit for ferrite cup core coils) the response of the filter was calculated on a computer with the results shown on Figure 14. Also shown are points measured on the completed filter. The filter has a smooth, almost flat, attenuation curve in the pass band, a transition region of ± 5 kc about the carrier frequency (1 Mc), and in the stop band, a minimum attenuation of 30 db. The phase response is sharply peaked at the carrier frequency. Observe that this filter attenuates the upper sideband of a 1 Mc modulated carrier, and the low frequency components of the modulation will be located near the carrier. Thus the phase

shift is much greater for low frequency components of the modulation than for the higher frequency components.

From the computed phase response of the filter, a 10-section equalizer was designed on a digital computer. This design is shown on Figure 15 and consists of 10 bridged -T sections, all having the same configuration. The computer design procedure ignores losses in the elements. When the singularities in the transfer function of these all-pass sections lay close to the jw axis, a very small amount of loss in the elements can cause a pronounced ripple in the attenuation curve. No modification of the design will compensate for this ripple. A computer calculation of the response of the equalizer is shown in Figure 16. Coil Q's of 500 were assumed, (unrealistically high for conventional inductors) and the attenuation ripple is probably too high to allow useful pulse transmission. A comparison calculation for the lossless case shows, however, that the phase response is almost unaffected by the losses in the elements. Even if the circuit elements were lossless, the ideal 10-section equalizer is not sufficient to correct the phase of the filter. This is shown on Figure 17 where the combined phase response for the filter and equalizer has been plotted, after subtracting a linear phase term. Figure 17 shows that the peak departure from linear phase is about 50 degrees. This is probably five or ten times the permissible phase error.

From the results described above, we conclude that a true PCM-SSB filter cannot be designed which will have acceptable attenuation and phase response, using systematic modern design methods and a PRACTICAL, for tactical radios, number of elements. Furthermore, it is concluded that any procedure dependent on conventional equalizer sections will be unsatisfactory. A vestigial sideband filter may be practical, but so far as is known there are no standard design procedures for controlling both amplitude and phase over a relatively broad transition region.

SECTION V

ERROR RATE

In this section the basic error rate equations for binary pulse transmission via a coherent SSB system are developed. The transmitter is assumed to be of conventional form in which an amplitude modulated suppressed carrier signal is modified by removal of most or all of one sideband (typically, though not necessarily) by a filter. The receiver consists of a device to generate a local carrier and perform a multiplication of this carrier by the received signal. Because of noise and circuit imperfections the local carrier is not precisely in phase with the transmitted carrier, however, this phase error is assumed to be constant at least during any single-bit interval. Phase error will vary slowly, compared with the bit rates and randomly, and can be described by some stationary probability distribution. Specifically we have assumed the distribution of phase error which would result from the addition of a small gaussian noise voltage to a carrier of correct phase. Bit detection is assumed to be a simple sampling process at the center of a bit interval. An error occurs whenever the voltage at the pulse center has its polarity inverted by the resultant effects of noise, phase error, and intersymbol interference.

It is shown in Appendix A, (equation A-8) that the signal detected by the system described can be written:

$$r(t) = a(t)\cos\varphi + b(t)\sin\varphi \qquad (16)$$

where: φ is the phase difference between the transmitted, and the locally generated carrier.
a(t) is the original modulation after system distortion, if any.
b(t) is related to the modulation, and is a consequence of modifying one sideband.

In addition to the detected signal, a gaussian noise voltage, n(t), will also be present. Assuming an equal probability of marks and spaces, the probability of bit error is the probability that

$$a_0 \cos\varphi - b_0 \sin\varphi + n < 0 \tag{17}$$

where: a_0, b_0 denote values at pulse center and a_0 is assumed positive.

For convenience we assume that n(t) has a gaussian density distribution with unit variance, or power, as follows:

$$p(n) = \frac{1}{\sqrt{2\pi}} e^{-\frac{1}{2}n^2} \tag{18}$$

With this convention, a_0^2 represents the peak pulse power to average noise power ratio. Thus the probability of bit error, at a time when phase error is φ, will be:

$$P_e = P_n\{n < -a'\} = \frac{1}{\sqrt{2\pi}} \int_{-\infty}^{-a'} e^{-\frac{1}{2}n^2}\, dn = \Phi(-a') \tag{19}$$

where: $a' = a_0 \cos\varphi - b_0 \sin\varphi$

For any assumed density distribution of phase angles, $p_\varphi(\varphi)$, the probability of error is the average over φ, or:

$$P_e = \int_{-\pi}^{\pi} \Phi(-a_0 \cos\varphi + b_0 \sin\varphi)\, p_\varphi(\varphi)\, d\varphi \tag{20}$$

Because of the complexity of phase locked oscillator (PLO) loops it was not possible to obtain the distribution of phase error which could be expected in an actual system. It is entirely reasonable, however, to represent the PLO behavior as follows. Assume that the incoming pilot carrier is disturbed by the addition of narrow band gaussian noise and that the PLO simply extracts the phase angle of this sum. The noise considered is the noise which falls

within the "noise bandwidth" of the PLO. The PLO must, by definition, "follow" the phase noise that this produces. For large carrier-to-noise ratios the phase error is small and is distributed in a gaussian manner. When α is the amplitude ratio of peak carrier-to-rms noise, it can be shown. (Reference 5, Page 411, equation 7-152) that the distribution of phase angle is:

$$P_\phi(\phi) = \frac{e^{-\frac{1}{2}\alpha^2}}{2\pi} + \frac{\alpha \cos\phi}{\sqrt{2\pi}} e^{-\frac{1}{2}\alpha^2 \sin^2\phi} \Phi(\alpha \cos\phi) \qquad (21)$$

where: $|\phi| \leq \pi$

$\Phi(x)$ is defined as an equation (19),

α = Peak Carrier/rms noise.

This rather cumbersome expression leads to the result that for large values of α (greater than 10) the rms value of ϕ is approximately $(1/\alpha)$ radians. For smaller values of α, Figure 5, of the Supplemental Report shows the numerically computed rms values of ϕ as a function of A, where A is expressed as a ratio of average carrier power-to-noise power, in db. No attempt has been made to relate the fictitious noise associated with the carrier to any real noise or disturbance in the system. Rather, it is assumed that when the PLO has a given rms phase error the distribution of phase angles will follow equation (21) providing only that α is appropriately chosen.

Using equation (21) in equation (20), the probability of error for any assumed pair of values for a_o and b_o can be computed. The results of such calculations are shown in Figure 3, of the Supplemental Report, where error rate is plotted as a function of the ratio (b_o/a_o) in db, with rms phase error as a parameter. Of more interest, however, is the situation where we consider a_o and b_o as the statistical quantities they are. Nominally, a_o is constant, being the peak pulse amplitude, but actually, due to pulse distortion and bandwidth limitations, a_o will vary from pulse to pulse depending on the

polarity of neighboring pulses. For example, phase or amplitude distortion of the low-frequency components of the pulse train will cause a very long, (though small in amplitude) "tail" on each pulse. The value of b_o will be very different from pulse-to-pulse and will appear almost noiselike. For a specific system, in which the pulse distortion is accurately known, calculations might be made of distribution functions for a_o and b_o, but in general this is not possible. It was determined, therefore, to consider the simpler case in which a_o is constant, and the system ideally SSB. A usable system must approach this case and the results are therefore considered to be a close approximation to those of an actual system. For an ideal SSB system, b(t) is the Hilbert transform of a(t), and as shown in Appendix D, b_o has a distribution described by Figure D-1. For any specified distribution of b_0, $\rho_b(b_0)$, the error probability described by equation (20), becomes:

$$P_e = \int_{-\infty}^{\infty} \rho_b(b_o) \int_{-\pi}^{\pi} \Phi(-a_o \cos\phi + b_o \sin\phi) \rho_\phi(\phi)\, d\phi\, db_o \quad (22)$$

From equation (22) error rates were calculated assuming various fixed values of a_o, the distribution of b_o described by Figure D-1, and the distribution of phase angle described by equation (21). The results are shown in Figure 2 where error rate is given as a function of a_0, with rms phase error as parameter. It should be noted that these results are based on the approximate distribution, derived in Appendix D, for quadrature voltage. Considering the assumption made in that derivation, the results in terms of resulting error rate would probably be slightly pessimistic. Intersymbol interference has been ignored, however, so the error rates given are most probably accurate.

SECTION VI

AFC FOR SSB RECEPTION

When a signal is transmitted via SSB, the greatest possible power economy is achieved with coherent reception. That is, the receiver must compare the incoming signal with a local oscillator exactly synchronized with the frequency and phase of the transmitted carrier. Ideally, the SSB signal would be processed to obtain the required frequency and phase information. Unfortunately there is no known method for doing this, and it is probably impossible. Thus, a pilot carrier signal must accompany the SSB signal in order to convey the required auxiliary information. According to the principles of information theory, very little information is conveyed by transmission of a signal of fixed phase and amplitude, and consequently, negligible power need be expended in the pilot carrier. If the transmitter operated at a precise carrier frequency, known to the receiver, a very small pilot carrier would probably be sufficient. However, when the transmitter frequency is not precisely controlled a considerably larger pilot carrier will be required. This section considers the theory, and some examples, of possible methods for extracting a frequency reference from a pilot carrier and PCM-SSB signal.

Any bandpass signal can be represented in either of the equivalent forms:

$$s(t) = R(t) \cos (\omega_o t + \varphi(t)) \tag{23}$$

$$s(t) = a(t) \cos \omega_o t - b(t) \sin \omega_o t \tag{24}$$

These forms have the following interrelationships:

$$\begin{aligned} a &= R \cos \varphi & R &= \sqrt{a^2 + b^2} \\ b &= R \sin \varphi & \varphi &= \tan^{-1} \frac{b}{a} \end{aligned} \tag{25}$$

In conventional modulation methods, either R(t) is constant while $\varphi(t)$ is modulated, as in FM, or R(t) is modulated while $\varphi(t)$ is constant, as in AM. For SSB, a(t) is the modulating signal while b(t) is a signal derived from a(t) either explicitly, by a 90° phase shift operation, or implicitly, by filtering. An SSB signal generally contains both envelope and phase modulation. For convenience in visualizing the relationships between components of bandpass signals, phasor diagrams are often employed. It is conventional to show the instantaneous phase and amplitude of the modulated carrier by a phasor drawn from the origin to a point (a(t), b(t)). In time this point will move and trace out a curve which is suggestive of the behavior of the carrier. Thus, when the curve encircles the origin, the carrier has gone through one "extra" cycle of oscillation (or one less cycle, depending on the direction of encirclement).

This possibility of "extra" carrier cycles raises a question as to the "frequency" of a phase modulated carrier. Two definitions of the frequency are often advanced. The basic definition of frequency as the average rate at which the signal passes through zero in a positive direction, is useful and seems to bear the closest relation to the primitive idea of frequency as the reciprocal of time required to complete a "cycle". A more useful mathematical definition is based on "instantaneous frequency":

$$\omega_i(t) = \frac{d}{dt}\left(\omega_0 t + \varphi(t)\right) = \omega_0 + \frac{d\varphi}{dt} \tag{26}$$

and average frequency over a specified time interval:

$$\overline{\omega(\tau)} = \frac{1}{\tau}\int_0^{\tau} \omega_i\, dt = \omega_0 + \frac{1}{\tau}\left\{\varphi(\tau) - \varphi(0)\right\} \tag{27}$$

Providing $\omega_o > \left|\frac{d\varphi}{dt}\right|_{max}$, the two definitions are equivalent if the specified time interval is taken between two positive-going zero crossings. Since an arbitrarily high carrier frequency can be assumed, no real conflict between the definitions need exist if $\frac{d\varphi}{dt}$ has an upper limit. The equivalence between zero-crossing rate and average instantaneous frequency is important, if the signal is to undergo limiting, for after ideal limiting only the zero crossing information is unchanged. It is advantageous to dwell on this equivalence of zero-crossing rate and average instantaneous frequency, for, by tracing the conditions necessary to equivalence, one gains an appreciation of the nature of phase behavior for SSB signals.

In equation (23) it is clear that if at all times $\omega_o > \left|\frac{d\varphi}{dt}\right|$ then the total phase angle $\left[\omega_o t + \varphi(t)\right]$ is a monotonically increasing function and $\cos\left[\omega_o t + \varphi(t)\right]$ is monotonic between minima and maxima, and these occur only at ± 1. (Without this restriction to monotonic behavior, a purely phase modulated carrier develops an apparent envelope fluctuation and the conventional distinction between envelope and phase is no longer clearcut.)

The phase modulated carrier will then trace out k complete "cycles" in a time T, if and only if:

$$\omega_o T + \varphi(t+T) - \varphi(t) = 2\pi k \qquad (28)$$

Thus, choosing the starting time, t, at the instant of a positive-going zero crossing we can say, from equation (27) that the average angular rate is:

$$\overline{\omega(T)} = \omega_o + \frac{1}{T}\left\{\varphi(t+T) - \varphi(t)\right\} = \frac{2\pi k}{T} \qquad (29)$$

This establishes the equivalence of the two definitions but not the requirement that $\omega_0 > \left|\frac{d\varphi}{dt}\right|$. Note that if we allow $\frac{d\varphi}{dt}$ to exceed ω_0, the total phase is not monotonic and can decrease with time. A condition may then arise where $\cos\left[\omega_0 t + \varphi(t)\right]$ has just made a zero crossing but the phase now begins to decrease until another zero crossing is made. Finally, phase again increases to the point where another zero crossing is made. This process introduces two extra zero crossings not reflected in the advancing of total phase by an additional 2π. Consequently, zero crossing and average instantaneous frequency cannot be equivalent during this interval. If the process described above is viewed with the aid of a phasor diagram, it will be found that with the condition $\omega_0 > \left|\frac{d\varphi}{dt}\right|$ an "extra" carrier cycle results every time that the phasor completes one encirclement of the origin, but not under any other condition. It should be noted that the condition $\omega_0 > \left|\frac{d\varphi}{dt}\right|$ is a sufficient, but not a necessary, condition for the equivalence of the two definitions of frequency.

An interesting test of these ideas was performed by adding the output of two oscillators and counting the rate of zero-crossings on a counter. It was found (the test preceded the above reasoning) that when the frequencies of the oscillators are close together, a very slight adjustment of the relative amplitudes of the signals cause the counter to show the exact frequency of the stronger, altogether ignoring the weaker signal. The adjustment of amplitudes is so critical as to appear discontinuous. Actually, there is a transition region. For two sinusoids:

$$\begin{aligned} &A_1 \sin \omega_1 t \\ &A_2 \sin \omega_2 t \qquad \omega_2 > \omega_1 \end{aligned} \tag{30}$$

it can be shown analytically that if $A_1/A_2 > \omega_2/\omega_1$, then the zero-crossing rate will be exactly that of the low-frequency signal. If A_1 is reduced below this

threshold, then during part of the time $\left|\frac{d\varphi}{dt}\right| > \omega_1$, and extra zero crossing may be observed, so that the apparent frequency lies between ω_1 and ω_2.

The critical behavior of zero-crossing rate as a function of relative signal strength is closely related to the capture effect observed in FM receivers, where limiting is used to obliterate all information but that contained in zero crossings.

Another experiment was performed in which a carrier tone was added at one edge of a narrow band of random noise, and zero crossings of the sum were displayed on a counter. For a high amplitude carrier the counter displayed a reading very nearly that of the correct carrier frequency. As expected, with no carrier the counter reading corresponded to a frequency near the center of the noise band. After allowing for the threshold voltage of the counter, the experimental results were in near agreement with the following theoretical expression:

$$\overline{\Delta f} = \frac{B_n}{2} e^{-C/N} \tag{31}$$

where: $\overline{\Delta f}$ is the difference between the "average frequency" and the carrier frequency.
B_n is the noise bandwidth
C/N is the carrier to Noise power ratio.

This expression is easily derived as follows: For narrow-band noise the envelope is relatively constant through many carrier cycles, and, on the average, the frequency of the noise is that of the mid-band frequency. As indicated, for those times when the carrier is only slightly greater than the noise envelope, only carrier cycles are counted, and conversely. The probability of the noise envelope exceeding the carrier is easily shown to be:

$$P_n\{R_n > C_a\} = e^{-C/N} \tag{32}$$

Thus the average number of cycles/second added by the noise, in addition to carrier cycles, is given by equation (31). While this equation is not an exact result it appears to be an accurate representation of the true situation.

After the preceding discussion of the behavior of phase and frequency in band-pass signals, attention was turned to SSB signals formed from binary PCM trains. In this section we are specifically interested in the characteristics of such signals, which can be used to locate carrier frequency. First, consider the behavior of $\varphi(t)$ in equation (23) when a(t) is a binary pulse train, and b(t) is its Hilbert transform. Since $\varphi = \tan^{-1} b/a$, note that in order for φ to increase by 2π radians it is necessary for a(t) and b(t) to pass through the following four conditions:

a. a positive, b positive, $0 < \varphi < \pi/2$

b. a negative, b positive, $\frac{\pi}{2} < \varphi < \pi$

c. a negative, b negative, $\pi < \varphi < \frac{3}{2}\pi$

d. a positive, b negative, $\frac{3\pi}{2} < \varphi < 2\pi$

Thus for φ to advance by 2π it is sufficient for the zero crossings of a and b to alternate. (For example if $a(t) = \cos \omega_1 t$ and $b(t) = \sin \omega_1 t$, the zero crossings alternate and $\varphi(t)$ advances linearly with time.) It is relatively easy to show that for full baud rectangular pulses this property of alternating zero crossings will hold for any sequence of pulse polarities. For pulses which do not have zero-rise times, however, it is possible to construct pulse sequences for which the zeros of a(t) and b(t) do not always alternate.

To visualize the behavior of a, b, R, and φ, a typical pulse train was constructed as shown on Figures 18 and 19. As shown on Figure 18 a sequence of gaussian pulses results in a quadrature component b(t) and an envelope R(t). For the example chosen, note that the zeroes of a(t) and b(t) do alternate and the phase $\varphi(t)$ must therefore advance 2π each time a(t) goes through a cycle from a positive pulse to one or more negative pulses and back

to a positive pulse. The behavior of $\varphi(t)$ is shown in Figure 19, with a(t) repeated for convenience. In Figure 19, φ is shown as the deviation of phase from a phase which increases linearly by $\pi/2$ radians-per-pulse interval. It will be noted that phase tends to advance whenever pulse polarity changes.

In a random pulse train there will be, on the average, one-quarter as many "cycles" of the train as there are pulses. Consequently, φ will advance an average $\pi/2$ radians per pulse interval, at least for rectangular pulses. For common pulse shapes, such as gaussian, this will also be true, except for certain sequences having an exceedingly small probability of occurrence. It is assumed that random pulse sequences will show this property, regardless of pulse shape, although this has not been rigorously proven, except for rectangular pulses.

From the previous argument it can be concluded that an SSB signal derived from a random binary pulse train has an average frequency:

$$\bar{f} = fo + 1/4T \qquad (33)$$

where: T is the pulse interval.

The average frequency referred to is the average instantaneous frequency. If random sequences were always being received then the carrier frequency could be accurately located by measuring the average frequency and subtracting out one-quarter of the "known" pulse rate. (Even the pulse rate is not "known" precisely at the receiver until after pulse synchronization has been achieved. Although it can be "known" to within approximately 100 cps with available oscillator stabilities.) Thus, for a bit rate of 576,000 pulses-per-second, averaged over one second, the measured frequency would differ from the carrier by 144,000 pulses-per-second. This difference would fluctuate with a gaussian distribution having a standard deviation of only 190 cycles. Consequently the derived carrier frequency would always be within

a few kc of the correct frequency, and a standard APC system could lock on a very small pilot carrier. A real PCM signal does not always have a random nature, however, and a practical system must be capable of acquiring phase reference for all possible transmitted signals.

Because of the possibly non-random nature of the transmitted signals, the two most extreme cases can be identified. One case is the alternate transmission of marks and spaces. This causes a degenerate SSB signal consisting of a single line component at a frequency offset from the carrier by one-half the bit rate. The other extreme is a transmission of all marks, or all spaces, which results in transmission of pure carrier. The average frequency for random transmission is midway between the frequencies which result from the two extreme cases.

Up to this point no explicit consideration has been given to the effect that the addition of a carrier signal to the SSB signal would have on average frequency. With the addition of a carrier voltage c cos $\omega_0 t$ equation (24) becomes:

$$S_C(t) = \left[a(t) + c \right] \cos \omega_0 t + b(t) \sin \omega_0 t \qquad (34)$$

From the foregoing discussion it is clear that when c is greater than the peak value of a, the phase function $\varphi(t)$ can never be outside the range $-\frac{\pi}{2} < \varphi < \frac{\pi}{2}$. Thus the average frequency of the carrier plus SSB signal would be exactly the carrier frequency. This simple result is important as it indicates that for the rectangular full baud case, without shaping, the addition of a carrier, having a power little more than half that of the sideband, a signal is obtained with an average frequency exactly the same as the carrier frequency. (For the gaussian shaped case carrier power must be almost equal to sideband power.) When noise is considered the situation is more complex. Nevertheless, when

the noise is small enough to permit tolerable error rates it would appear that a very slight increase in carrier power, beyond that indicated, would be sufficient to ensure that the average frequency, of the total signal, would be extremely close to the exact carrier frequency. When the carrier is not sufficient to dominate the SSB signal, it appears that the average frequency would be strongly influenced by the sidebands.

While an AFC system based on a measurement of average frequency of the total signal, should perform very well, when a dominating carrier is transmitted, it will in all probability obtain little, if any, benefit from the transmission of a small carrier. Consideration must therefore be given to the means of deriving frequency information, other than by average frequency measurements, before making a final choice of AFC. A general means of frequency location is based on an operation on the received power spectrum. A great many such methods could be devised, but in practice the tendency would be to choose a method which could be realized with standard and thoroughly tested circuits. Thus consideration must be given to the possible use of a limiter, a discriminator, and one of a number of detectors.

As discussed in Appendix E a discriminator (but no limiter) and square law envelope detector can provide an AFC system with a control voltage derived from an operation on the power spectrum of the signal. For a linear discriminator, control will depend on the centroid of the power spectrum, and under steady state conditions, the frequency error is equal to the centroid of the sideband power spectrum, referred to baseband. In the following, we consider the frequency error that will result from such a system for the case of a SSB signal, derived from a random binary pulse train.

From equations (A.9), (A.11), and (B.1) the baseband power spectrum is:

$$|s'(\omega)|^2 = T\left(\frac{\sin \omega T/2}{\omega T/2}\right)^2 e^{-\left(\frac{\omega}{\omega_\sigma}\right)^2} \tag{35}$$

Except for frequency translation the rf spectrum is described by the same function, on one side of the carrier. Applying equation (E.15) to this spectrum, the frequency error is

$$\omega_e = \frac{\int_0^\infty T\left(\frac{\sin \omega T/2}{\omega T/2}\right)^2 e^{-\left(\frac{\omega}{\omega_\sigma}\right)} \omega d\omega}{\int_0^\infty T\left(\frac{\sin \omega T/2}{\omega T/2}\right)^2 e^{-\left(\frac{\omega}{\omega_\sigma}\right)^2} d\omega} \tag{36}$$

The denominator is just π E/T, where E is pulse energy, evaluated in Appendix B as equation (B.14). With the substitution $y = \omega T/2$, the numerator is normalized so that:

$$\omega_e = \frac{4}{\pi E} \int_0^\infty \frac{\sin^2 y}{y} e^{-\left(\frac{2y}{T\omega_\sigma}\right)^2} dy \tag{37}$$

The integral is evaluated in terms of a tabulated function, equation (B.30) in Appendix B, and a plot of this function is shown in Figure B-3. It is worth stating that the integral diverges as the gaussian bandwidth parameter ω_σ becomes infinite. The above expression was evaluated and the results are shown in Figure B-4, where frequency error, f_e, (not radian frequency) is divided by bit rate, 1/T, and shown as a function of the bandwidth parameter $a = \omega_\sigma T/2$. This parameter has a typical value 2.02, for which $f_e = .225$ times the bit rate. It is interesting that this result is very close to the average instantaneous frequency expected for a random binary train, i.e., the carrier plus 0.25 times the bit rate.

Suppose a carrier signal is transmitted in addition to the SSB signal considered above. If the power in the pilot is R times the sideband power, then the denominator in equation (36) is increased by the factor (1 + R), but, as stated in Appendix E, the numerator is unaffected. Thus the frequency error becomes:

$$f_e = \frac{1}{1+R} \quad f_e' \tag{38}$$

where: f_e' is the frequency error when no carrier is transmitted.

Applying this modification to the results shown in Figure B-4 the results shown in Figure 20 are obtained. This figure shows the carrier power required to obtain a frequency error which is 1/2, 1, 2, 4, or 10 percent of the bit rate, as a function of the gaussian bandwidth and the bit rate. If it is considered that AFC should provide frequency control to within a few kilocycles in order for the APC loop to work properly, the results shown in Figure 20 are disappointing.

The foregoing discussion indicates that a simple centroid-controlled AFC system will not be satisfactory. It is possible to improve AFC performance by filtering the signal spectrum before presenting it to the linear discriminator system described above. This type of system is analyzed as follows, where it is assumed that a rectangular bandpass filter of bandwidth 2W precedes the discriminator and the center frequency of the filter is the same as that for the discriminator. To ensure the presence of the carrier within the filter bandwidth requires an overall frequency stability for transmitter and receiver, of ± W cycles/second. The implications of this stability requirement are discussed in a succeeding paragraph. For the assumed filter, the frequency error is calculated as previously indicated except that equation (E. 15) must be modified as follows:

$$\omega_e = \frac{\int_0^{\omega_e + 2\pi W} |S'(\alpha)|^2 \alpha \, d\alpha}{\int_0^{\omega_e + 2\pi W} |S'(\alpha)|^2 \, d\alpha} \tag{39}$$

When carrier power is present the denominator is modified by the addition of πP_c, where P_c is the carrier power. The factor π is introduced because the denominator of equation (39) is equal to π times sideband power when $W \to \infty$. Equation (39) can be solved by assuming a value for the limit on the integrals, $\omega_e + W$, and evaluating the ratio to obtain ω_e and thus W. For the full baud gaussian power spectrum, however, the integrals would have to be numerically evaluated. When W is small however, the power spectrum can be assumed constant over the range of integration, and equation (39) solved explicitly with the result that:

$$\frac{W}{f_o} = \sqrt{\left(\frac{f_e}{f_o}\right)^2 + \frac{f_e}{f_o^2} \frac{P_c}{|S(0)|^2}} \tag{40}$$

Using the relation between carrier power and sideband spectral density given by equation (B.37) there results:

$$\frac{W}{f_o} = \sqrt{\left(\frac{f_e}{f_o}\right)^2 + \frac{f_e}{f_o} R K(\omega_\sigma, T)} \tag{41}$$

where: $K(\omega_\sigma, T)$ is a system constant ≈ 0.72, defined by equation (B.35) and shown in Figure B-2.
R is the ratio of carrier to sideband power.

For larger values of W the integrands can be approximated by two terms of their power series, and the result integrated term by term. For example, assuming a $\sin^2 X/X^2$ power spectrum and neglecting the effect of the gaussian filter over the range of integration, and noting that:

$$\sin^2 y = y^2(1 - 1/3\, y^2) \tag{42}$$

we have:

$$\omega_e = \frac{\frac{4}{\pi}\int_0^{\chi}(1-\frac{1}{3}y^2)\,y\,dy}{\pi P_c + 2\int_0^{\chi}(1-\frac{1}{3}y^2)\,dy}$$

where: $y = \omega \cdot T/2$

$x = (\omega_e + 2\pi W)\cdot T/2$

$$\omega_e = \frac{4/\pi\left[\frac{\chi^2}{2} - \frac{\chi^4}{12}\right]}{\pi P_c + 2\left[\chi - \frac{\chi^3}{9}\right]} = \frac{3/\pi\,\chi^2\left[1 - \chi^2/6\right]}{\pi P_c + 2\chi\left[1 - \frac{\chi^2}{9}\right]} \tag{43}$$

It is convenient at this point to define:

$$z = x/\pi = \frac{f_e + W}{f_0} \tag{44}$$

where: $f_e = \frac{\omega_e}{2\pi}$, $f_0 = \frac{1}{T}$

Using these variables, there results:

$$\frac{f_e}{f_0} = \frac{z^2\left[1 - \pi^2 z^2/6\right]}{R\frac{E}{T} + 2z\left[1 - \frac{\pi^2}{9}z^2\right]} \tag{45}$$

where: $z = (f_e + W)/f_o < \frac{1}{\pi T}$

R = Ratio of carrier power to transmitted sideband power.

E = Pulse energy, equation (B.14)..

From this equation values of W/f_o are found by assuming values for z, solving for f_e/f_o and then obtaining $W/f_o = z - f_e/f_o$. In this way, curves of W/f_o as functions of f_e/f_o are obtained as shown in Figure 21 for $a = \omega_o T/2 = 2.425$. The exact value chosen for a has very little effect on the results.

It is now necessary to guarantee that the carrier will always fall within the filter bandwidth 2W in order that the AFC can operate on it. Hence the over-all stability of the transmitter and receiver must be such that the total carrier displacement (before AFC) be less than ± W cps. Assuming equal stability for transmitter and receiver,

$$S = \pm W/2/f_c \qquad (46)$$

where: S = stability of Xmtr = stability of receiver.

f_c = RF carrier frequency

The equipment stability necessary to achieve a prescribed frequency error is shown in Figure 22.

SECTION VII

APC DESIGN FOR PCM-SSB RECEPTION

7.1 INTRODUCTION

If there is no distortion in the signal-forming process or in transmission, the received SSB data signal is:

$$s(t) = a(t) \cos \omega t + b(t) \sin \omega t \qquad (47)$$

Where a(t) is the modulating signal, b(t) is its Hilbert transform, and ω is the carrier frequency. To detect a(t), it is necessary to have a demodulating carrier which is coherent (phase-locked) with the carrier of the received signal. Phase information is necessary since we must detect a(t) and reject b(t). Thus the ideal reference at the receiver is the form cos (ωt + 0). It is assumed that a carrier pilot tone is transmitted along with the modulated signal. The receiver must pick out this pilot from the total signal-plus-noise. The questions to be answered are:

a. How well can this be done?

b. How much pilot power is required?

It has been concluded that the task requires a PLO together with a relatively tight AFC loop. Without AFC, PLO could extract the reference only at the cost of an unreasonable amount of pilot power. If the PLO must look at a wide frequency band, it will see a large amount of SSB energy located to one side of the desired pilot. This is in effect a large asymmetrical noise which causes large phase perturbations unless the pilot power is large compared to the SSB power at the PLO input. Alternatively, the PLO could be designed with a wide capture range but extremely narrow noise bandwidth; this would

result however, in an unreasonably long lock-in time. The situation would be improved if there could be a guard band between the pilot and the signal band. This is possible to only a limited extent due to the requirement of this system for transmission of low-frequency components of the modulation.

7.2 REVIEW OF THE PLO

The basic PLO uses a phase detector, a low-pass filter, and a voltage-controlled oscillator. A block diagram is shown in Figure 23. The input and output quantities are considered to be the phases of the input and oscillator output signals, or alternatively, the time derivatives of these phases (frequencies).

The phase detector output voltage is some function of the difference, φ, between the two phases as its input. Two of the various possible phase detector characteristics $v = f(\varphi_1 - \varphi_2) = f(\varphi)$ are shown in Figure 24. In the locked condition, it is only the slope of the characteristic at some fixed φ with which we are concerned. Assume a unity slope, and absorb this constant in the overall loop gain.

The low pass filter, which is usually used, is shown in Figure 25. It is a standard "lag" filter with unity d-c transmission. Its purpose is to eliminate the high frequency component of the phase detector output, and allow a suitable choice of PLO parameters. The two time constants provide a desirable degree of design flexibility.

The voltage-controlled oscillator generates a periodic wave whose frequency is ω_o (its free-running frequency) plus a constant, K, times its input voltage.

The basic system equation is:

$$\dot{\varphi} + K\,L(\varphi)\,f(\varphi) = \Delta\omega \tag{48}$$

where: $\Delta\omega = \omega_1 - \omega_0$

$L(\varphi)$ = Linear Operator

With our assumptions this becomes:

$$\ddot{\varphi} + \left(\frac{1}{\tau} + Ka\right)\dot{\varphi} + \frac{K}{\tau}\varphi = \frac{\Delta\omega}{\tau} + (\dot{\Delta\omega}) \tag{49}$$

from which it is seen that at equilibrium (derivatives $\longrightarrow$ o) there is a "static phase error", $\varphi_{\infty} = \frac{\Delta\omega}{K}$, equal to the open-loop frequency error divided by the open-loop gain.

The equivalent "servo" block diagram is shown in Figure 26. The system transfer function is:

$$\frac{\Phi_2}{\Phi_1} = Ka\,\frac{s + 1/a\tau}{s^2 + \left(\frac{1}{\tau} + Ka\right)s + \frac{K}{\tau}} \tag{50}$$

The "hold range" is defined as that open-loop frequency difference beyond which synchronization (sync) will be lost, in the case where the system is initially in sync and $\Delta\omega$ is slowly increased. If for example we assume a sine-characteristic phase detector $v = f(\varphi) = \sin\varphi$, the largest voltage it can provide is unity, so that from equation (48) hold range = $|\Delta\omega|_{max}$ = K.

The "capture" or "pull-in" range is that maximum open-loop frequency difference for which sync can be established if $\Delta\omega$ is slowly decreased from the out-of-sync condition. This may be made smaller than the hold range.

It is the significant frequency range of the system, since there is no assurance (due to the nonlinear nature of the PLO) that frequencies outside this band will be recaptured if sync is momentarily lost.

Pull-in time (the time required to achieve frequency synchronism starting from a given initial frequency difference) can be found only approximately, even after involved non-linear analysis. It is given by Richman (in Ref. 9) as approximately:

$$T_F \cong 4 \frac{(\Delta f)^2}{(B_n)^3} \tag{51}$$

where: B_n = noise bandwidth = $\int_0^\infty \left| \frac{\Phi_2(\omega)}{\Phi_1(\omega)} \right|^2 df$

This holds except near the limits of the capture range, where the pull-in time becomes arbitrarily large.

Another important quantity is the output phase jitter. If the jitter caused by the local oscillator is negligible, output jitter is a function of input jitter and the transfer function of the PLO. The mean squared output jitter (for minute jitter) can be calculated if the power density spectrum of the input jitter is known, by:

$$\overline{\varphi_2^2} = \frac{1}{2\pi} \int_0^\infty |\Phi_1(\omega)|^2 \cdot \left| \frac{\Phi_2(\omega)}{\Phi_1(\omega)} \right|^2 df \tag{52}$$

which becomes equal to AB_n if φ, has a uniform power density A. To completely describe the jitter, its probability density or distribution must be known. In the case where the input has a gaussian density, the output will approach gaussian for the high probability, i.e., low amplitude values.

7.3 PROBLEMS FACED BY THE PLO IN PCM-SSB

The PLO must be able to acquire, and remain locked to, a signal which is anywhere in the expected frequency range. Normally the PLO should be designed for a "capture range" greater than this (perhaps by a factor of two) since pull-in time increase rapidly toward the extremes of the capture range.

The effect of thermal noise alone is handled in a straightforward manner. If the noise is narrowband and symmetrical about the carrier frequency it can be represented in the form:

$$n(t) = x(t) \cos \omega t + y(t) \sin \omega t \tag{53}$$

where: x and y are independent gaussian random variables.

The noise power is:

$$\overline{n^2} = N_o B_n = \frac{\overline{x^2}}{2} + \frac{\overline{y^2}}{2} = \overline{x^2} = \overline{y^2} \tag{54}$$

If this is added to a pilot tone of amplitude Q, the result is:

$$(Q + x) \cos \omega t + y \sin \omega t \tag{55}$$

with a phase:

$$\varphi_1(t) = \tan^{-1} \frac{y}{Q + x} \tag{56}$$

For useful S/N ratios, this is approximated closely by:

$$\varphi_1(t) \cong \frac{y}{Q} \tag{57}$$

This is the input quantity (due to thermal noise) to the PLO. It is assumed that n(t) has a flat power density spectrum over the bandwidth of the PLO, of density N_0. This is then also the density of y(t) in baseband, and $\varphi_i(t)$ has a density N_e/Q^2. The mean squared phase jitter at the PLO output is therefore:

$$\overline{(\varphi_2)^2} = 2\frac{N_e}{Q^2}\int_0^\infty \left|\frac{\Phi_2(\omega)}{\Phi_1(\omega)}\right|^2 df = \frac{2N_0 B_n}{Q^2} \qquad (58)$$

where B_n is the noise bandwidth of the PLO as defined by equation (51). (The factor of two (2) enters because the PLO is sensitive to noise on both sides of the carrier frequency.)

Now, using equations (B-35) and (B-36), the carrier can be expressed in terms of two ratios as:

$$Q = \sqrt{2\ R\ \ E/T} \qquad (59)$$

where: R is the ratio of carrier to sideband power
E/T is the ratio of pulse energy to bit interval (average sideband Power)

Using this relation in equation (58) there results:

$$\varphi_{rms}\sqrt{R} = \sqrt{\frac{B_n}{f_0}\cdot\frac{1}{E/N_0}} \qquad (60)$$

where: f_0 = 1/T the bit rate
E/N_0 = pulse energy noise power density.

The quantity E/N_0 is a fundamental parameter in theoretical studies of bit error rate in binary systems. As an example, refer to Ref. 11, page 1602. Typically, E/N_0 = 16.

Substituting equation (51) in equation (60) there results:

$$\varphi_{rms}\sqrt{R} = \sqrt{\frac{4^{1/3}}{E/N_o}\left(\frac{\Delta f}{f_o}\right)\left(\frac{1}{T_F\,\Delta f}\right)^{1/3}} \qquad (61)$$

where: Δ f is the capture range

T_F is the time to achieve lock.

In practical design, factors such as pull-in range, pull-in time, RMS phase jitter, and static phase error, are taken into account and a balance determined. Design relationships are presented in the article by Richman (Ref. 9).

In PCM-SSB, the PLO is confronted with the additional problem of the asymmetrical sideband power. It must lock to the pilot, and yet ignore the SSB signal. Since all of the SSB energy is concentrated to one side of the pilot tone, the tendency will be to pull the PLO away from the pilot frequency. The SSB signal pulse pilot tone is:

$$s(t) = \left[Q + a(t)\right]\cos\omega t + b(t)\sin\omega t \qquad (62)$$

with an instantaneous phase,

$$\varphi_1(t) = \tan^{-1}\frac{b(t)}{Q + a(t)} \qquad (63)$$

Depending on the relative strengths of sideband and pilot at the PLO input, this can be a comparatively small phase perturbation which may be analyzed by linear approximations, or a large rapidly varying function perhaps even involving a random frequency error.

7.4 RELATION BETWEEN PILOT AMPLITUDE AND PHASE JITTER

We now want to relate the pilot amplitude to the phase jitter in the PLO output.

The signal at the receiver consists of pilot, sideband, and noise:

$$f(t) = [Q + a(t) + x(t)] \cos \omega_c t + [b(t) + y(t)] \sin \omega_c t \qquad (64)$$

The instantaneous phase of this signal is:

$$\varphi_1(t) = \tan^{-1} \frac{b(t) + y(t)}{Q + a(t) + x(t)} \qquad (65)$$

This is analytically intractable due to the statistical nature of a, b, x, and y, and even more so because of the non-linear nature of the function. The following assumptions are therefore made:

a. Filtering ahead of the PLO input will make the pilot much larger than the noise or filtered remnants of the sideband

b. The angle remains sufficiently small so that almost all the time $\tan^{-1} u \cong u$.

c. S/N is sufficient so that b >> y.

With these assumptions, at the PLO input:

$$f'(t) = Q \cos \omega_c t + b'(t) \sin \omega_c t,$$
$$\varphi_1'(t) \cong \frac{b'(t)}{Q} \qquad (66)$$

The quantity b(t) represents the quadrature component of the signal after having gone through filtering, to be described.

7.4 RELATION BETWEEN PILOT AMPLITUDE AND PHASE JITTER

We now want to relate the pilot amplitude to the phase jitter in the PLO output.

The signal at the receiver consists of pilot, sideband, and noise:

$$f(t) = [Q + a(t) + x(t)] \cos \omega_c t + [b(t) + y(t)] \sin \omega_c t \tag{64}$$

The instantaneous phase of this signal is:

$$\varphi_1(t) = \tan^{-1} \frac{b(t) + y(t)}{Q + a(t) + x(t)} \tag{65}$$

This is analytically intractable due to the statistical nature of a, b, x, and y, and even more so because of the non-linear nature of the function. The following assumptions are therefore made:

a. Filtering ahead of the PLO input will make the pilot much larger than the noise or filtered remnants of the sideband

b. The angle remains sufficiently small so that almost all the time $\tan^{-1} u \cong u$.

c. S/N is sufficient so that b >> y.

With these assumptions, at the PLO input:

$$f'(t) = Q \cos \omega_c t + b'(t) \sin \omega_c t,$$
$$\varphi_1'(t) \cong \frac{b'(t)}{Q} \tag{66}$$

The quantity b(t) represents the quadrature component of the signal after having gone through filtering, to be described.

The actual transmitter is assumed to include a high-pass filter in the signal path of the baseband pulse train to eliminate low frequency components of the modulation. Assume an ideal high-pass filter with cutoff at f_h. This acts on a(t) at the transmitter, and therefore also removes components of b(t) below f_h, since the power spectrum of b(t) must be identical with that of a(t).

It is assumed that the PLO is preceded by AFC, which makes possible the use of a band-pass filter in the signal path, with pass-band $f_c \pm B/2$. (This has a low-pass equivalent with cutoff at B/2.) This filter reduces the amount of sideband energy (and noise) appearing at the PLO input. The joint effect of the filter and the high-pass filter is that b(t) contains only those components of the original quadrature signal which lie between f_h and B/2.

It is assumed that B/2 is much smaller than the standard deviation frequency $\frac{\omega_\sigma}{2\pi}$ of the SSB filter. Therefore b(t) will have a power density in the band of interest closely equal to the density of the original baseband signal at $\omega = 0$. The single side power density spectrum of the original signal, in the limited band of interest is:

$$|G(0)|^2 = 2T \tag{67}$$

A typical PLO with a damping constant:

$$\zeta = \frac{1}{2}\left[a\sqrt{KT} + \frac{1}{\sqrt{KT}}\right] = \frac{\sqrt{2}}{2} \tag{68}$$

will have a transfer function of the form:

$$|H(\omega)|^2 = \left|\frac{\Phi_2}{\Phi_1}\right|^2 = \frac{1+(\omega/\omega_1)^2}{1+(\omega/\omega_2)^4} \tag{69}$$

This is found in a straightforward manner from equation (51). However, for our purposes this is close enough to

$$\left|H(\omega)\right|^2 = \frac{1}{1+\left(\frac{\omega}{4B_n}\right)^2} = \frac{1}{1+\left(\frac{\pi}{2}\right)^2\left(\frac{f}{B_n}\right)^2} \qquad (70)$$

where B_n is the noise bandwidth of the PLO, defined by equation (52). Figure 27 shows the complete signal path relevant to the discussion.

This single-sided power density spectrum of φ_1' is:

$$\left|\Phi_1\right|^2 = \frac{|G(0)|^2}{Q^2} = \frac{2T}{Q^2}, \quad 2\pi f_n \le \omega \le 2\pi\frac{B}{2} \qquad (71)$$

Therefore, the power density spectrum of φ_2 is

$$\left|\Phi_2\right|^2 = \left|\Phi_1\right|^2\left|H(\omega)\right|^2 = \frac{2T}{Q^2}\left|H(\omega)\right|^2, \qquad (72)$$

and,

$$\overline{\varphi_2^2} = \int_{f_n}^{B/2}\left|\Phi_2\right|^2 df$$

$$= \frac{2\pi}{Q_2}\int_{f_n}^{B/2}\frac{df}{1+\left(\frac{\pi}{2}\right)^2\left(\frac{f}{B_n}\right)^2} \qquad (73)$$

The result is:

$$\varphi_{2\,rms}\cdot Q = \left[\frac{4}{\pi}T'B_n\right]^{1/2}\left[\tan^{-1}\frac{\pi}{2}\frac{B/2}{B_n} - \tan^{-1}\frac{\pi}{2}\frac{f_n}{B_n}\right]^{1/2} \qquad (74)$$

We now specify that when the initial frequency difference (between the pilot and the PLO) is B/2 the pull-in time is to be some particular T_F. Equation (52) becomes:

$$T_F \cong \frac{B^2}{B_n^3} \tag{75}$$

Using this relation, and defining the parameters,

$$A = \frac{4}{\pi}\left[\frac{1}{B T_F}\right]^{1/3} = \frac{4}{\pi}\frac{B_n}{B} \tag{76}$$

$$u = \left(\frac{B}{2f_h}\right)^{1/2} \tag{77}$$

equation (74) becomes:

$$\varphi_{2\,rms} \cdot Q = \left[TB \tan^{-1}\left(\frac{u - 1/u}{Au + 1/Au}\right)\right]^{1/2} \tag{78}$$

In our 12-channel system, T = 1.736 x 10^{-6}, and the relation becomes:

$$\varphi_{2\,rms} \cdot Q = \frac{0.00149\, B^{1/3}}{T_F^{1/6}}\left[\tan^{-1}\left(\frac{u - 1/u}{Au + 1/Au}\right)\right]^{1/2} \tag{79}$$

This is plotted vs. B/2 in Figure 28, for two values of T_F (0.1 and 0.01 sec) and three values of f_h (0.5, 1, and 1.4 Kc). For a particular set of parameters T, f_h and B/2, the relation is of the form $\varphi_{2\,rms} \cdot Q$ = constant (a hyperbola). In practical applications, the value of Q is usually only known in terms of the ratio, R, of carrier to sideband power. The required relationship is given by equation (B.36) as:

$$Q = \sqrt{2RK(\omega_0, T)} \tag{80}$$

(The constant, A, in equation (B.36) has been taken as unity in the above development. The constant K (ω_c, T) is typically 0.72, and is defined by equation (B.35).

The relation of static phase error to the parameters involved in Figure 28 is also of interest. For this purpose, assume the frequency instability of the PLO is negligible; the natural (open-loop) frequency of the PLO is at the center of the band of uncertainty $\frac{\omega_c}{2\pi} \pm B/2$, but the pilot may be located at the edge of this band. The required pull-in range is then B/2; however, we will assume a design having a greater pull-in range by a factor n since pull-in time increases rapidly toward the extremes of the range. By manipulating several of the relations in Richman's article (Ref. 9) and assuming, for the system damping constant, the typical value $\zeta = \sqrt{2}/2$, the following result is obtained:

$$\varphi_{\infty m} = \frac{16}{3\pi n^2}\left[\frac{1}{T_F B}\right]^{1/3} = \frac{4}{3n^2} A \qquad (81)$$

where $\varphi_{\infty m}$ is the static phase error resulting from an initial (open-loop) frequency difference B/2 cps, and T_F is the time required to lock in from this maximum expected difference.

Equation (81) shows that $\varphi_{\infty m}$ can be made as small as desired, by making the pull-in range larger than necessary, while holding T_F and B, and consequently B_n, fixed. This can be done by simultaneously adjusting the open-loop gain and the ratio of the two filter time constants. Static phase error of the PLO is therefore not a serious problem; its contribution to overall error-rate can be made negligible in comparison with other factors. It is in fact theoretically possible to reduce static phase error to zero by means of a somewhat more complex automatic phase control system, but this does not seem worth while in the present case.

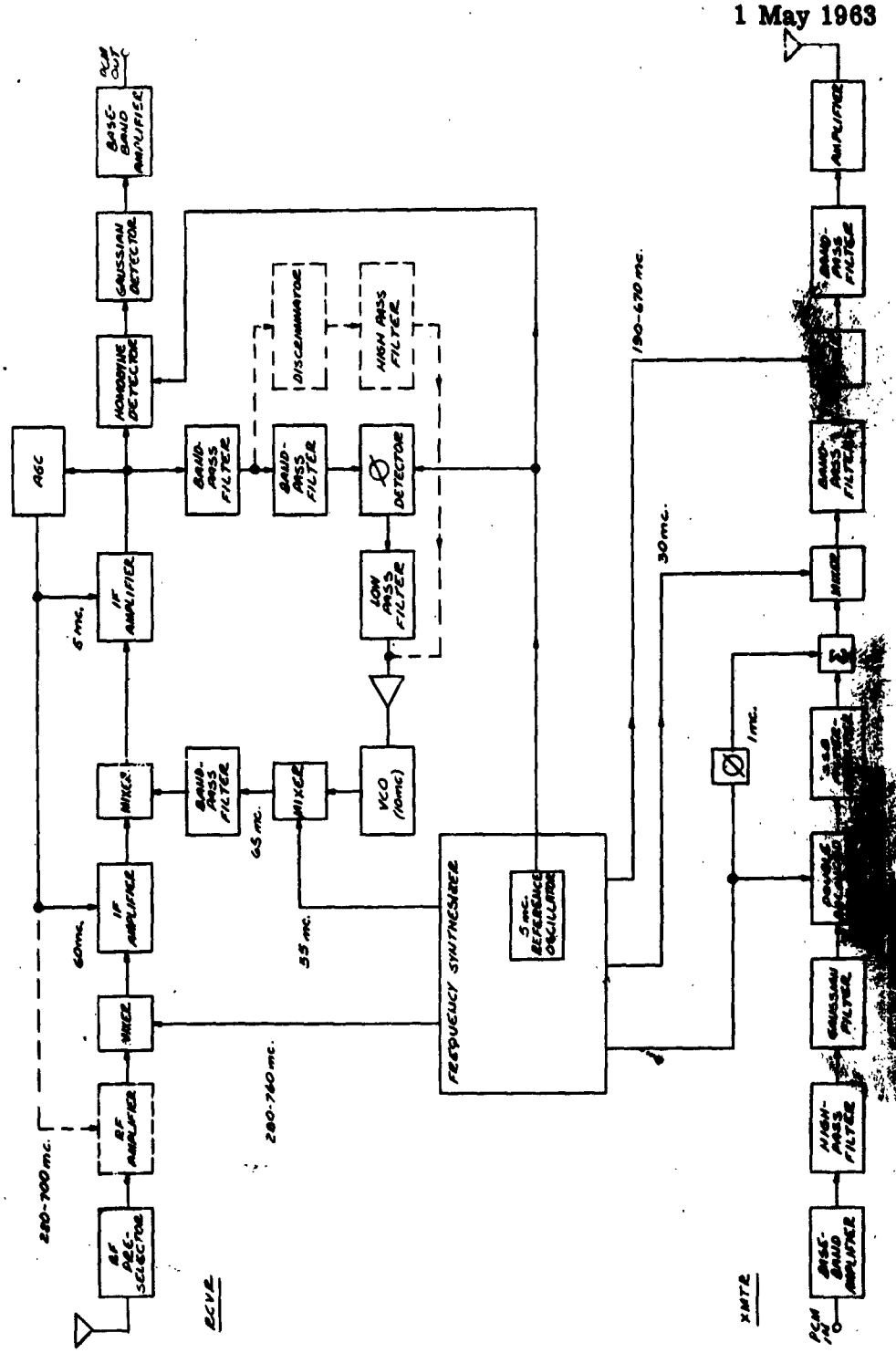

Figure 1. Block Diagram of Illustrative System

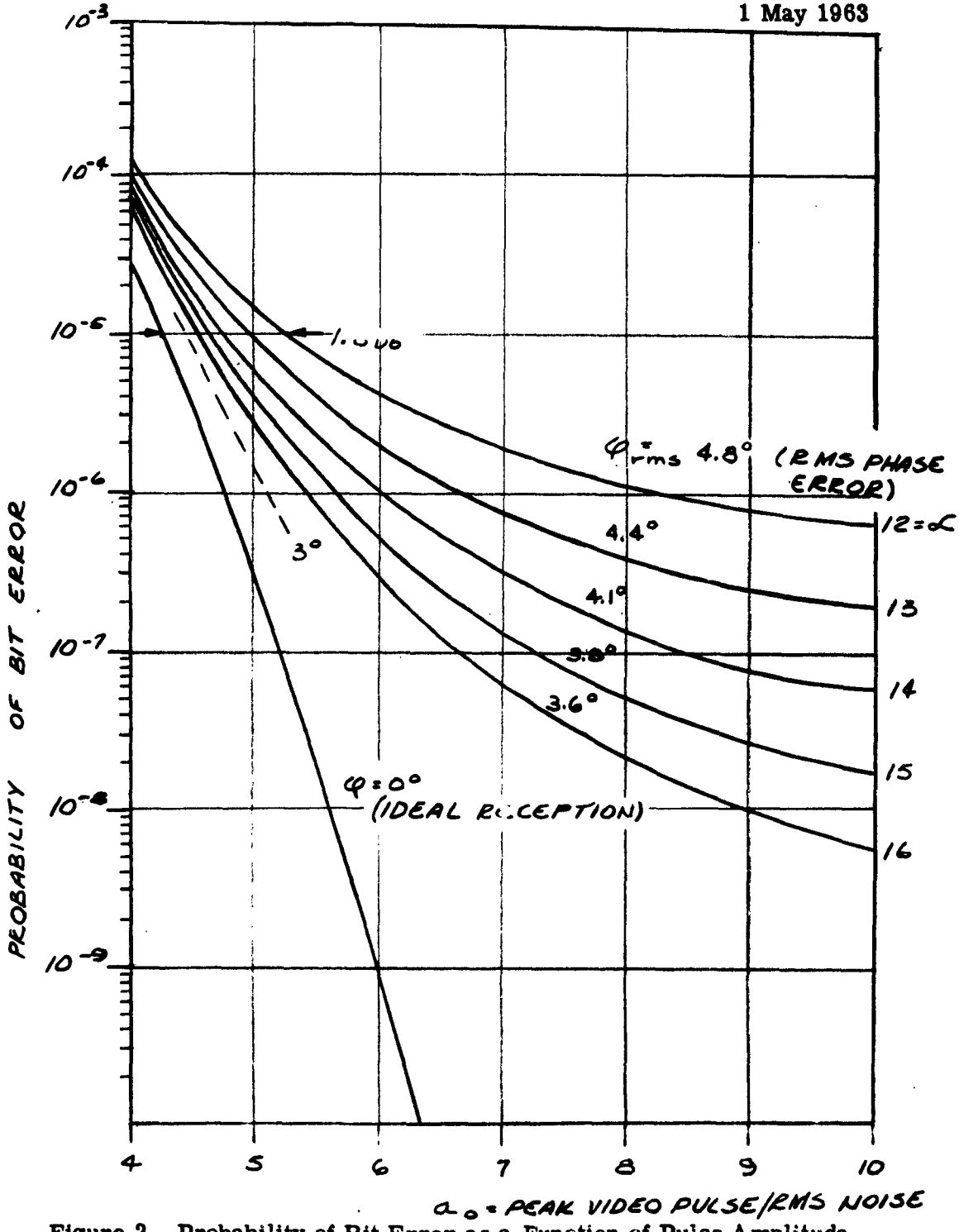

Figure 2. Probability of Bit Error as a Function of Pulse Amplitude with rms Phase Error as Parameter

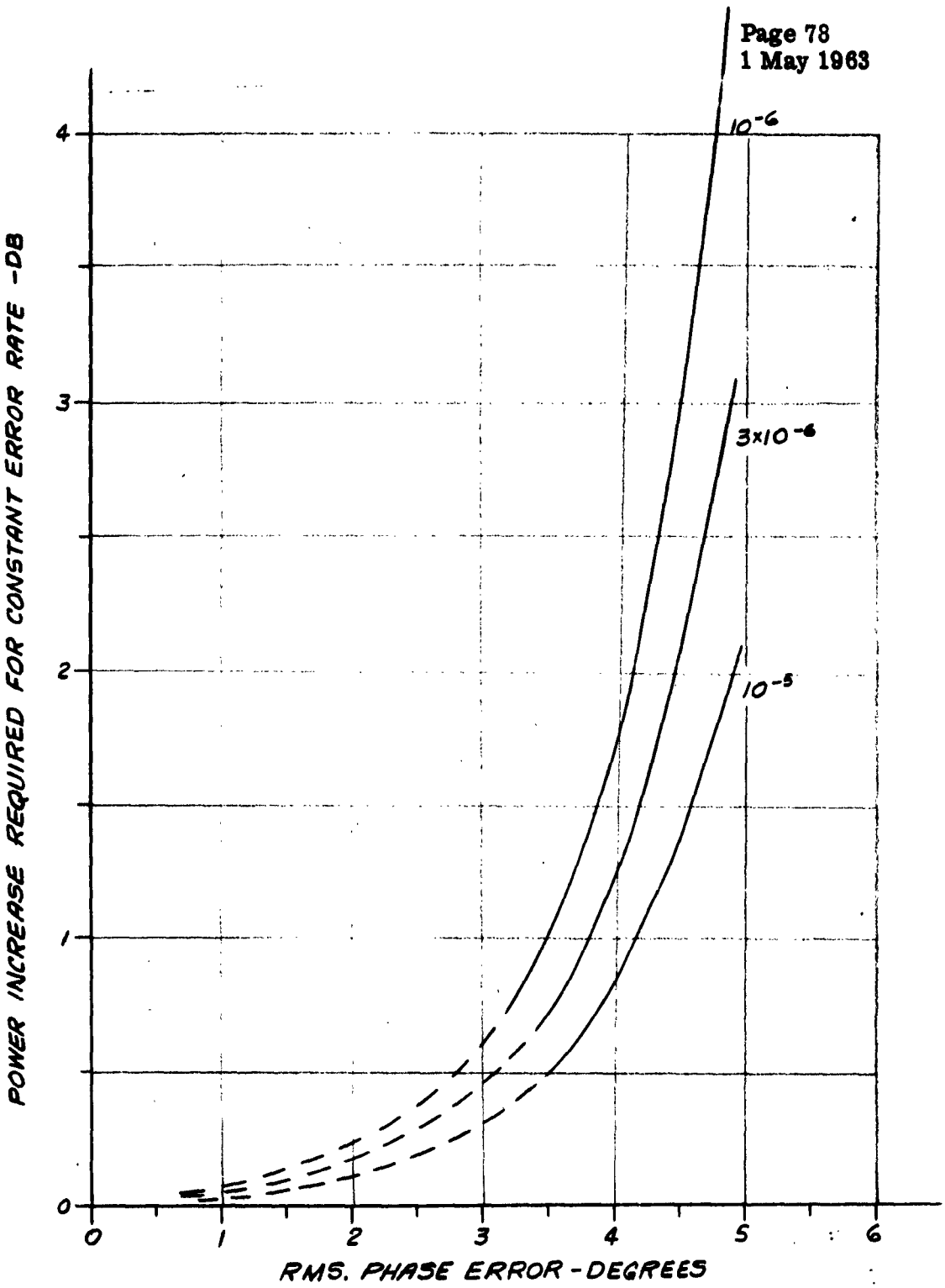

Figure 3. Power Increase Required for Constant Error Rate as a Function of rms Phase Error

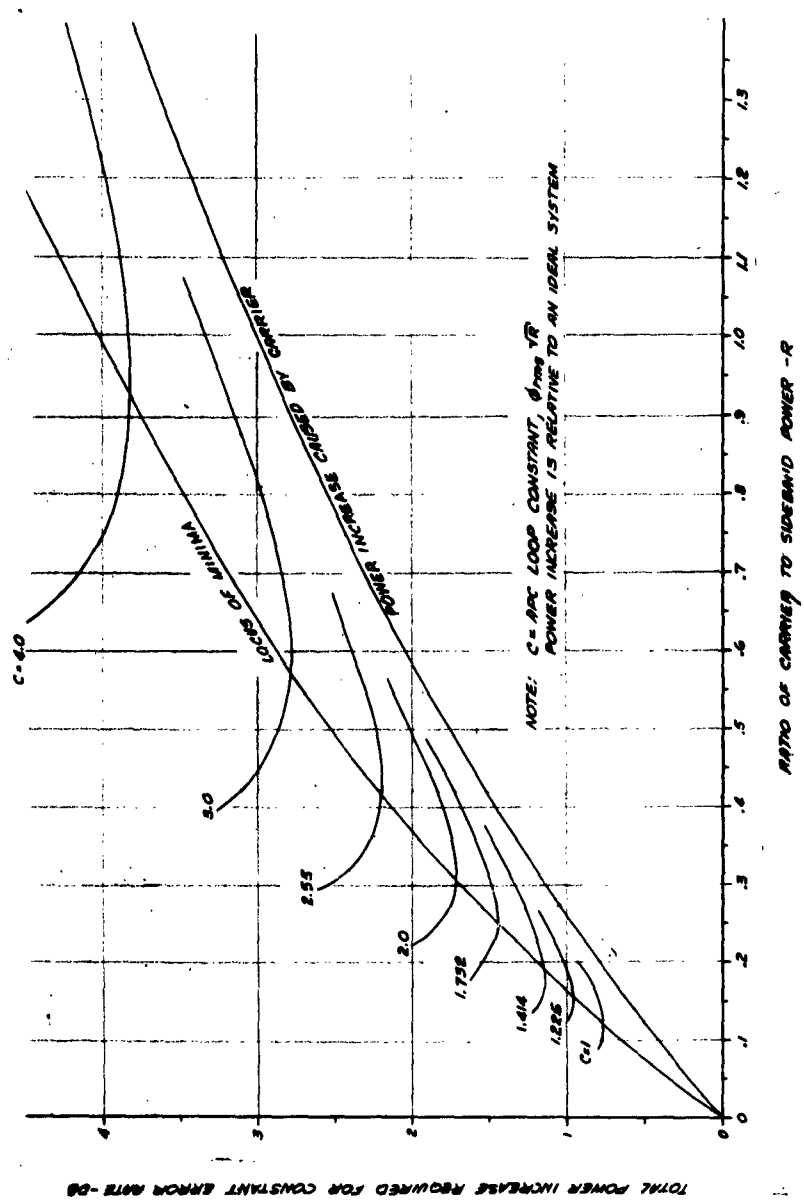

Figure 4. Total Power Increase Required to Maintain an Error Rate of 10^{-5}, as a Function of R

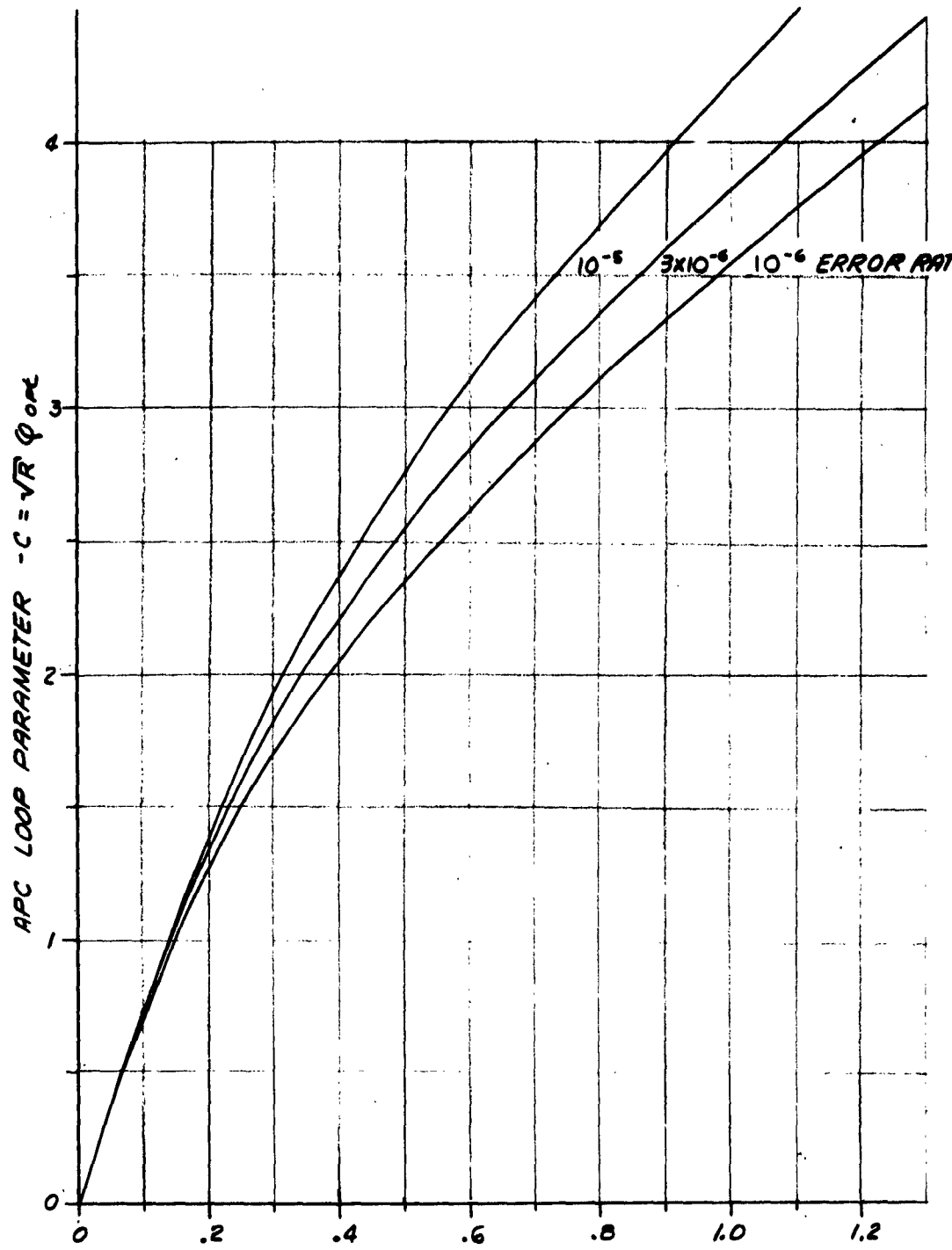

Figure 5. Optimum Value for the Ratio of Carrier to Sideband Power as a Function of an APC Loop Parameter, For a Specified Error Rate

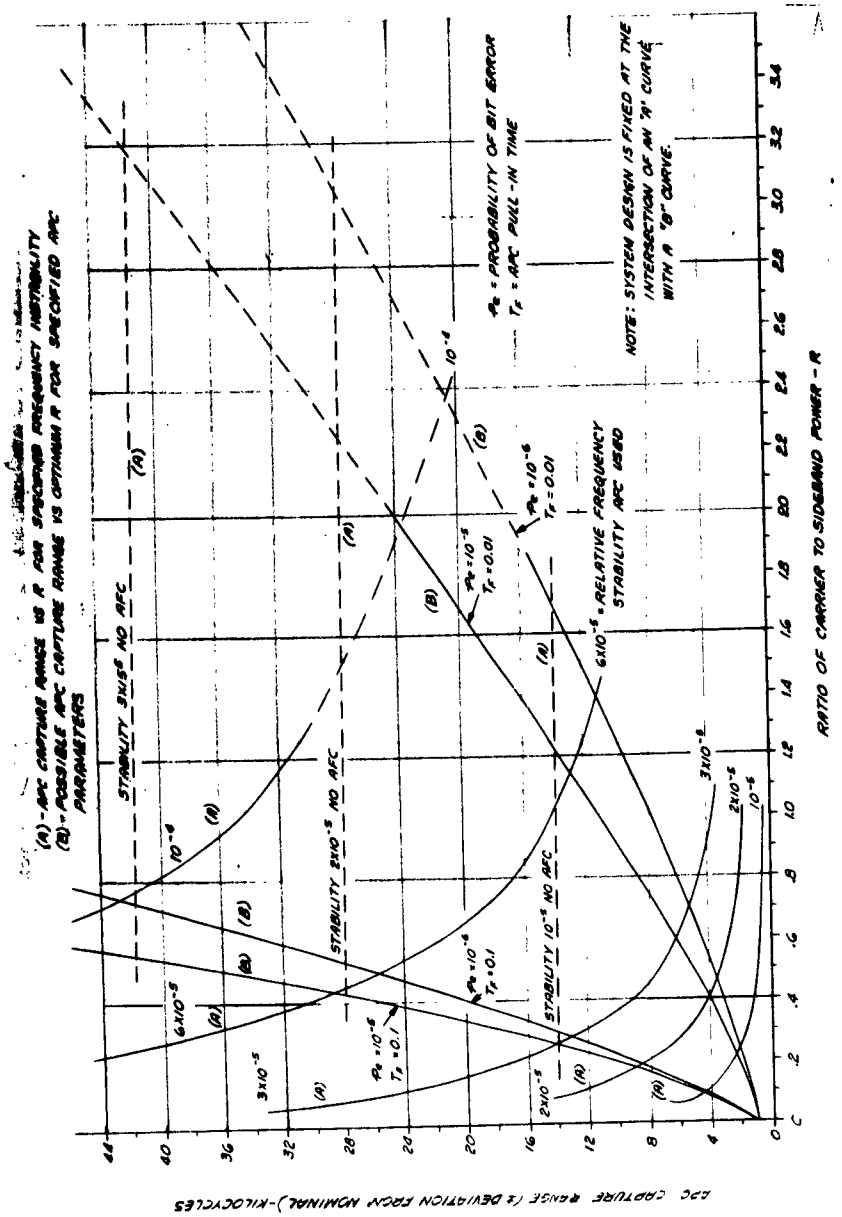

Figure 6. System Design Curves

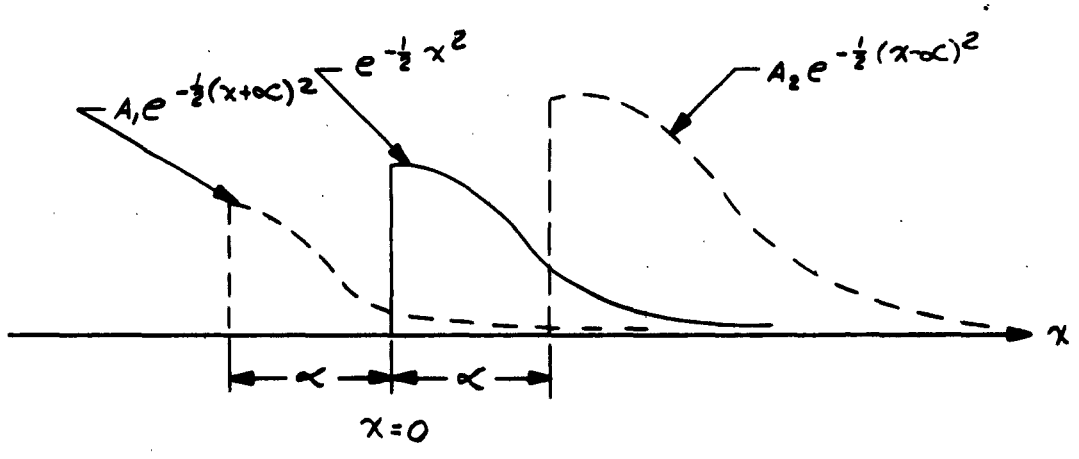

SSB CASE

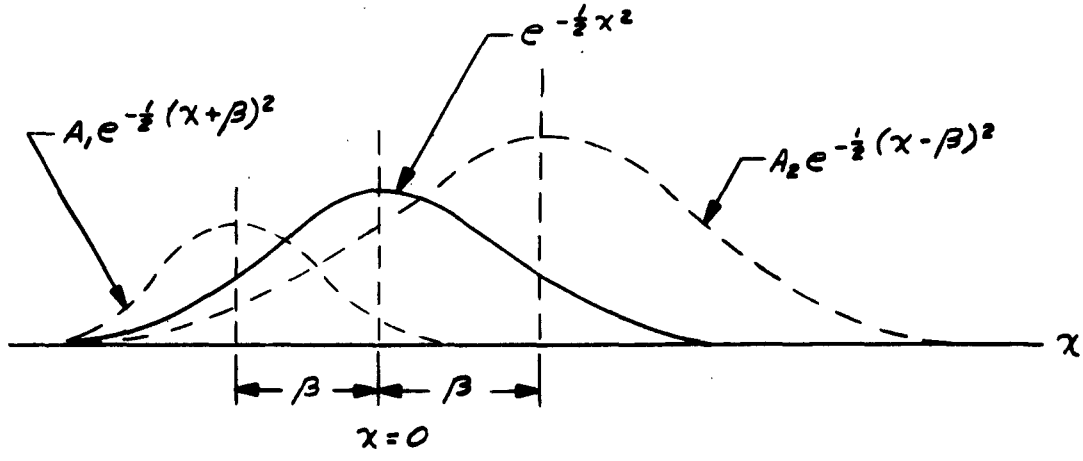

FM CASE

Figure 7. Adjacent Channel Interference

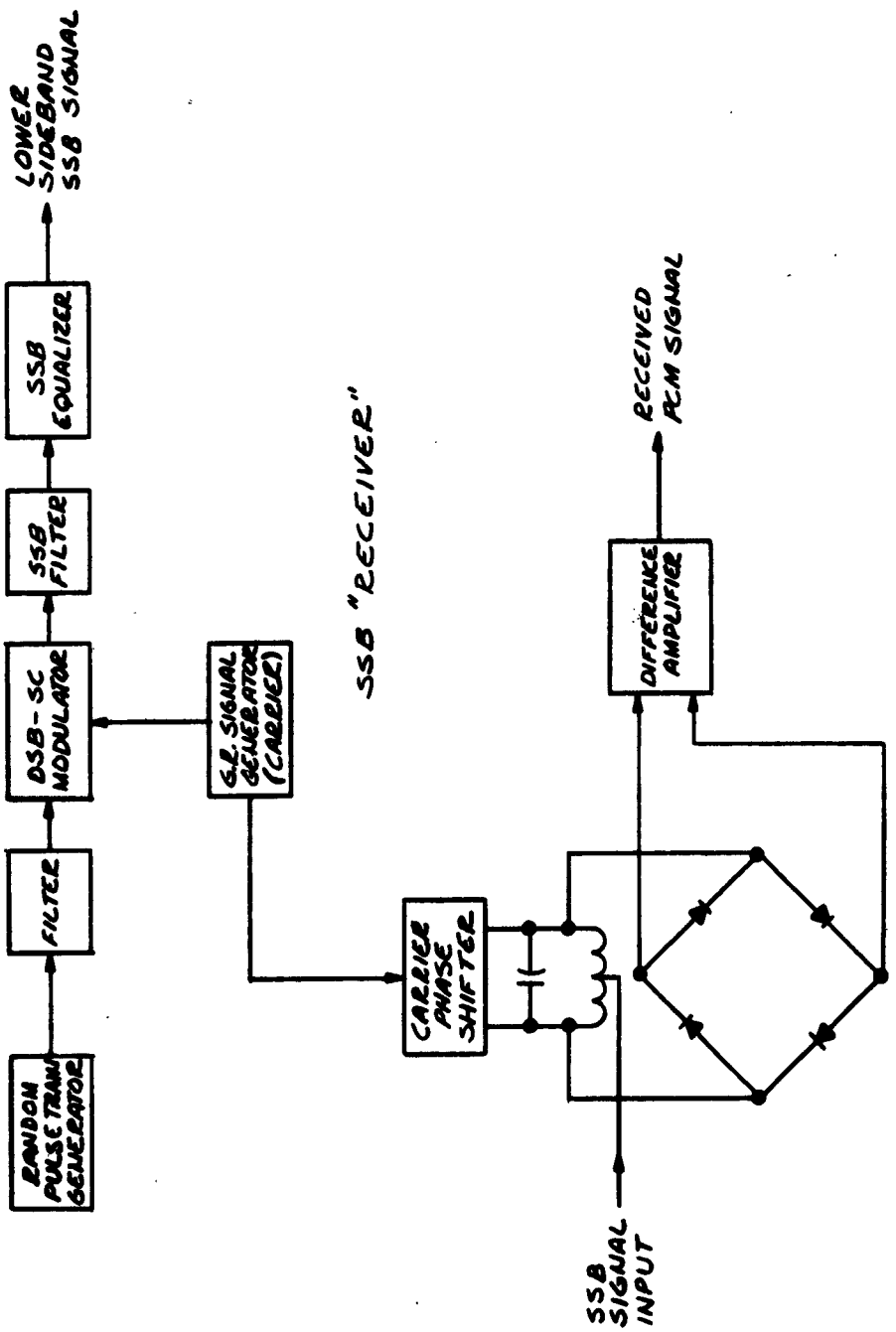

Figure 8. Block Diagram of Experimental System

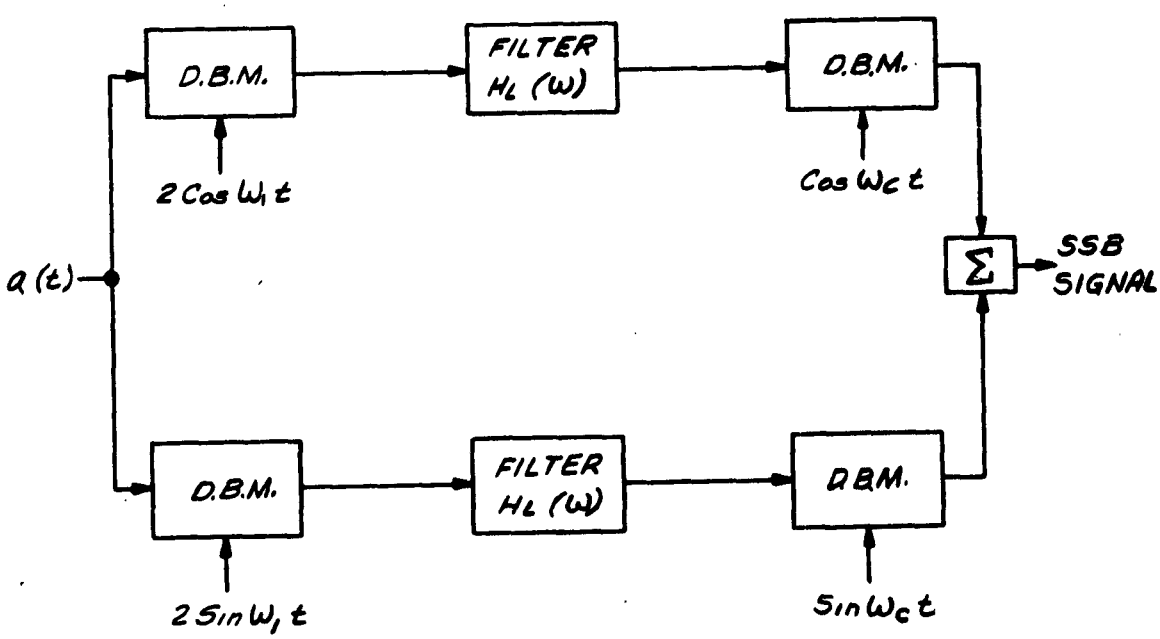

Figure 9. Weaver's "Third Method of SSB Generation"

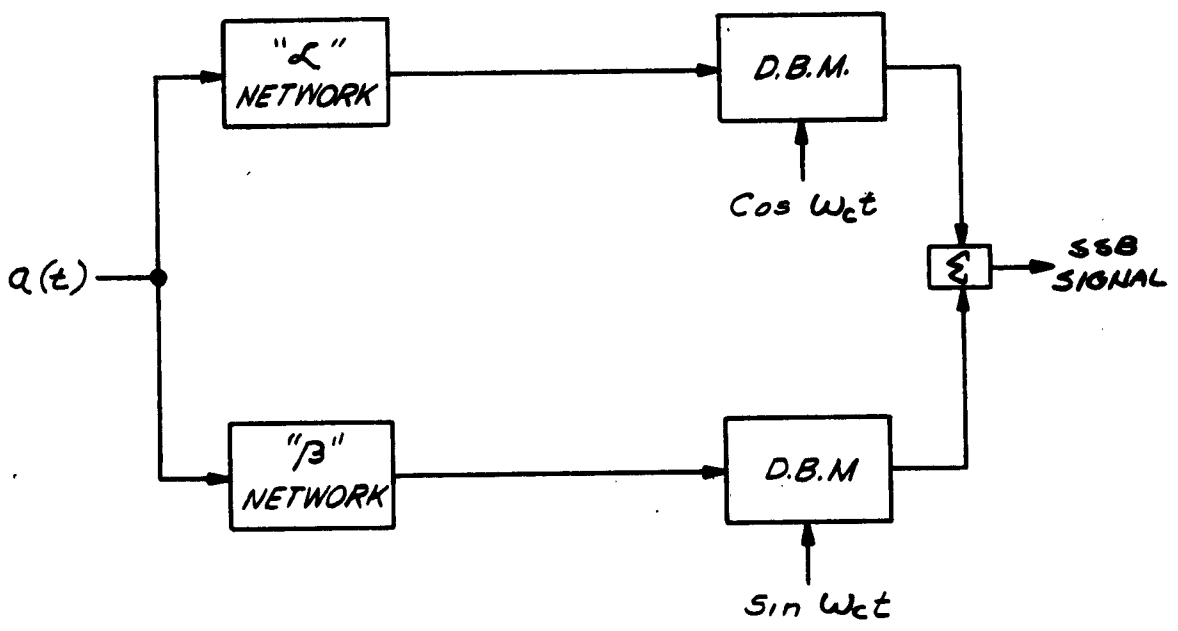

NOTE: PHASE OF "α" NETWORK MINUS PHASE OF "β" NETWORK IS APPROXIMATELY 90° AT ALL MODULATION FREQUENCIES

Figure 10. Phase Shift Method of SSB Generation

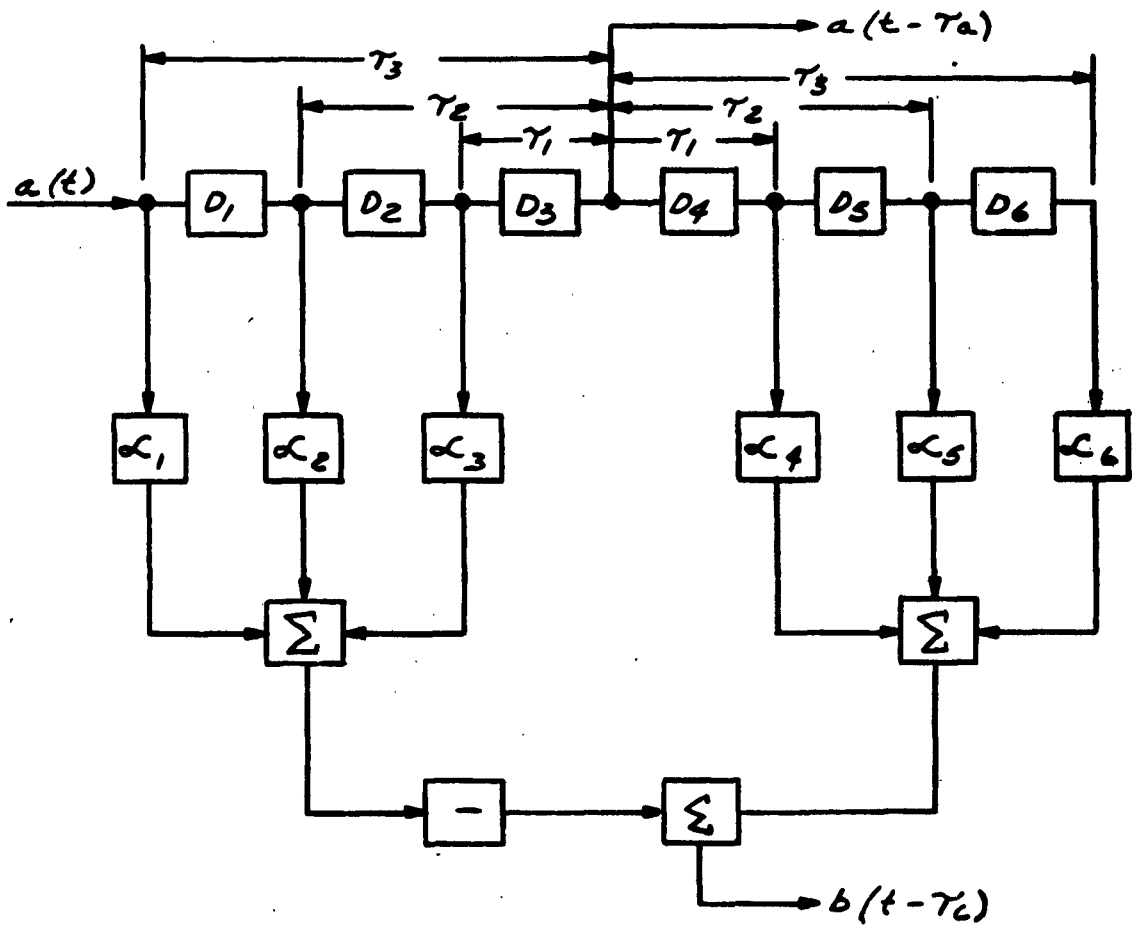

Figure 11. Delay Line Phase Shifter

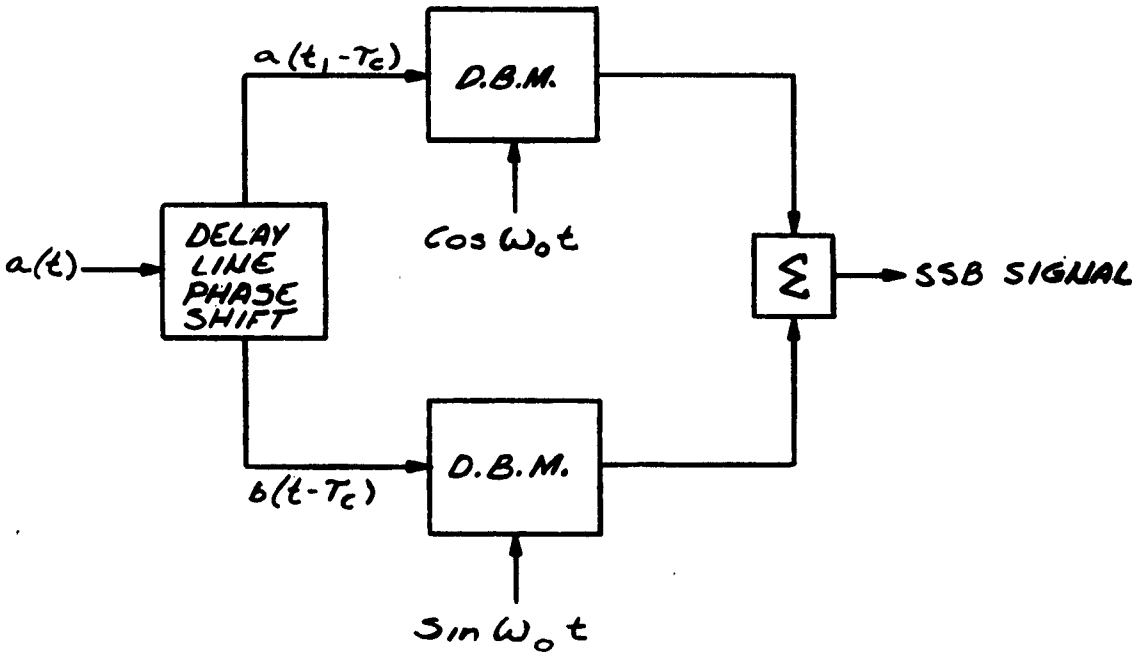

NOTE: $b(t-T_c)$ IS DERIVED FROM $a(t)$ BY SHIFTING THE PHASE OF EACH FREQUENCY COMPONENT OF $a(t-T_c)$ BY 90°, WHILE MAINTAINING APPROXIMATELY CONSTANT AMPLITUDE

Figure 12. SSB Generation Using a Delay Line Phase Shifter

NINTH ORDER CA ER FILTER:
50% REFLECTION FACTOR, MODULUS Q=86°

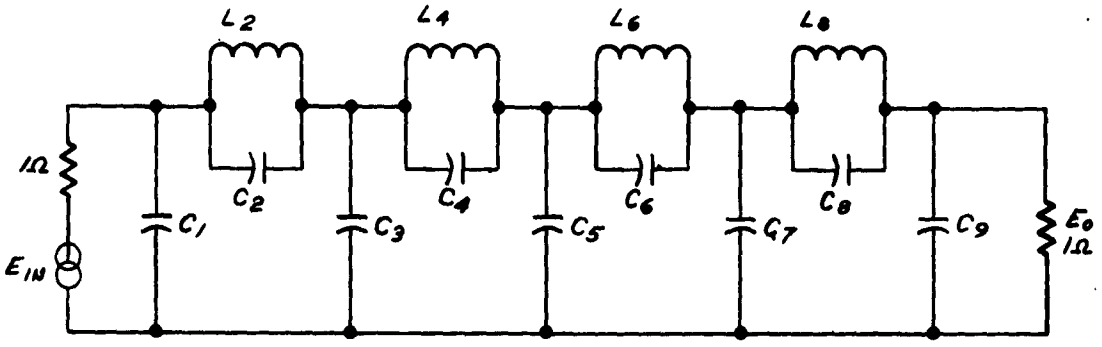

$$\frac{E}{E_0} = T(S) = \frac{\sum_0^9 a_n S^n}{\sum_0^9 b_n S^n}$$

TRANSFER FUNCTION

S IN MEGARADIANS

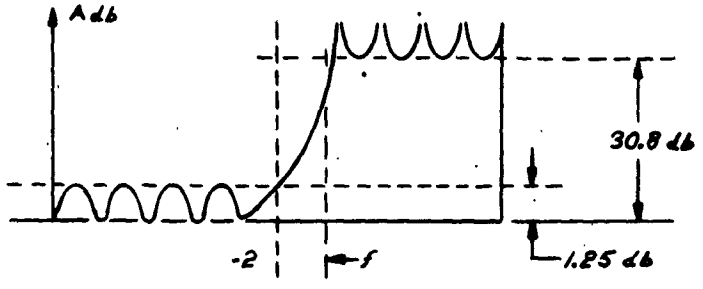

SCHEMATIC ATTENUATION

Subscript	C (F)	L (H)	a	b
0	-	-	2.0037430	1.0000
1	.2879	-	1.0218095	1.7117936×10^{-3}
2	.1152	.1125	3.2875877×10^{-1}	8.5590760×10^{-2}
3	.2120	-	1.442900×10^{-1}	1.0790901×10^{-4}
4	1.168	.02125	1.7648794×10^{-2}	2.6977622×10^{-3}
5	.05943	-	4.7367025×10^{-3}	2.2143592×10^{-6}
6	2.376	.0106	3.9156594×10^{-4}	3.6906328×10^{-5}
7	.1074	-	8.6098532×10^{-5}	1.4662904×10^{-3}
8	.5286	.0428	3.1128288×10^{-6}	$1.83286314 \times 10^{-2}$
9	.1614	-	5.8081886×10^{-7}	-

Figure 13. SSB Low-Pass Filter Design

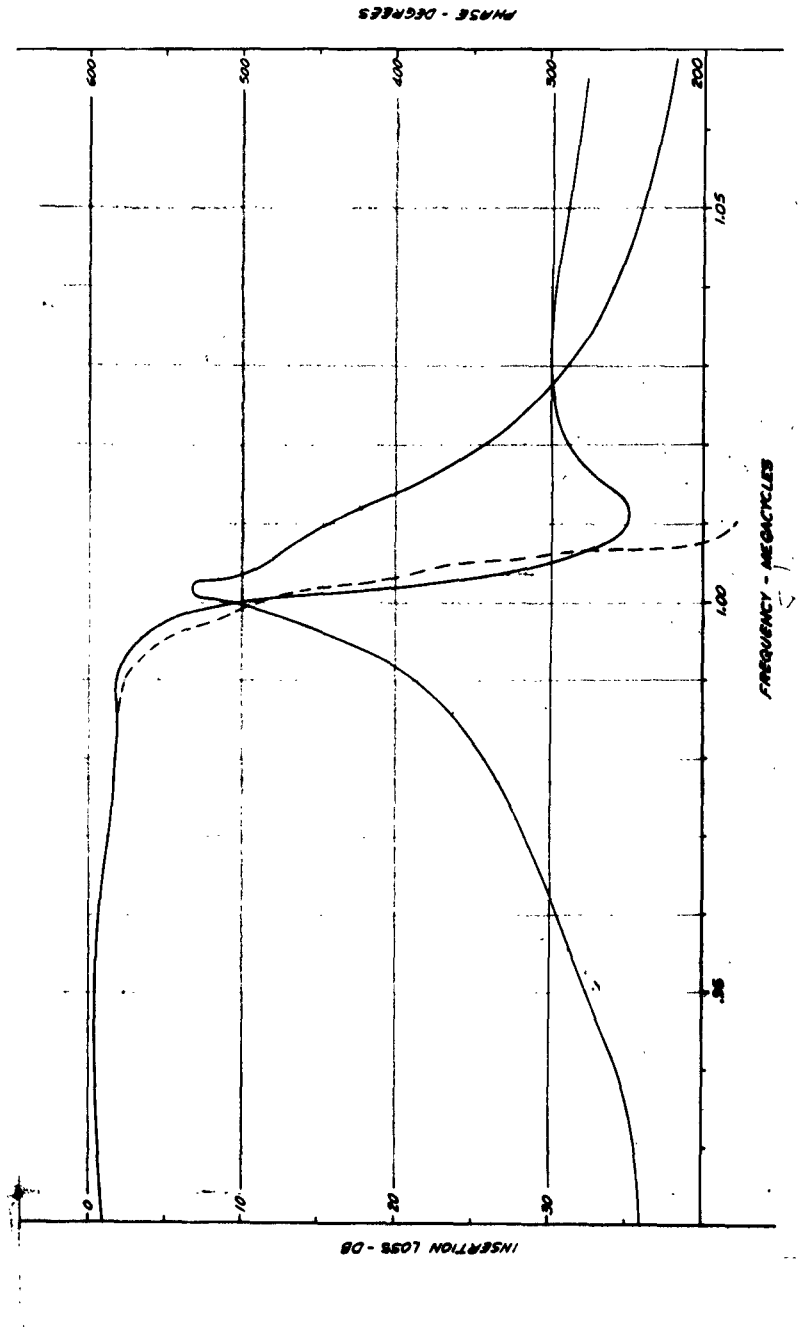

Figure 14. Calculated Response For SSB Low Pass Filter

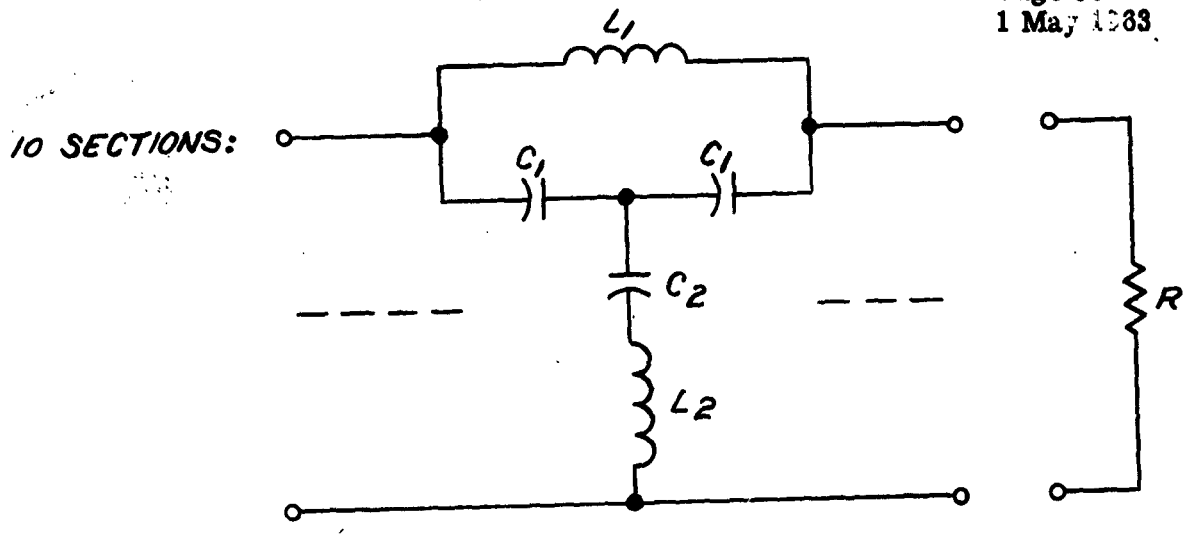

Section	L_1	L_2	C_1	C_2
1	24.48	2,875	5,750	24.53
2	8.16	7,582	15,160	8.162
3	5.684	10,958	21,916	4.965
4	16.39	2,981	5,962	16.42
5	3.564	12,290	24,580	3.564
6	15.54	2,535	5,070	15.56
7	4.576	7,853	15,710	4.576
8	4.270	7,626	15,250	4.271
9	12.56	2,397	4,794	12.57
10				

NOTE: INDUCTOR VALUES ARE IN MICROHENRIES.
CAPACITOR VALUES ARE IN PICOFARADS.

Figure 15. SSB Equalizer Design

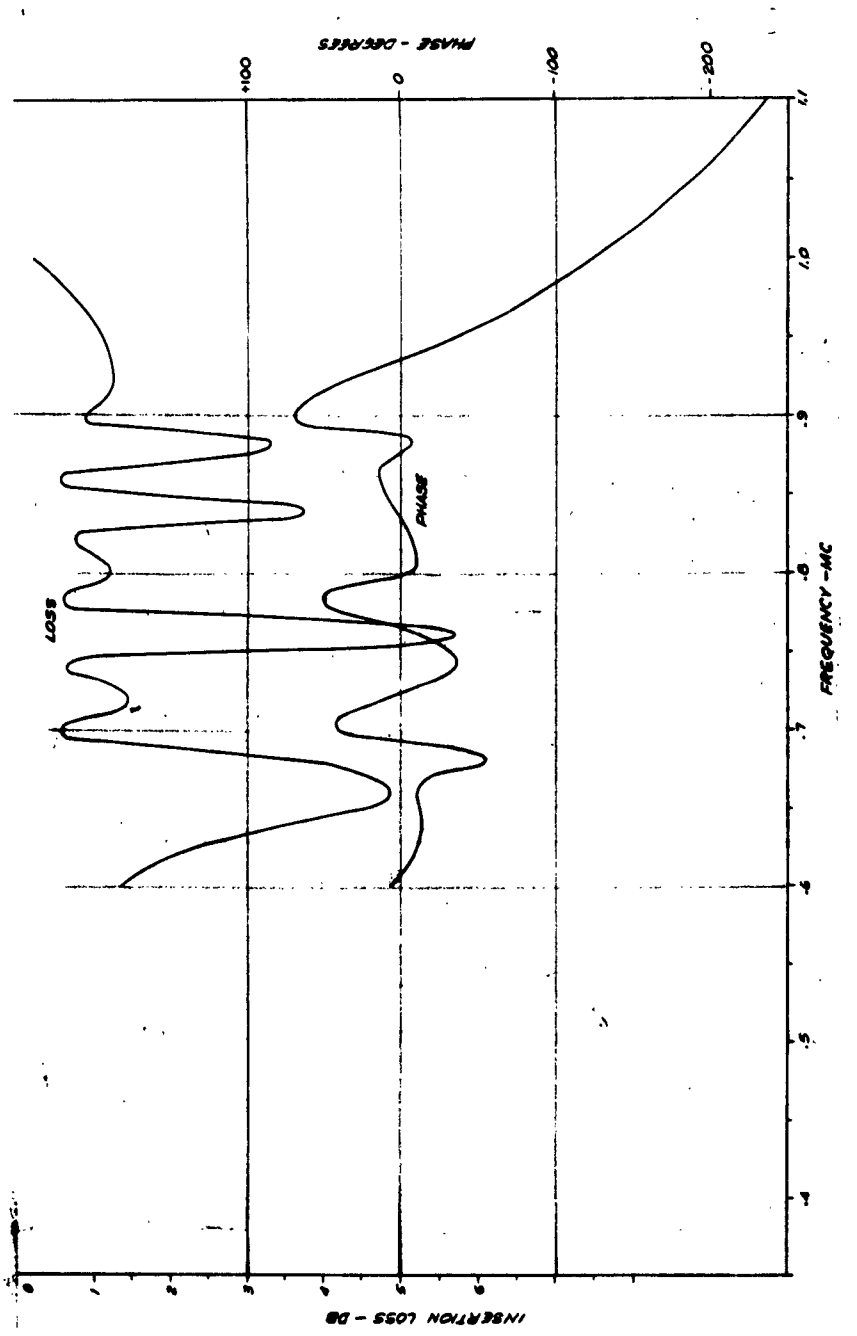

Figure 16. Calculated Response For Equalizer

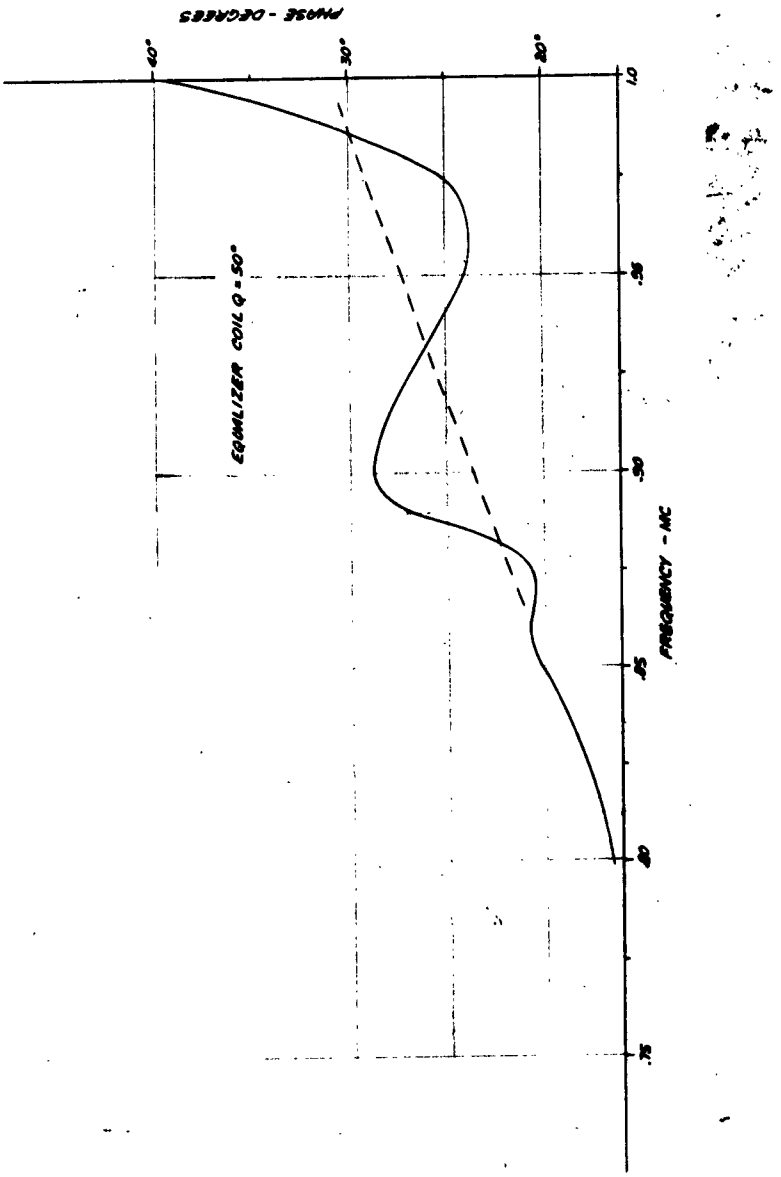

Figure 17. Calculated Phase Characteristics of Filter and Equalizer - Departure From Linear Phase

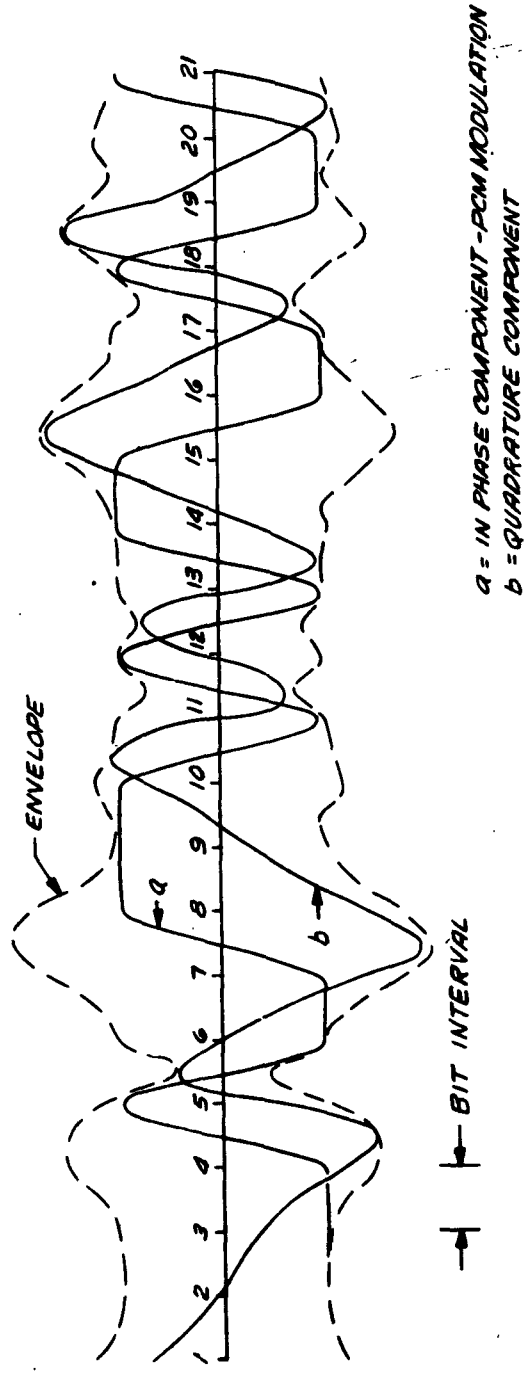

Figure 18. Component Waveforms in a PCM-SSB Signal

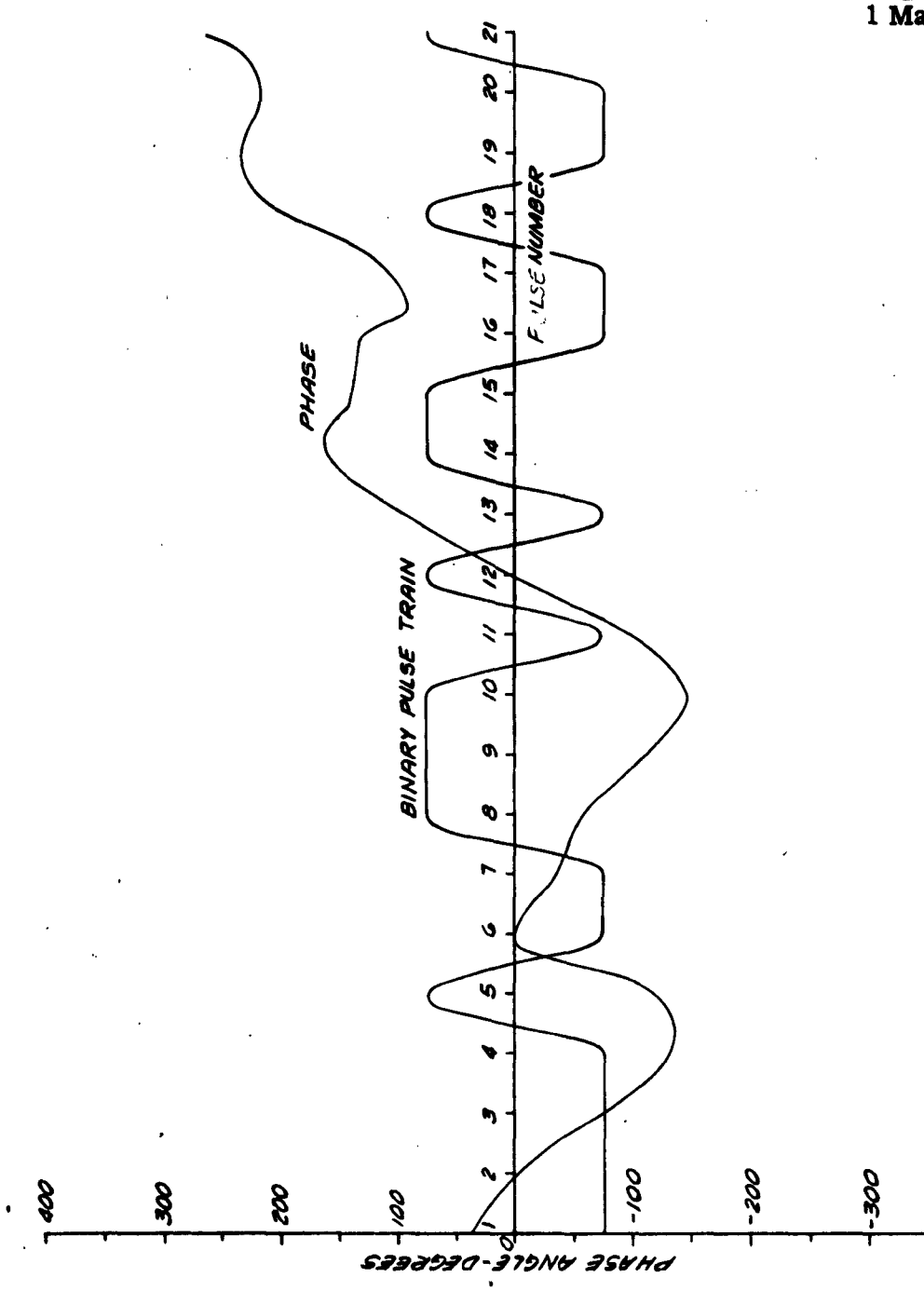

Figure 19. Phase Deviation From Linearly Increasing Phase For a SSB-PCM Binary Train - 21 Pulse Sample

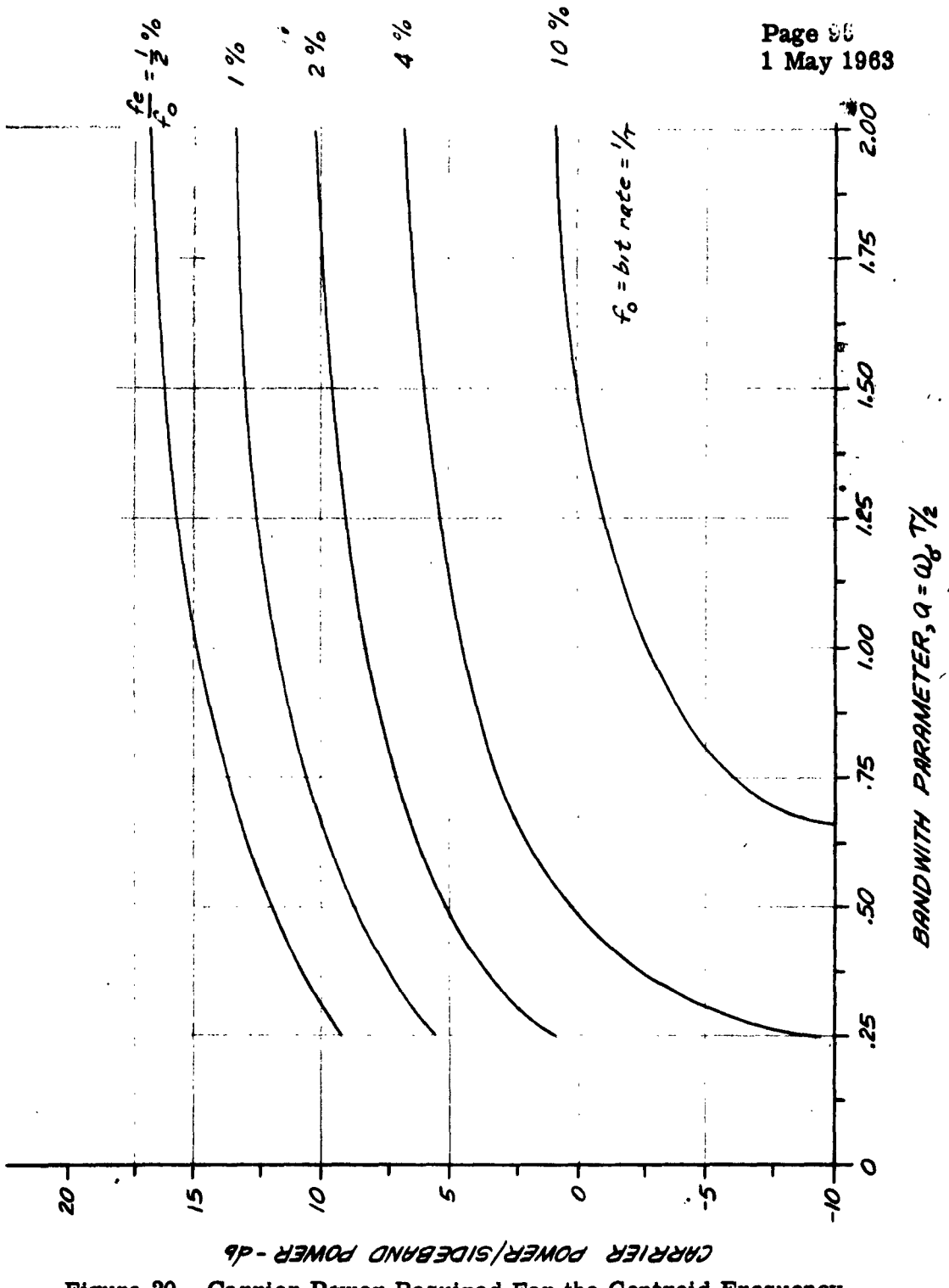

Figure 20. Carrier Power Required For the Centroid Frequency to be a Given Fraction of the Bit Rate, as a Function of Gaussian Bandwidth

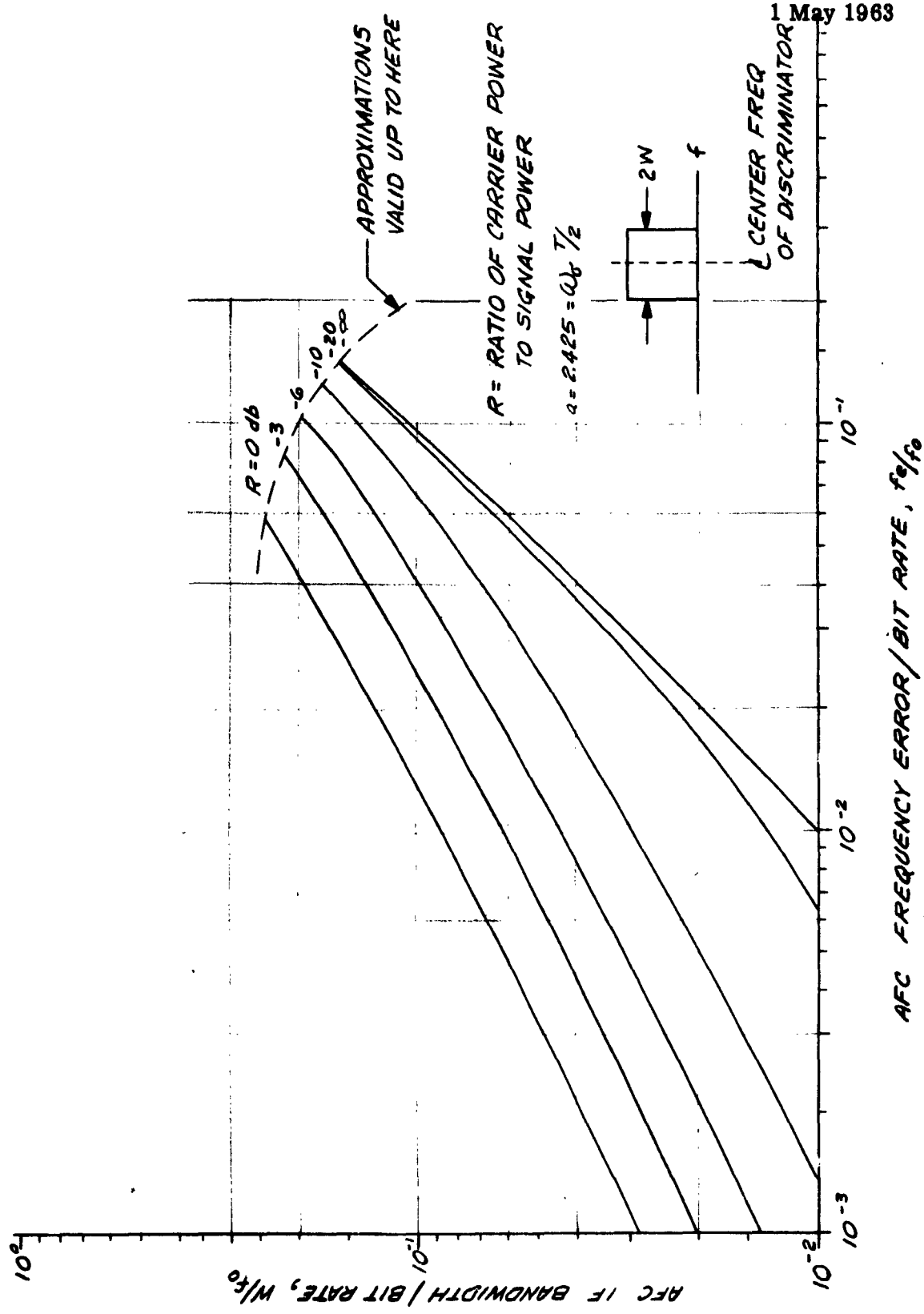

Figure 21. AFC Frequency Error as a Fu[illegible] Bandwidth

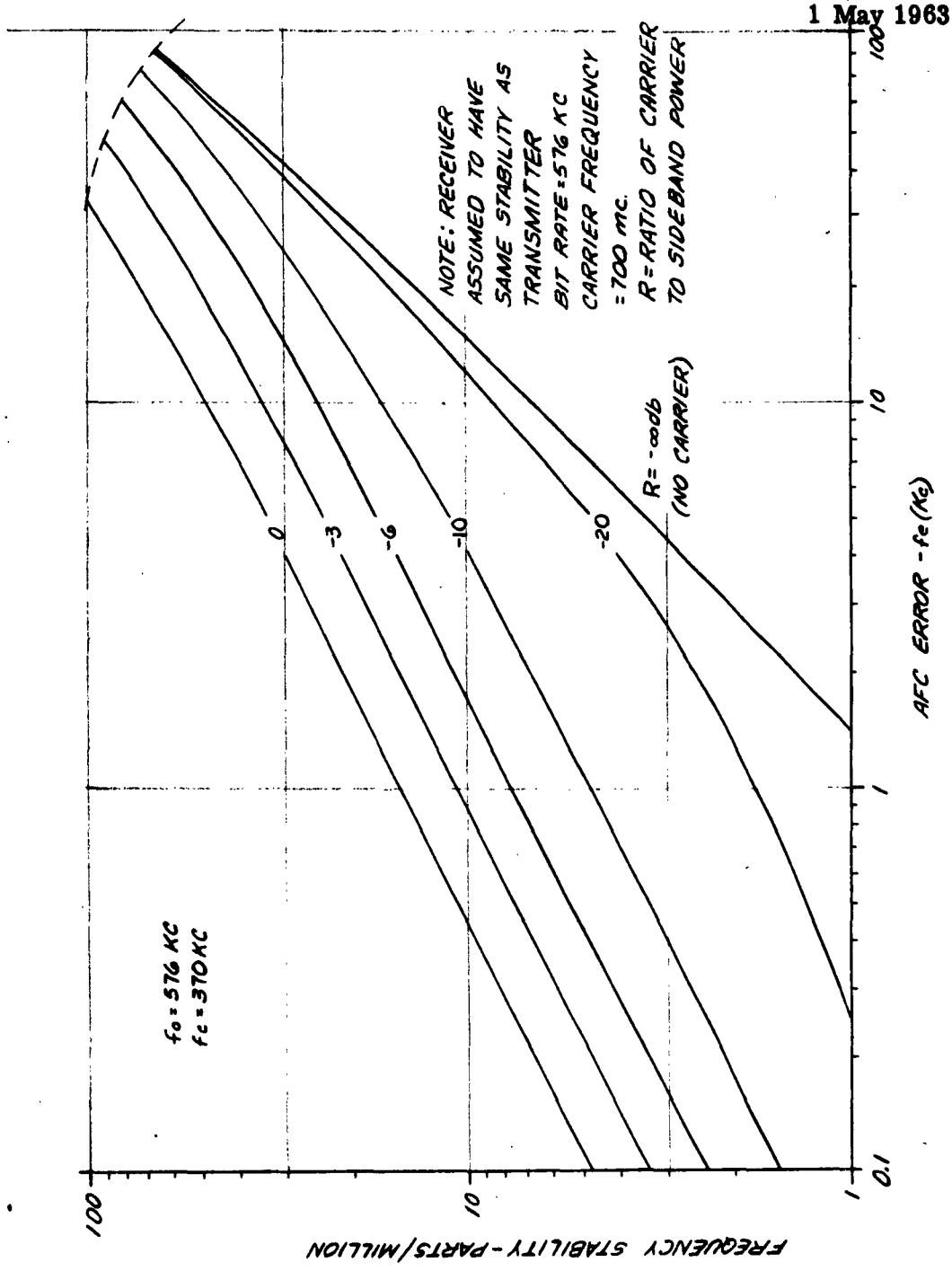

Figure 22. Frequency Stability of SSB Transmitter Required For a Specified AFC Frequency Error

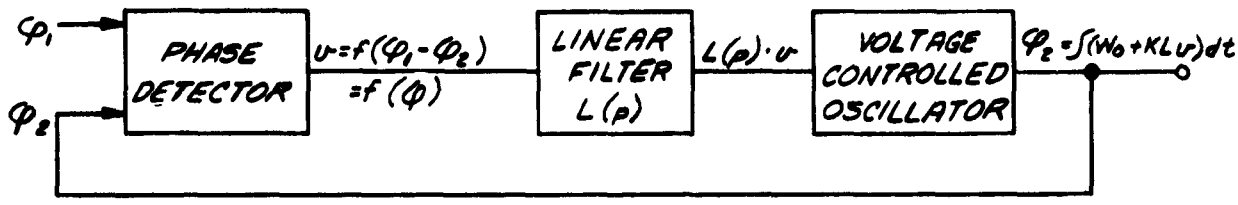

Figure 23. Phase Locked Oscillator, Block Diagram

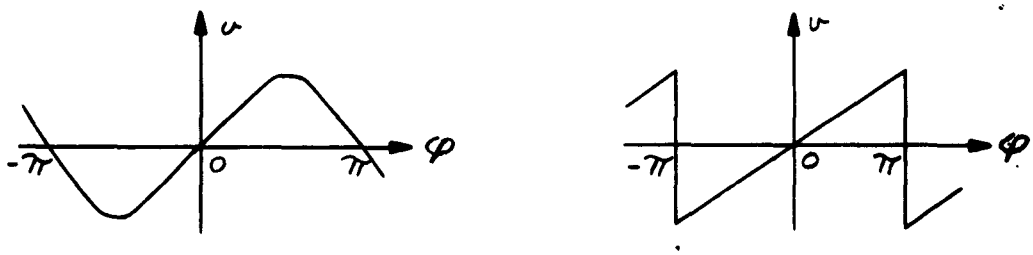

Figure 24. Phase Locked Oscillator, Phase Detector Characteristics

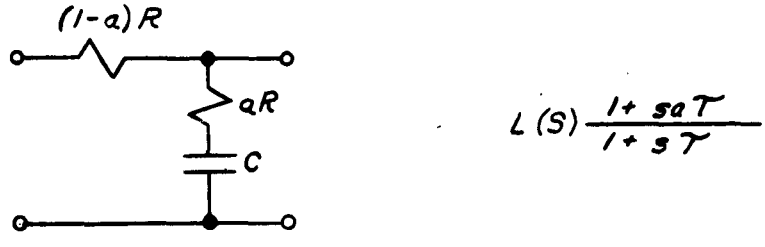

Figure 25. Phase Locked Oscillator, Low Pass Filter

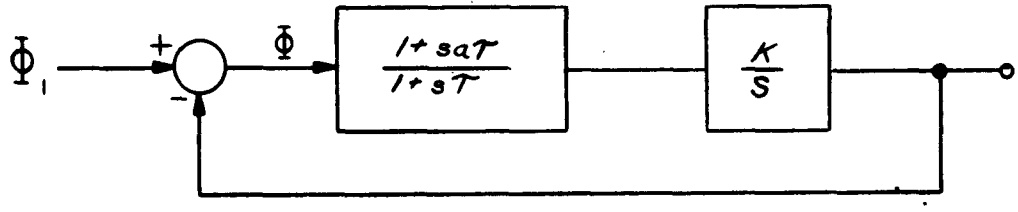

Figure 26. Phase Locked Oscillator, Equivalent Servo Block Diagram

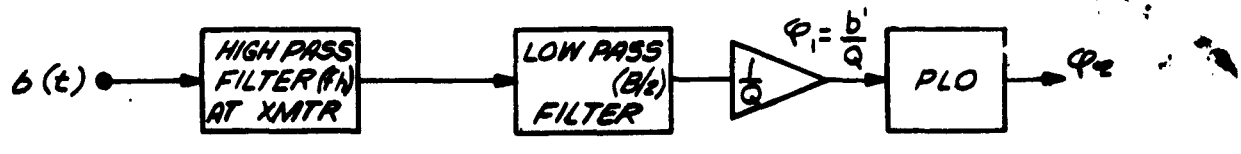

Figure 27. Signal Path in PLO Circuit

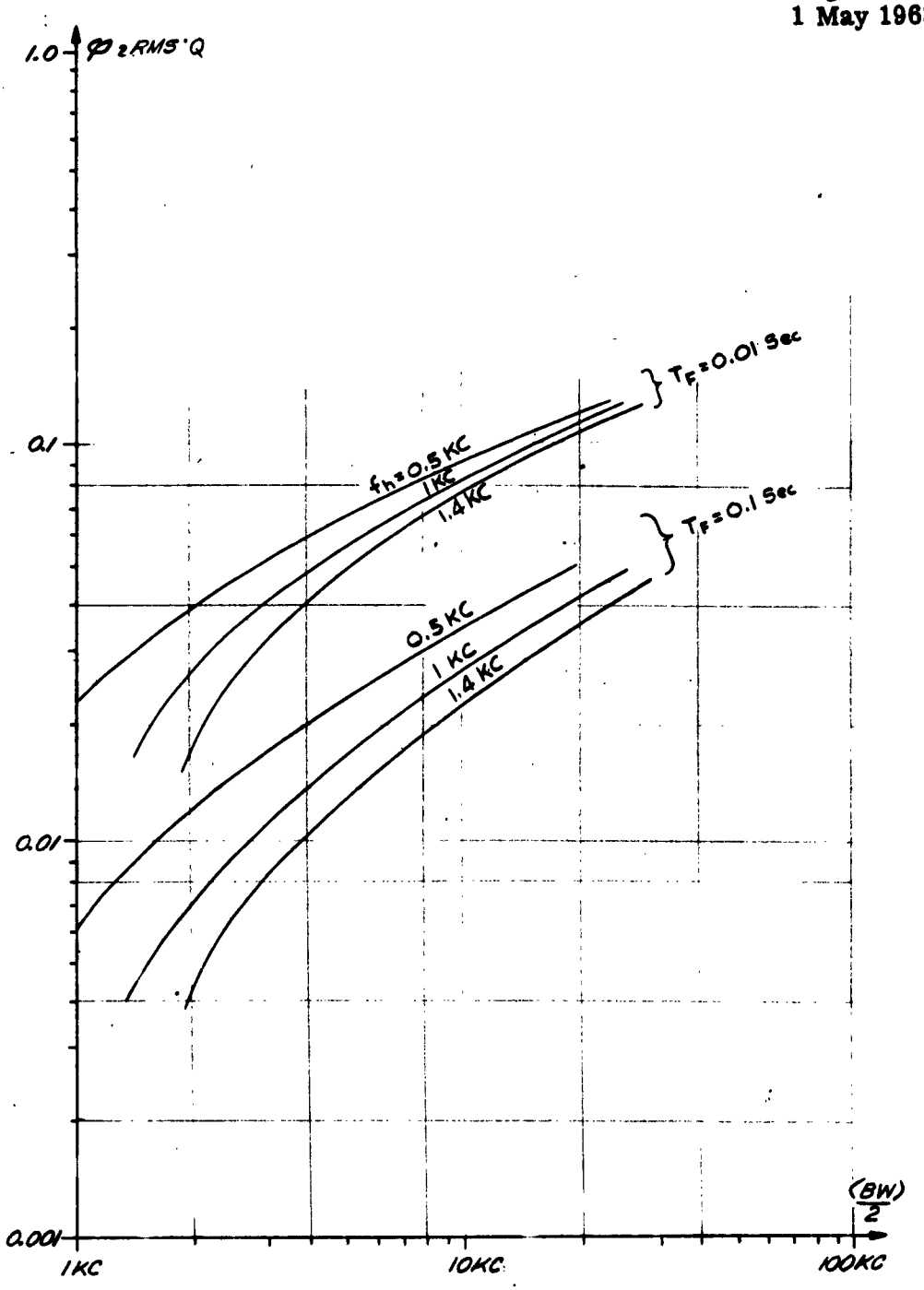

Figure 28. APC Capture Range as a Function of the Parameter $\varphi_{rms} \times Q$

APPENDIX A

MATHEMATICAL METHODS AND NOTATION

A. 1 FOURIER TRANSFORMS AND FREQUENCY TRANSLATION

In this report the principle mathematical tools are based on Fourier transforms methods. The Fourier transform is defined as:

$$F(\omega) = \int_{-\infty}^{\infty} f(t)\, e^{-j\omega t}\, dt$$

$$f(t) = \frac{1}{2\pi} \int_{-\infty}^{\infty} F(\omega)\, e^{j\omega t}\, dw \qquad w = 2\pi f$$

In conventional circuit analysis the symbol, f, is reserved for the real frequency of a sinusoid. Although we maintain this convention, in some discussions the term frequency is also used to refer to angular rate, w. Frequently we are concerned with the transform of the function $2f(t)\cos[\omega_0 t + \theta]$ This is readily found by using the substitution:

$$2\cos[\omega_0 t + \theta] = e^{j[\omega_0 t + \theta]} + e^{-j[\omega_0 t + \theta]}$$

Thus:

$$F_T(\omega) = \int_{-a}^{\infty} f(t) e^{j(\omega_0 t + \theta)} e^{-j\omega t}\, dt + \int_{-\infty}^{\infty} f(t) e^{-j(\omega_0 t + \theta)} e^{-j\omega t}\, dt$$

(A.1)

$$F_T(\omega) = e^{j\theta} F(\omega - \omega_0) + e^{-j\theta} F(\omega + \omega_0)$$

If the signal $2f(t)\cos(\omega_0 t+\theta)$ is filtered by a filter having a transfer function $H(\omega)$, the spectrum of the result is simply equation (A. 1) multiplied by $H(\omega)$. When $H(\omega)$ is a high-pass or low-pass filter having a cutoff frequency near f_0 the result is an essentially single sideband signal. When this signal is multiplied, at the receiver by $2\cos(\omega_0 t+\beta)$ the result, by application of equation (A. 1), is:

$$\begin{aligned} F_{T_D} &= e^{j\beta}\left[F_T(\omega-\omega_0)H(\omega-\omega_0)\right]+e^{-j\beta}\left[F_T(\omega+\omega_0)H(\omega+\omega_0)\right] \\ &= e^{j\beta}\left[\{e^{j\theta}F(\omega-2\omega_0)+e^{-j\theta}F(\omega)\}H(\omega-\omega_0)\right] \\ &+ e^{-j\beta}\left[\{e^{j\theta}F(\omega)+e^{-j\theta}F(\omega+2\omega_0)\}H(\omega+\omega_0)\right] \end{aligned} \qquad \text{(A.2)}$$

$$\begin{aligned} F_{T_D} &= F(\omega)\left[e^{-j(\beta-\theta)}H(\omega-\omega_0)+e^{-j(\beta-\theta)}H(\omega+\omega_0)\right] \\ &+ F(\omega+2\omega_0)\left[e^{j(\beta+\theta)}H(\omega-\omega_0)+e^{-j(\beta+\theta)}H(\omega+\omega_0)\right] \end{aligned}$$

Equation (A. 2) is the mathematical result of coherent detection of an SSB signal. In practice $F(\omega+2\omega_0)$ is negligible except for frequencies near $2\omega_0$, and is filtered out by the equipment used to amplify and process the detected signal. For these reasons the second term in equation (A. 2) may be ignored. The spectrum of the signal which is received by coherent detection is, consequently:

$$F_R(\omega)=F(\omega)\left[e^{j(\beta-\theta)}H(\omega-\omega_0)+e^{-j(\beta-\theta)}H(\omega+\omega_0)\right] \qquad \text{(A.3)}$$

A.2 THE SSB SIGNAL

It was shown in paragraph A. 1, that a modulating signal, f(t), after multiplication by a carrier, $2\cos\omega_o t$, has a spectrum:

$$F_T(\omega) = F(\omega-\omega_o) + F(\omega+\omega_o)$$

If this signal is passed through an ideal low-pass filter with cutoff frequency at ω_o , the result is an SSB signal. The waveform of this SSB signal is calculated as:

$$r(t) = \frac{1}{2\pi}\int_{-\omega_o}^{+\omega_o} \left[F(\omega-\omega_o)+F(\omega+\omega_o)\right] e^{j\omega t}\, d\omega \qquad \text{(A.4)}$$

After a simple change of variable and substitution of $e^{jx} = \cos x + j\sin x$, one obtains:

$$r(t) = \cos\omega_o t \left\{\frac{1}{2\pi}\int_{-2\omega_o}^{+2\omega_o} F(u) e^{jut}\, du\right\}$$
$$+\sin\omega_o t \left\{\frac{1}{2\pi}\left[j\int_{-2\omega_o}^{0} F(u)e^{jut}\,du - j\int_{0}^{2\omega_o} F(u)e^{jut}\,du\right]\right\} \qquad \text{(A.5)}$$

The coefficient of $\cos\omega_o t$ is identical with f(t), if f(t) is bandlimited to twice the first conversion frequency. In practice this will always be the case.

The coefficient of $\sin\omega_o t$ is the Fourier transform of the spectrum of f(t) modified by a factor -j for positive ω , and +j for negative ω . This modification of the spectrum of f(t) is identical to a 90° phase lag for all frequencies, and can be used to define the Hilbert transform relation. The resulting time function will be referred to as the quadrature function $\hat{f}(t)$. Thus equation (A. 5) is written more simply:

$$r(t) = f(t)\cos\omega_o t + \hat{f}(t)\sin\omega_o t \qquad \text{(A.6)}$$

The equation can be expanded to a more useful explicit form by using the substitution:

$$e^{j(\beta-\theta)} = e^{j\varphi} = \cos\varphi + j\sin\varphi$$

The parameter, φ, is simply the difference in phase between the transmitted and locally generated carrier, and ordinarily is the error in phase detection. Equation (A.3) can then be written:

$$F_R(\omega) = \cos\varphi\, F(\omega)\left[H(\omega-\omega_0)+H(\omega+\omega_0)\right] + \sin\varphi\, F(\omega)\left[jH(\omega-\omega_0)-jH(\omega+\omega_0)\right] \qquad (A.7)$$

This is a fundamental equation which describes the spectrum of the signal which is received after double sideband suppressed carrier modulation, sideband filtering, and coherent reception by a local carrier having phase error, φ. The equation applies equally well to DSB, SSB, VSB transmission. To obtain the time waveform of the received signal Fourier transform the coefficients of cos φ, and sin φ which are constants. Thus, the received waveform is:

$$r(t) = a(t)\cos\varphi + b(t)\sin\varphi$$

$$\text{WHERE: } a(t) = \frac{1}{2\pi}\int_{-\infty}^{\infty}\frac{1}{4}F(\omega)\left[H(\omega-\omega_0)+H(\omega+\omega_0)\right]d\omega \qquad (A.8)$$

$$b(t) = \frac{1}{2\pi}\int_{-\infty}^{\infty}\frac{j}{4}F(\omega)\left[H(\omega-\omega_0)-H(\omega+\omega_0)\right]d\omega$$

A.3 THE AVERAGE POWER SPECTRUM OF A RANDOM PULSE TRAIN

In this report we are generally considering a full baud NRZ pulse train after gaussian filtering. The voltage density spectrum for a single full baud pulse of unit amplitude is obtained as follows:

$$F(\omega) = \int_{-T/2}^{T/2} e^{-j\omega t}\,dt = T\,\frac{\sin\omega T/2}{\omega T/2} \qquad (A.9)$$

Note that $F(\omega)$ is zero for $\omega T/2 = k\pi, k = 1, 2, \ldots$. Thus, at frequencies which are multiples of the pulse rate there is no energy, and this result is true after any subsequent linear filtering.

A pulse train can be expressed mathematically by:

$$f(t) = \sum_{n=-\infty}^{\infty} \alpha_n f(t - nT) \tag{A.10}$$

For a binary train, the coefficients α_n can have either of the values + 1 or - 1. When these values are selected at random, and each selection is independent of all others, the train is referred to as a random, binary train. Usually it is assumed that the probability of α_n being + 1 is 1/2 so that the train has a zero average value, i.e., is unbiased.

For any particular finite pulse train the spectrum of f(t) may be extremely complicated. For may purposes, however, the average power spectrum of f(t) is sufficient, and it has a relatively simple form. In general, average power spectrum is defined as the Fourier transform of the autocorrelation function:

$$r(\tau) = \lim_{N \to \infty} \frac{1}{2NT} \int_{-NT}^{NT} f(t - \tau) f(\tau) \, dt$$

It can be shown (Ref. 3, page 221) that the average power spectrum of an unbiased random pulse train is:

$$|S(\omega)|^2 = \frac{A}{T} |F(\omega)|^2 \tag{A.11}$$

where: $F(\omega)$ is the Fourier energy spectrum of f(t)
T is the pulse interval
A is a constant equal to the mean squared value of α_n in equation (A.10).

For a binary train, $\overline{\alpha_n^2} = 1$. When the selection of polarities of α_n is biased, in general there is also a set of discrete frequency components in the average power spectrum. For pulse shapes, where the spectrum vanishes at multiples of the pulse rate, however, no discrete components are present, even for a biased train. As previously stated,this is true for any filtered full baud pulse. Note that equation (A. 11) is the two-sided power spectrum, whereas Middleton uses the one-sided form and therefore an additional factor 2.

The utility of equation (A. 11) is based on Parseval's formula (see Ref. 10, page 27)

$$\int_{-\infty}^{\infty} |f(t)|^2 dt = \int_{-\infty}^{\infty} |F(\omega)|^2 df \quad f = \omega/2\pi \tag{A. 12}$$

In words, the energy of a time waveform is equal to the integral of the absolute - squared value of its Fourier transform. For deterministic waveforms, f(t), if the waveform is filtered, in a filter having a transfer function $H(\omega)$, the energy out of the filter is given by:

$$E = \int_{-\infty}^{\infty} |F(\omega)|^2 |H(\omega)|^2 df \tag{A. 13}$$

Similarly, for probabilistic waveforms, such as random pulse trains, the average power after filtering is calculated as:

$$P = \int_{-\infty}^{\infty} |s(\omega)|^2 |H(\omega)|^2 df \tag{A. 14}$$

where: $|s(\omega)|^2$ is the average power spectrum given by equation (A. 11)

APPENDIX B

PULSE SHAPES AND SPECTRA

Particular mathematical results, pertaining to pulses and their spectra used in this report, are collected in this appendix.

B.1 GAUSSIAN PULSE

Assume that the basic PCM pulse shape is formed by gaussian filtering of a rectangular full baud pulse. The resulting pulse, as a time function, is found as follows:

A gaussian filter has a transfer function:

$$G(\omega) = e^{-\frac{1}{2}\left(\frac{\omega}{\omega_\sigma}\right)^2} \tag{B.1}$$

and a corresponding impulse response:

$$h(t) = \frac{1}{2\pi}\int_{-\infty}^{\infty} e^{-\frac{1}{2}\left(\frac{\omega}{\omega_\sigma}\right)^2} e^{j\omega t}\, d\omega \tag{B.2}$$

$$= \frac{1}{\sqrt{2\pi}}\,\omega_\sigma\, e^{-\frac{1}{2}(\omega_\sigma t)^2}.$$

The step response is the integral of the impulse response, thus:

$$s(t) = \frac{\omega_\sigma}{\sqrt{2\pi}}\int_{-\infty}^{t} e^{-\frac{1}{2}(\omega_\sigma t^2}\, dt = \frac{1}{\sqrt{2\pi}}\int_{-\infty}^{t\omega_\sigma} e^{-\frac{1}{2}y^2}\, dy \tag{B.3}$$

$$s(t) = \Phi(t\omega_\sigma) \quad \text{WHERE: } \Phi(x) = \frac{1}{2\pi}\int_{-\infty}^{x} e^{-\frac{1}{2}y^2}\, dy$$

From the step response, the response to a full baud pulse centered at t = 0 is obtained as:

$$\varphi(t) = \Phi\left(\left[t + \tfrac{T}{2}\right]\omega_\sigma\right) - \Phi\left(\left[t - \tfrac{T}{2}\right]\omega_\sigma\right) \tag{B.4}$$

The function is plotted in Figure B.1 for a value of the parameter, $\frac{T\omega_\sigma}{2}$, corresponding to a typical pulse shape at the receiver. Thus, in the AN/GRC-50 radio (FM) set this parameter would be as follows:

$$T = \frac{1}{576,000 \text{ bits/sec}} = 1.736 \times 10^{-6} \text{ seconds}$$

$\omega_\delta = 2.325 \times 10^6$ radians/sec for the transmitter filter

$\omega_\delta = 1.642 \times 10^6$ radians/sec for combined transmitter and receiver filter

$\frac{T\omega_\sigma}{2} = 2.018$ at the transmitter

$\frac{T\omega_\sigma}{2} = 1.425$ at the receiver

B.2 PULSE ENERGY

From the pulse shape, equation (B.4), pulse energy can be obtained as the integral of $p^2(t)$ over all time. In discussion the term energy is used for convenience although usually no physical units are explicitly used. This usage, besides being convenient, is correct if the time functions describing pulse shapes are regarded as voltages across a resistance of one ohm. Instead of integrating $p^2(t)$ to obtain pulse energy, it is simplier to use Parseval's formula, equation (A.12). The voltage spectrum of a rectangular pulse is defined by equation (A.9), and filter response by equation (B.1). Thus, pulse energy, E. is:

$$E = \frac{1}{2\pi} \int_{-\infty}^{\infty} T^2 \frac{\sin^2 \omega T/2}{(\omega T/2)^2} e^{-\left(\frac{\omega}{\omega_\delta}\right)^2} d\omega \qquad \text{(B.5)}$$

This integral is not a standard tabulated result, but can be evaluated in a number of ways. The simplest method is to differentiate with respect to $a = 1/\omega_\sigma$, integrate with respect to ω and again, with respect to a. A different method of evaluation based more directly on physical concepts will be shown in the following paragraphs.

Integral (B.5) can be regarded as a Fourier transform of a spectrum, evaluated at the particular point t = 0. The spectrum involved is that of a triangular pulse after gaussian filtering. However, because a triangular pulse is the integral of three step functions, it is necessary only to integrate equation (B.3) and apply the result to the required three step functions to evaluate at t = 0.

A triangular pulse beginning at t = - T, rising to unity at t = 0, and then following to zero at t = T, has the required spectrum:

$$\frac{T^2 \sin \omega T/2}{(\omega T/2)^2} \qquad \text{(B.6)}$$

The derivative of this pulse consists of a unit step at t = - T, two negative unit steps at t = 0, and positive unit step at t = T. In the integral, it is convenient to substitute: $\sqrt{2}\,\omega_1 = \omega_\sigma$ so that the gaussian function has the form specified by equation (B.1). Adhering to the procedure described in the preceding paragraph, and using equation (B.3):

$$E = \int_{-\infty}^{\infty} \left\{ \Phi\left([t-T]\omega_1\right) - 2\Phi(t\omega_1) + \Phi\left([t+T]\omega_1\right) \right\} dt \qquad \text{(B.7)}$$

The integral of function Φ is readily evaluated as follows:

$$I = \int \Phi(x)\,dx = x\Phi(x) - \int \Phi'(x)\,x\,dx + c \qquad \text{(B.8)}$$

and,

$$\int \Phi'(x)\,x\,dx = \frac{1}{\sqrt{2\pi}} \int e^{-\frac{1}{2}x^2} x\,dx = -\frac{1}{\sqrt{2\pi}} e^{-\frac{1}{2}x^2} \qquad \text{(B.9)}$$

Thus:

$$I = x\Phi(x) + \frac{1}{\sqrt{2\pi}} e^{-\frac{1}{2}x^2} + c \qquad \text{(B.10)}$$

When evaluated over definite limits $-\infty$ to y:

$$I = y\Phi(y) + \frac{1}{\sqrt{2\pi}} e^{-\frac{1}{2}y^2} \qquad \text{(B.11)}$$

Also,

$$\int_{-\infty}^{\circ} \Phi(kx+m)\,dx = \frac{1}{k}\int_{-\infty}^{m} \Phi(u)\,du = \frac{m}{k}\Phi(m) + \frac{1}{k\sqrt{2\pi}} e^{-\frac{1}{2}m^2} \qquad \text{(B.12)}$$

Applying equations (B.12) to (B.7), we have:

$k = \omega_1 \; ; \; y = 0$

$$E = \frac{1}{\omega_1}\left\{-T\omega_1\Phi(-T\omega_1) + \frac{1}{\sqrt{2\pi}} e^{-\frac{1}{2}(T\omega_1)^2} - \frac{2}{\sqrt{2\pi}} + T\omega_1\Phi(+T\omega_1) + \frac{1}{\sqrt{2\pi}} e^{-\frac{1}{2}(T\omega_1)^2}\right\} \qquad \text{(B.13)}$$

After rearranging, replacing ω_1 by $\omega_b/\sqrt{2}$, and setting $a = \omega_b \frac{T}{2}$ we have:

$$E = T\left[\Phi(\sqrt{2}\,a) - \Phi(-\sqrt{2}\,a) - \frac{1}{\sqrt{\pi}}\left\{\frac{1-e^{-a^2}}{a}\right\}\right] \qquad \text{(B.14)}$$

$$E = T\,\mathrm{erf}(a) - \frac{T}{\sqrt{\pi}}\left\{\frac{1-e^{-a^2}}{a}\right\}$$

where: $\mathrm{erf}(a) = \frac{2}{\sqrt{\pi}}\int_0^a e^{-x^2}\,dx \; ; \quad a = \omega_b T/2$

Pulse energy is easily calculated from equation (B.14) using standard tables. For the typical constants specified in paragraph B.1, the pulse energy relative to the bit interval is given in Table B.1.

TABLE B.1

PULSE ENERGY RELATIVE TO BIT INTERVAL

	$a = \omega_b T/2$	E/T
At Transmitter	2.018	0.72
At Receiver	1.425	0.612

Observe that the quantity E/T is equal to the ratio of power available when a gaussian filter is used, to power available if no gaussian filter were used. A plot of this function is shown in Figure B.2.

B.3 QUADRATURE PULSE

As shown in paragraph A.2 of Appendex A, an SSB signal consists of a modulating signal and a derived quadrature signal which separately modulate two carriers in quadrature. In this paragraph, the quadrature pulse corresponding to a guassian pulse is derived. Consider a gaussian pulse defined by quation (B.2) with a spectrum defined by equation (B.1). Subsequent to applying a 90° phase shift to the spectrum, the quadrature pulse is obtained from:

$$g_i(t) = \frac{1}{2\pi}\int_{-\infty}^{0} j e^{-\frac{1}{2}\left(\frac{\omega}{\omega_\delta}\right)^2} e^{j\omega t}\, d\omega - \frac{1}{2\pi}\int_{0}^{\infty} j e^{-\frac{1}{2}\left(\frac{\omega}{\omega_\delta}\right)^2} e^{j\omega t}\, d\omega \qquad \text{(B.15)}$$

Completing the squares in the exponents:

$$g_i(t) = \frac{j}{2\pi} e^{b^2}\int_{-\infty}^{0} e^{-\left[\frac{\omega}{\sqrt{2}\omega_\delta}+b\right]^2} d\omega - \frac{j}{2\pi} e^{b^2}\int_{0}^{\infty} e^{-\left[\frac{\omega}{\sqrt{2}\omega_\delta}+b\right]^2} d\omega \qquad \text{(B.16)}$$

where: $b = -jt\omega_\delta/\sqrt{2}$

Changing the variable of integration as follows:

$$z = j\left[\frac{\omega}{\sqrt{2}\omega_\delta}+b\right] \;;\; dz = \frac{j\,d\omega}{\sqrt{2}\omega_\delta}$$

$$g_i(t) = -\frac{1}{2\pi} e^{b^2}\sqrt{2}\,\omega_\delta \int_{-\infty}^{jb} e^{+z^2} dz + \frac{1}{2\pi} e^{b^2}\sqrt{2}\,\omega_\delta \int_{jb}^{\infty} e^{z^2} dz \qquad \text{(B.17)}$$

In the first integral, substitute z = - y, and interchange the limits, to obtain:

$$g_i(t) = \frac{\sqrt{2}}{\pi}\,\omega_\delta\, e^{-\frac{1}{2}(\omega_\delta)^2} \int_{0}^{t\omega_\delta/\sqrt{2}} e^{z^2} dz \qquad \text{(B.18)}$$

The result is somewhat complicated but numerical values can be obtained from published tabulations. The integral is known as Dawson's integral, and tables have been published in "The Journal of the Franklin Institute", Vol. 237, June 1944, pg. 495-497; and Vol. 238, Sept. 1944, pages 220-222. (See also Jahnke and Emde "Tables of Functions", Dover.)

The function defined by equation (B.18) is the quadrature pulse corresponding to a gaussian pulse. For the full baud rectangular pulse after gaussian filtering, the corresponding quadrature pulse is the integral of equation (B.18). To establish this result note that any linear operation, such as differentiation or integration, has a corresponding operation on the spectrum. The operation on the spectrum is identical for the original pulse and for the quadrature pulse. Thus, if a pulse is integrated, the corresponding quadrature pulse is the integral of the original quadrature pulse. The quadrature step response is:

$$S_g(t) = \int_{-\infty}^{t} g_i(t)\,dt \tag{B.19}$$

and the response to a full baud rectangular pulse is therefore:

$$g(t) = \int_{-\infty}^{t+T/2} g_i(t)\,dt - \int_{-\infty}^{t-T/2} g_i(t)\,dt = \int_{t-T/2}^{t+T/2} \left\{ \frac{\sqrt{2}}{\pi}\omega_b e^{-\frac{1}{2}(u\omega_b)^2} \int_0^{u\omega_b/\sqrt{2}} e^{z^2}\,dz \right\} du \tag{B.20}$$

By a change of variable: $v = \omega_b \frac{u}{\sqrt{2}}$, there results:

$$g(t) = \frac{2}{\pi} \int_{(t-T/2)\frac{\omega_b}{\sqrt{2}}}^{(t+T/2)\omega_b/\sqrt{2}} e^{-v^2} \int_0^v e^{z^2}\,dz\,dv \tag{B.21}$$

In this form, q(t) can be calculated from values of the function:

$$I(b) = \int_0^b e^{-v^2}\,dv \int_0^v e^{z^2}\,dz \tag{B.22}$$

which is tabulated by J. B. Rosser: in Theory and Application of $\int_0^\gamma e^{-x^2}dx$ and $\int_0^\gamma e^{-\rho^2y^2}dy \int_0^y e^{-x^2}dx$, Mapleton House, Brooklyn, N.Y., 1948, pages 174-191. A plot of this function is shown in Figure B.1 for a value of $\alpha_f T$ = 2.85, corresponding to the case of gaussian filtering at both transmitter and receiver.

B.4 EVALUATION OF A DEFINITE INTEGRAL

In Section VI, use is made of the following integral:

$$I = \int_0^\infty \frac{\sin^2 y}{y^2} e^{-a^2y^2} dy$$

Although this can be evaluated as a formal mathematical problem, it can be derived easily using results previously established.

I can be rewritten as:

$$I(b) = \int_0^\infty \frac{\sin y}{y} e^{-a^2y^2}\left[\frac{e^{jby} - e^{-jby}}{2j}\right] dy \qquad \text{(B.23)}$$

$$= -j\int_0^\infty \frac{\sin y}{2y} e^{-a^2y^2} e^{jby} dy + j\int_{-\infty}^0 \frac{\sin y}{2y} e^{-a^2y^2} e^{-jby} dy$$

and then noted that I(b) is identical in form to the expression for the quadrature pulse described in equation (A.5) when:

$$F(y) = \frac{\sin y}{2y} e^{-a^2y^2}$$

In this form, F(y) is the spectrum of a full baud rectangular pulse after gaussian filtering.

Consequently, I(b) is the quadrature pulse corresponding to this spectrum. But, from equations (B.1), (B.21), and (A,9) the result that a pulse having a spectrum differential:

$$P(\omega) = T \frac{\sin \omega T/2}{\omega T/2} e^{-\frac{1}{2}\left(\frac{\omega}{\omega_b}\right)^2} \frac{d\omega}{2\pi} \qquad \text{(B.24)}$$

will have a quadrature pulse:

$$q_\delta(t) = \frac{2}{\pi} \int_{(t-T/2)\omega_\delta/\sqrt{2}}^{(t+T/2)\omega_\delta/\sqrt{2}} e^{-v^2} \int_0^v e^{z^2} dz\, dv \tag{B.25}$$

Thus, it is only necessary to identify variables as follows:

$$\begin{aligned} y &= \omega T/2 \\ dy &= \frac{T}{2} d\omega \\ a^2 y^2 &= 1/2 \left(\frac{\omega}{\omega_\delta}\right)^2 = a^2 \omega^2 \frac{T^2}{4} \\ a^2 &= \frac{2}{T^2 \omega_\delta^2} \\ by &= \omega t \\ b &= 2t/T \end{aligned} \tag{B.26}$$

With these changes the given spectrum becomes:

$$\frac{\sin y}{2y} e^{-a^2 y^2} = 1/2 \quad \frac{\sin \omega T/2}{\omega T/2} e^{-1/2\left(\frac{\omega}{\omega_\delta}\right)^2} \frac{T}{2} d\omega \tag{B.27}$$

which is $\frac{\pi}{2} P(\omega) df$. Thus, the desired integral, I(b) is $\frac{\pi}{2}$ times $q_\delta(t)$ with the substitutions:

$$\begin{aligned} \omega_\delta &= \frac{\sqrt{2}}{aT} \\ t\frac{\omega_\delta}{\sqrt{2}} &= \frac{t}{aT} = \frac{b}{2a} \\ \frac{T}{2}\frac{\omega_\delta}{\sqrt{2}} &= \frac{1}{2a} \end{aligned} \tag{B.28}$$

Therefore:

$$I(b) = \int_{\left(\frac{b}{2a}-\frac{1}{2a}\right)}^{\left(\frac{b}{2a}+\frac{1}{2a}\right)} e^{-v^2} \int_0^v e^{z^2} dz\, dv \tag{B.29}$$

For the original problem, b = 1, so we have:

$$\int_0^\infty \frac{\sin^2 y}{y} e^{-a^2 y^2} dy = \int_0^{1/a} e^{-v^2} \int_0^v e^{z^2} dz\, dv \qquad \text{(B.30)}$$

The integral is plotted in Figure B.3. In the plot, which is used in Section VI, the interpretation which is given to the parameter a is slightly different than that used in the derivation.

B.5 POWER IN AN SSB SIGNAL WITH CARRIER

Considering a SSB power spectrum it is convenient to regard it as being identical to the power spectrum of the baseband modulating signal (except for a translation in frequency of each half of the spectrum). Thus, given a baseband power spectrum, $|S(\omega)|^2$ the corresponding SSB power spectrum is described by:

$$\begin{aligned} |S_s(\omega)|^2 &= |S(\omega-\omega_0)|^2 && \omega > \omega_0 \\ &= 0 && |\omega| < \omega_0 \\ &= |S(\omega+\omega_0)|^2 && \omega < -\omega_0 \end{aligned} \qquad \text{(B.31)}$$

With this convention, sideband power is equal to power in the baseband modulating signal. When a carrier, Q Cos $\omega_0 t$, accompanies the sideband the total signal, using equation (A.6) is:

$$r(t) = [Q + f(t)] \cos \omega_0 t + \hat{f}(t) \sin \omega_0 t \qquad \text{(B.32)}$$

The power in this signal is $P_C + P_S$, the carrier plus sideband power, where

$$P_c = \frac{Q^2}{2} \quad \text{and} \quad P_s = \tfrac{1}{2} P_f + \tfrac{1}{2} P_{\hat{f}}$$

The quantity P_f is the power associated with f(t), and similarly $P_{\hat{f}}$. Since f and $\hat{f}$ have the same power spectrum, they contain equal power, so $P_S = P_f$. The factor 1/2 in the expression for sideband power accounts for the fact that f(t) is reduced in amplitude by the factor $\text{Cos}\,\omega_o t$, and similarly for $\hat{f}(t)$. For the special case of $\omega_o = 0$, then $\text{Cos}\,\omega_o t = 1$, $\text{Sin}\,\omega_o t = 0$, and $P_S = 1\ (P_f) + 0\ (P_{\hat{f}})$, as required for the, now, baseband signal.

When considering a specific design problem it is usually desirable to express carrier power as:

$$P_c = R P_s \tag{B.33}$$

where: R is a constant.

The sideband power can be written:

$$P_s = \frac{1}{2\pi} \int_{-\infty}^{\infty} \frac{1}{T} |F(\omega)|^2 d\omega = A^2 K(\omega_\beta, T) \tag{B.34}$$

This form is convenient for the purpose of normalizing results; the terms have the following significance: $F(\omega)$ is the voltage spectrum of an individual pulse; T is the pulse interval; A^2 is the pulse train power prior to baseband filtering; $K(\omega_\beta, T)$ is a function of filter bandwidth and pulse interval, and is the ratio of power out of the pulse-forming baseband filter to the pulse train power input. For the typical case considered in this report, the full baud input pulses have unit amplitude, and a train of such pulses have unit power, so $A^2 = 1 = A$. As shown above, a unit full baud pulse after gaussian filtering has an energy described by equation (B.14). Since pulse energy per pulse interval is average power, and there is unit power into the gaussian filter, the function $K(\omega_\beta, T)$ is:

$$K(\omega_\beta, T) = \frac{E}{T} = \text{erf}(a) - \left\{ \frac{1 - e^{-a^2}}{\sqrt{\pi}\, a} \right\} \tag{B.35}$$

Where: $\operatorname{erf}(a) = \frac{2}{\sqrt{\pi}} \int_0^a e^{-x^2} dx$

$$a = \omega_\delta \frac{T}{2}$$

Carrier amplitude Q can now be related to the ratio of carrier to sideband power, R, as follows:

$$P_c = \frac{Q^2}{2} = R P_s = R A^2 K(\omega_\delta, T) \qquad \text{(B.36)}$$

$$\frac{Q}{A} = \sqrt{2RK(\omega_\delta, T)}$$

This equation is used in Section VI. An additional relation which is required is that between carrier power, and power spectral density in the vicinity of the carrier. For a full baud rectangular pulse train of amplitude A, $|S(0)|^2 = A^2 T$, as may be seen from equations (A.9) and (A.11). Therefore:

$$\frac{P_c}{|S(0)|^2} = \frac{R}{T} K(\omega_\delta, T) \qquad \text{(B.37)}$$

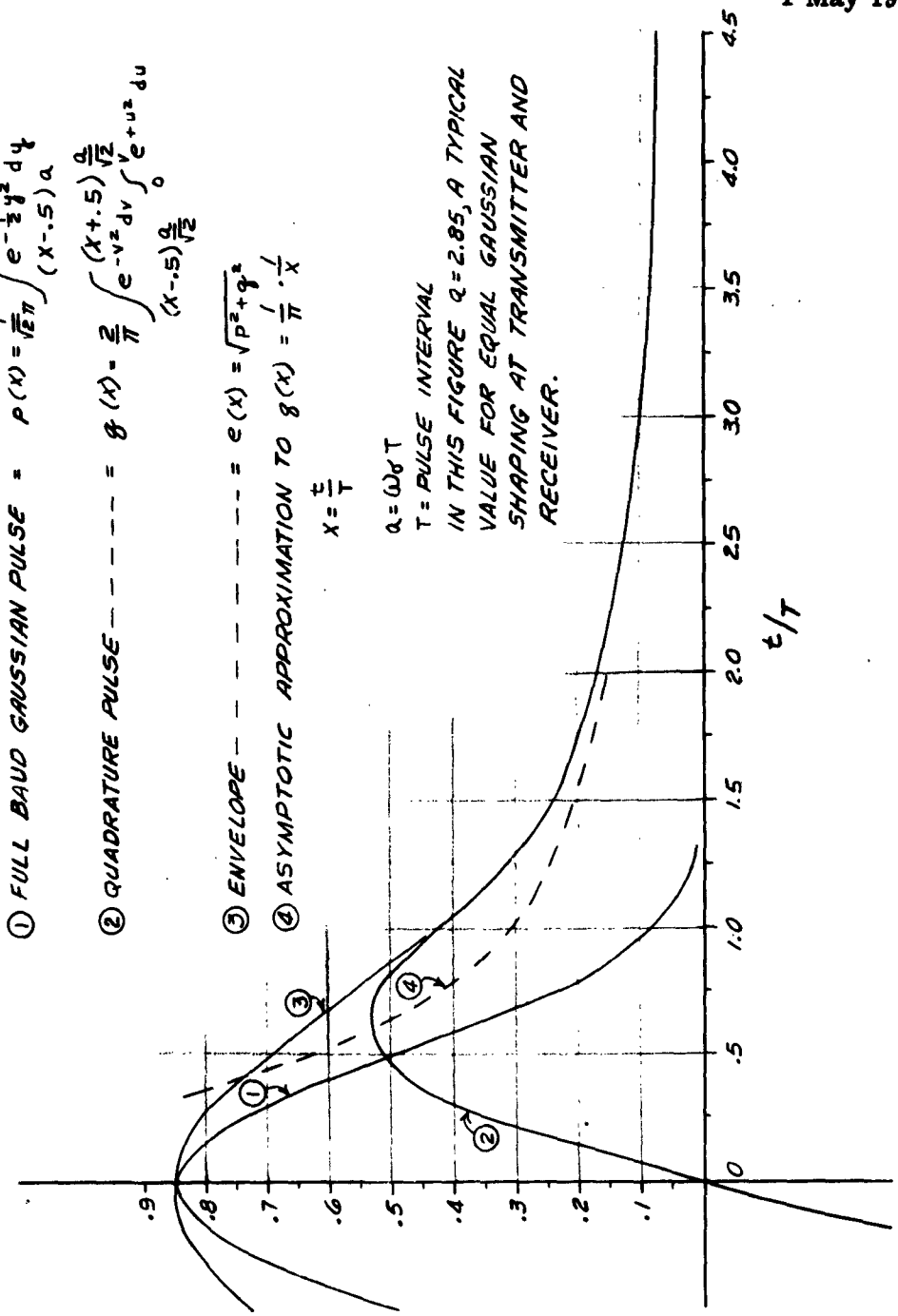

Figure B.1. Full Baud Gaussian Pulse and Derived Waveforms in an SSB System

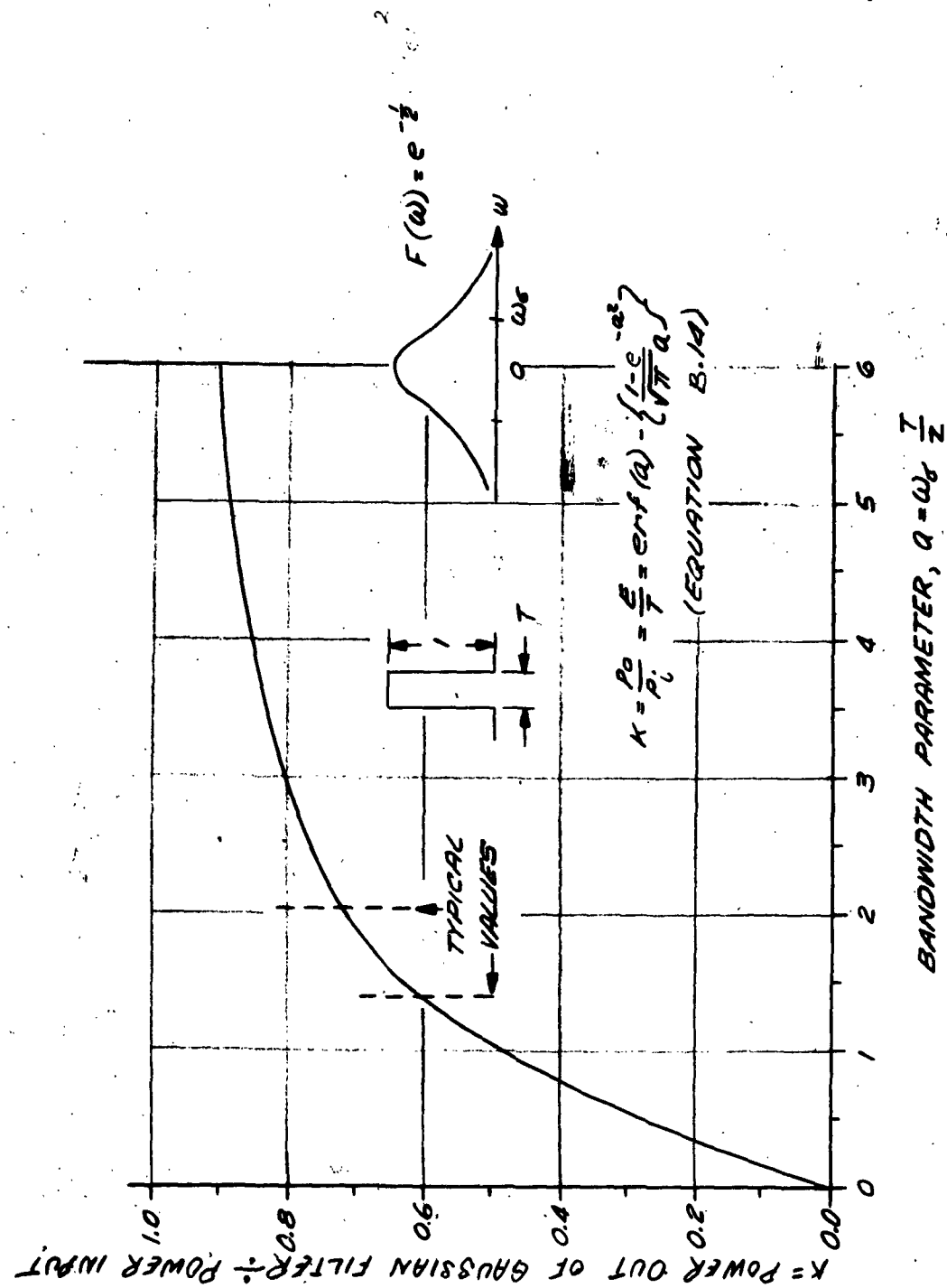

Figure B.2. Power Out of a Gaussian Filter Divided by Power Input From a Full Baud Rectangular Pulse Train, as a Function of Bandwidth

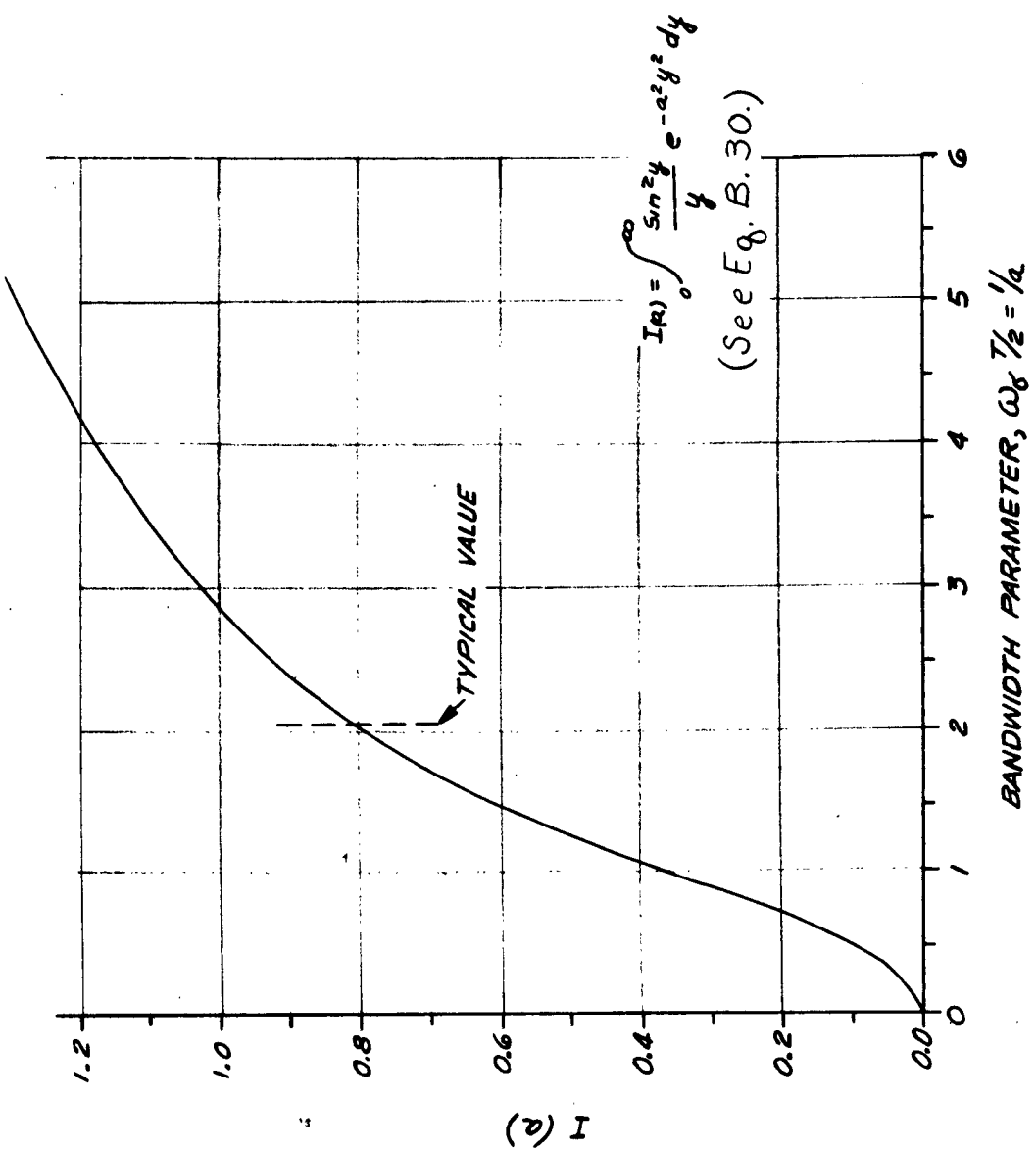

Figure B.3. Centroid of a Full Baud Gaussian Power Spectrum as a Function of Bandwidth

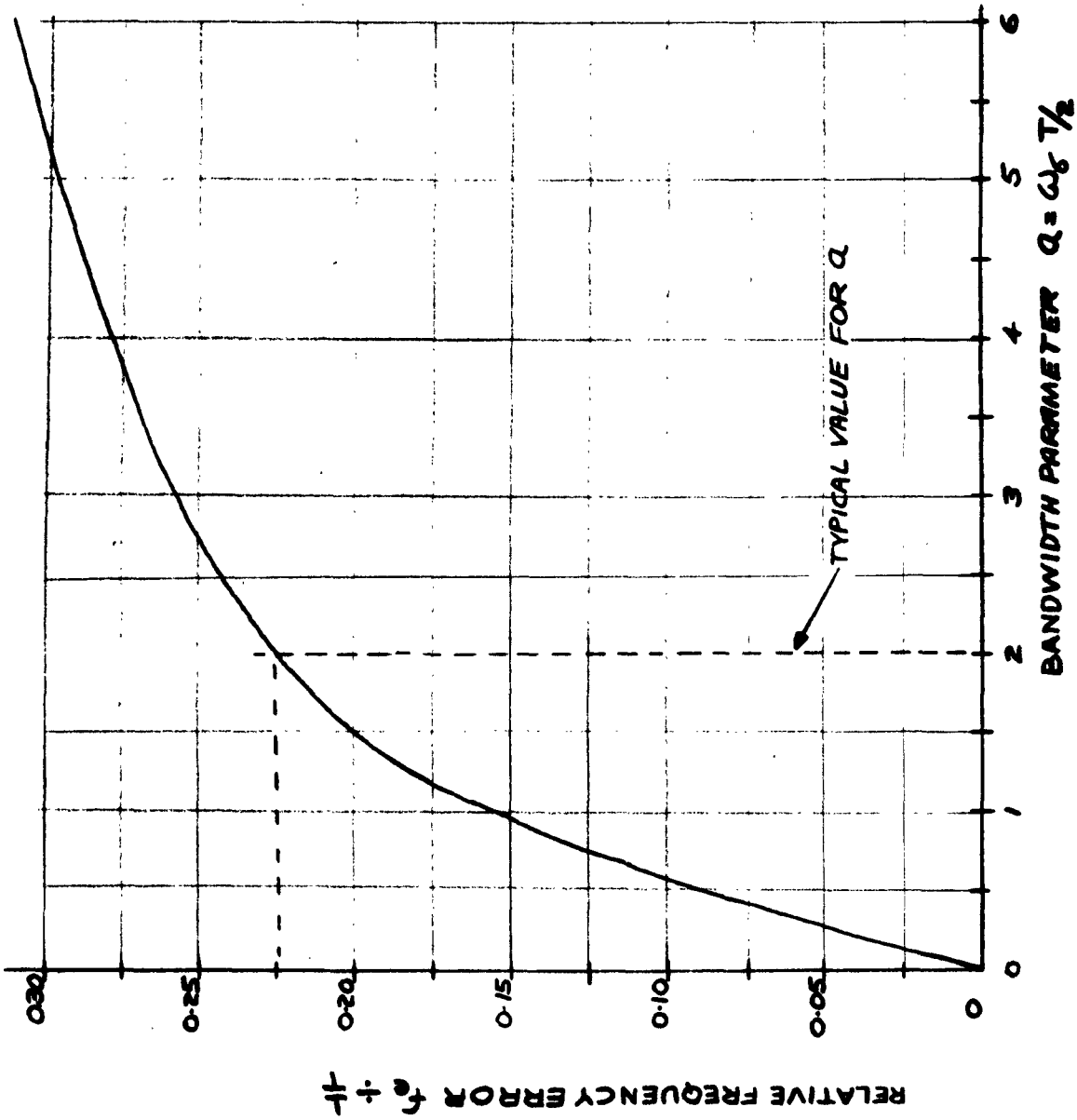

Figure B.4. AFC Error For the Power Spectrum of a Full Baud Gaussian Pulse Train, as a Function of Bandwidth

APPENDIX C

AN ESTIMATE OF THE AMOUNT OF SIDEBAND REJECTION OBTAINABLE FROM PHASE SHIFTER

The spectrum of an SSB signal formed with a tapped delay line phase shifter is: (Refer to paragraph 3.2.2)

$$\begin{aligned} S(\omega) &= A(\omega-\omega_0)\left[1-\sum^{N} 2\alpha_n \sin(\omega-\omega_0)\tau_n\right] \\ &\quad + A(\omega+\omega_0)\left[1+\sum' 2\alpha_n \sin(\omega+\omega_0)\tau_n\right] \\ &= S_1(\omega)+S_2(\omega) \end{aligned} \tag{C.1}$$

Assume that $A(\omega)$, the spectrum of the baseband modulation is band limited, being zero for $|\omega|>\frac{\pi}{\tau_0}$. The spectrum of the SSB signal is then zero except in the range $\omega_0-\frac{\pi}{\tau_0}<|\omega|<\omega_0+\frac{\pi}{\tau_0}$. Considering only positive frequencies, the second term in the expression for $S(\omega)$ can be ignored. The ratio of power in the unwanted sideband to total power can be calculated as follows:

$$\frac{P_{s_1}}{P_T} = \frac{\int_{\omega_0}^{\omega_0+\pi/\tau_0} |S_1(\omega)|^2 d\omega}{\int_{\omega_0-\frac{\pi}{\tau_0}}^{\omega_0+\pi/\tau_0} |S_1(\omega)|^2 d\omega} = \frac{\int_{0}^{\pi/\tau_0} |S_1(\omega+\omega_0)|^2 d\omega}{\int_{-\frac{\pi}{\tau_0}}^{+\pi/\tau_0} |S_1(\omega+\omega_0)|^2 d\omega} \tag{C.2}$$

For the purpose of estimating the number of delay reactions necessary to achieve a given power ratio, the modulation spectrum can be approximated by:

$$A(\omega) \cong \tfrac{1}{2}(1+\cos\omega\tau_0)\,;\ \tau_0=\frac{\tau}{2}\,;\ |\omega|<\frac{\pi}{\tau} \tag{C.3}$$

Also, note that: $1-\sum_{n=1}^{N} 2\alpha_n \sin\omega\tau_n = \sum_{N+1}^{\infty} 2\alpha_n \sin\omega\tau_n$ when $\omega > 0$.
Thus the integrand of the numerator has the form:

$$S_1(\omega+\omega_o) = \tfrac{1}{2}(1+\cos\omega\tau_o)\sum_{N+1}^{\infty} 2\alpha_n \sin\omega\tau_n$$

$$= \sum_{N+1}^{\infty} \alpha_n \sin\omega\tau_n + \tfrac{1}{2}\sum_{N+1}^{\infty} 2\alpha_n \sin\omega(\tau_n-\tau_o) + \tfrac{1}{2}\sum_{N+1}^{\infty} 2\alpha_n \sin\omega(\tau_n+\tau_o) \qquad (C.4)$$

Because τ_n is always an odd integer multiple of τ_o then $\tau_n \pm \tau_o$ is an even multiple of τ_o, thus, the last two sums consist of terms having common frequencies and can be combined so that $S_1(\omega+\omega_o)$ can be written:

$$S_1(\omega+\omega_o) = \sum_{N+1}^{\infty} \alpha_n \sin\omega\tau_n + \tfrac{1}{2}\alpha_{N+1}\sin\omega(\tau_{N+1}-\tau_o) + \tfrac{1}{2}\sum_{N+1}^{\infty}(\alpha_n+\alpha_{n+1})\sin\omega(\tau_n+\tau_o) \qquad (C.5)$$

Now when S_1 is squared we obtain many terms of the form:

$$\sin mx \sin nx = \tfrac{1}{2}\cos(m-n)x - \tfrac{1}{2}\cos(n+m)x$$

Upon integration over a half period, or over a full period, such terms have a zero contribution except when m = n. But m = n only for terms from the same summation. Thus:

$$N = \int_0^{\pi/\tau_o} |S_1(\omega+\omega_o)|^2 d\omega = \frac{\pi}{2\tau_o}\left[\sum_{N+1}^{\infty}\alpha_n^2 + \tfrac{1}{4}\alpha_{N+1}^2 + \tfrac{1}{4}\sum_{N+1}^{\infty}(\alpha_n+\alpha_{n+1})^2\right]$$

$$= \frac{\pi}{2\tau_o}\left[\tfrac{3}{4}\sum_{N+1}^{\infty}\alpha_n^2 + \tfrac{1}{2}\sum_{N+1}^{\infty}\alpha_n\alpha_{n+1}\right] \qquad (C.6)$$

Upon substitution of the values of $\alpha_n = \frac{2}{\pi(2n-1)}$

$$N = \frac{3}{2\pi\tau_o}\sum_{N+1}^{\infty}\frac{1}{(2n-1)^2} + \frac{1}{\pi\tau_o}\sum_{N+1}^{\infty}\frac{1}{(2n-1)(2n+1)} \qquad (C.7)$$

The second sum can be evaluated exactly with the aid of the formula:

$$\sum_{1}^{N} \frac{1}{[qk+p][qk+p-q]} = \frac{N}{p(qN+p)} \qquad (C.8)$$

which follows directly from formula (222) given by Jolley (Ref. 7). Setting q = 2, p = 1, and noting that as $N \to \infty$ the sum becomes 1/2, we have:

$$\sum_{N+1}^{\infty} \frac{1}{(2n+1)(2n-1)} = 1/2 - \frac{N}{(2N+1)} = \frac{1}{2(2N+1)} \qquad (C.9)$$

The first sum can be very accurately approximated with the aid of the formula used above, as follows:

$$\sum_{N+1}^{\infty} \frac{1}{(2n-1)^2} = \sum_{N+1}^{\infty} \frac{1}{2n(2n-2)} \cdot \frac{(2n)}{(2n-1)} \cdot \frac{(2n-2)}{(2n-1)} \qquad (C.10)$$

$$\text{BUT:} \quad \frac{2n(2n-2)}{(2n-1)^2} = \frac{4n^2-4n}{4n^2-4n+1} = 1 - \frac{1}{4n^2-4n+1} \qquad (C.11)$$

Thus:

$$\sum_{N+1}^{\infty} \frac{1}{(2n-1)^2} = \sum_{N+1}^{\infty} \frac{1}{2n(2n-2)} - \sum_{N+1}^{\infty} \frac{1}{2n(2n-2)(2n-1)^2} \qquad (C.12)$$

But the last summation has a magnitude less than:

$$\frac{1}{(2N+1)^2} = \sum_{N+1}^{\infty} \frac{1}{2n(2n-2)} \qquad (C.13)$$

Thus the relative error in the desired sum is less than $(2N + 1)^{-2}$ which is less than 1/4 percent even for N = 10.

The sum:

$$\sum_{N+1}^{\infty} \frac{1}{2n(2n-2)} = 1/4 - \frac{N}{4(N+1)} = \frac{1}{4(N+1)} \qquad \text{(C. 14)}$$

as found by setting p = q = 2 in the general formula used above. As a result, the numerator of the desired ratio is approximately:

$$N = \frac{1}{2\pi\tau_0}\left[\frac{3}{4(N+1)} + \frac{1}{2N+1}\right] \qquad \text{(C. 15)}$$

The denominator of the desired ratio is accurately given by the expression:

$$D \cong \int_{-\pi/\tau_0}^{0} 4A^2(\omega)\, d\omega \qquad \text{(C. 16)}$$

This approximation is obtained by noting that:

$$S_1(\omega+\omega_0) \cong 2 \quad \text{for} \quad -\frac{\pi}{\tau_0} < \omega < 0, \qquad \text{(C. 17)}$$

and ignoring the small energy contribution from the undesired sideband. Thus:

$$D \cong \int_{-\pi/\tau_0}^{0} (1+\cos\omega\tau_0)^2 d\omega = \int_{-\pi/\tau_0}^{0} (1+2\cos\omega\tau_0 + \cos^2\omega\tau_0)\, d\omega \cong \frac{3\pi}{2\tau_0} \qquad \text{(C. 18)}$$

The desired ratio is therefore:

$$\frac{P_{U_0}S_0}{P_T} \cong \frac{1}{3\pi^2}\left[\frac{3}{4(N+1)} + \frac{1}{2N+1}\right] \cong \frac{5}{12\pi^2(N+1)} \cong 0.042 \qquad \text{(C. 19)}$$

APPENDIX D

AMPLITUDE DISTRIBUTION OF THE QUADRATURE COMPONENT AND ENVELOPE OF A PCM-SSB SIGNAL

As shown in the Section V, the bit detection process will be disturbed by the quadrature voltage when any phase error exists in the demodulating carrier. In a random pulse train, the quadrature voltage will appear as a random quantity at the pulse sampling instant. To evaluate average error rate the statistical distribution of the disturbing quadrature voltage must be known. Furthermore, the quadrature voltage contributes directly to the magnitude of the SSB envelope. For these reasons an estimate of the probability distribution of the quadrature voltage is developed in the following paragraphs.

D.1 THE QUADRATURE DISTRIBUTION

A random binary pulse train can be described mathematically as:

$$a(t) = \sum_{n=-\infty}^{\infty} \alpha_n p(t - nT) \qquad \text{(D.1)}$$

where: α_n = ± 1 chosen independently, at random

p(t) is the pulse function

A similar expression describes the quadrature pulse train, b(t), except that p(t) is replaced by the quadrature pulse, q(t). The particular functions, p, and q, used here as typical examples of PCM pulses are described in Appendix B by equations (B.4) and (B.21) respectively, and are shown in Figure (B.1). Now if b(t) is sampled at the bit rate, one obtains a set of random quantities having some statistical distribution. The mean square value of this distribution is shown to be:

$$\overline{b^2(t)} = \sum_{n=-\infty}^{\infty} q^2(t - nT) \qquad \text{(D.2)}$$

and a similar expression represents $\overline{a^2(t)}$. Theoretically this sum can be evaluated in terms of the pulse energy spectra by means of Poisson's sum formula (Ref. 10), as follows:

$$\overline{b^2(t)} = \frac{1}{T}\sum_{n=-\infty}^{\infty} e^{jn\omega_0 t} Q_E(n\omega_0);\ \omega_0 = 2\pi/T \qquad \text{(D.3)}$$

where: T = pulse interval

$Q_E(\omega)$ is the Fourier transform of $q^2(t)$

$Q_E(\omega) = \frac{1}{2\pi}\int_{-\infty}^{\infty} Q(y)\, Q(z-y)\, dy$

$Q(\omega)$ is the Fourier transform of $q(t)$

In this formula, when n = o, $Q_E(n\omega_0)$ represents the quadrature pulse energy. The remaining terms of the sum form a Fourier series with rapidly decreasing coefficients. For pulses of the form considered in this report, only the first term is significant. Thus equation (D.3) is, approximately:

$$\overline{b^2(t)} \cong \frac{E}{T} + Q_E(\omega_0)\cos\omega_0 t \qquad \text{(D.4)}$$

Similarly,

$$\overline{a^2(t)} \cong \frac{E}{T} + P_E(\omega_0)\cos\omega_0 t \qquad \text{(D.5)}$$

where: $P_E(\omega_0)$ is the pulse energy spectrum for the original pulse.

In (D.4) and (D.5) the simple cosine variation results from the assumption that the original pulse is symmetrical about the sampling instant. In general, a phase angle is associated with the cosine term. It can be shown that $P_E(\omega_0)$ and $Q_E(\omega_0)$ are of opposite sign and almost equal amplitude. When interested in the behavior of $\overline{a^2(t)}$ and $\overline{b^2(t)}$ it is generally easier to use equation (D.2) and calculate the quantities directly, especially when the pulse shapes are know explicitly. In this manner, using the pulse shapes given in Figure B.1, the extreme values for $\overline{a^2(t)}$ and $\overline{b^2(t)}$ were obtained, as shown in Table D.1.

TABLE D.1

Quantity	Sampling Instant	
	Pulse Center	Pulse Edge
$\sqrt{\overline{a^2(t)}}$	0.8526	0.7043
$\sqrt{\overline{b^2(t)}}$	0.6892	0.8631
$\sqrt{\overline{a^2(t)}} \Big/ \sqrt{E/T}$	1.09	0.90
$\sqrt{\overline{b^2(t)}} \Big/ \sqrt{E/T}$	0.882	0.11

$\sqrt{E/T}$ = Rms value of a(t) and b(t) = 0.781

$p(0)$ = Peak Pulse Amplitude = 0.846

From the table it may be observed that in general the distribution of a(t) and b(t) must depend on the particular sampling instant chosen within the pulse interval. Although a(t) and b(t) have the same average rms value over all possible sampling instants, for a particular instant (e.g., the desired case of sampling at pulse center), a and b have different rms values.

To determine bit error probability, the distribution of the quadrature voltage at pulse centers is the only consideration. In principle, this distribution can be determined from the expression:

$$b(0) = b_0 = \sum_{n=-\infty}^{\infty} \alpha_n q(nT) \; ; \; \alpha_n = \pm 1 \text{ at random,} \qquad \text{(D.6)}$$

for any particular quadrature pulse shape. It is actually impractical to carry out this procedure due to the very large number of terms which are required to adequately approximate the sum. Instead, advantage can be taken of an interesting property of quadrature pulses i.e., for any practical pulse shape, p(t), which is narrowly confined in time, the corresponding quadrature pulse rapidly approaches the asymptotic form K/t, where K is a constant. The

asymptotic form is shown graphically on Figure B.1 where it may be seen that for times greater than 1.5 pulse-intervals, the approximation is excellent. Also, for symmetrical pulses, the quadrature pulse is zero at pulse center. Thus equation (D.6) is approximately:

$$b_o \cong \sum_{\substack{n=-\infty \\ \neq 0}}^{\infty} \alpha_n \frac{K}{n} \qquad \text{(D.7)}$$

The distribution described by this equation can be obtained, at least numerically, and this basic distribution can be used with a correction process to obtain the distribution for any particular quadrature pulse. A correction process of this type has not been applied for it is believed that the basic distribution is sufficiently close to the desired distribution. The process for obtaining the distribution of b_0 as described by equation (D.7) is outlined below.

First, consider the variable, x, defined by:

$$x = \sum_{1}^{\infty} \frac{\alpha_n}{n} \qquad \text{(D.8)}$$

Since x is the sum of independent random variables, the characteristic function for the distribution of x is the product of the individual characteristic functions. The characteristic function for the n^{th} component is:

$$\varphi_n(t) = \tfrac{1}{2} e^{-i\frac{t}{n}} + \tfrac{1}{2} e^{+i\frac{t}{n}} = \cos\left(\frac{t}{n}\right) \qquad \text{(D.9)}$$

Thus, the characteristic function for x is:

$$\varphi_n(t) = \prod_{1}^{\infty} \cos\left(\frac{t}{n}\right) \qquad \text{(D.10)}$$

It has been shown by J. Dutka that this infinite product can be expressed as:

$$\varphi_x(t) = \prod_{j=1}^{\infty} \frac{\sin \beta_j t}{\beta_j t} \; ; \; \beta_j = \frac{2}{2j-1} \qquad \text{(D. 11)}$$

In this form the characteristic function is recognized as that which results from an infinite sum of random variables, each having a rectangular distribution of different widths. A close approximation to the distribution of x can be obtained by considering the sum of a limited number of these rectangularly distributed variables.

Mathematically, a repeated convolution of the rectangular distribution must be performed. Further accuracy is obtained by assuming a normal distribution for those terms which were ignored. Using some results of J. Dutka (see acknowledgements) which give explicit formulas for the results of convolving rectangular distributions, M. Landis obtained a very good approximation to the distribution of x. The excellence of the approximation obtained by hand calculation was confirmed by a computer calculation which was programmed by M. S. Corrington and T. C. Hilinsky. The computer program involved a calculation of the distribution function $\varphi_x(t)$ in the form of equation (D. 11). The first 1000 terms of the product were used. A Fourier transform program was then used to compute $f_1(x)$, the probability density function for x.

Having computed the distribution of x, the distribution of the sum of two such variables can be computed by direct convolution, or, by squaring the characteristic function $\varphi_x(t)$ and Fourier transforming. The results of the calculations described above are shown in Table D. 2. In this table are given the probability density and distribution functions for x and y, where x and y are random variables formed as follows:

$$x = \sum_{-\infty}^{\infty} \frac{\alpha_n}{n} \qquad \alpha_n = +1, -1 \text{ each with probability } 1/2, \text{ with random independent choices.} \qquad \text{(D. 12)}$$

$$y = \sum_{n=-\infty,\, n\neq 0}^{\infty} \frac{\alpha_n}{n}$$

The variance and standard deviation of these distributions are:

$$\sigma_x^2 = 1.64493 \qquad \sigma_x = 1.28256$$
$$\sigma_y^2 = 3.28986 \qquad \sigma_y = 1.81382 \qquad \text{(D. 13)}$$

The probability density function for the normalized variable $y/\sigma_y = b_0/a_0$ is plotted in Figure D. 1. Normal distribution having the same variance is also shown for comparison.

The normalized distribution described is the required distribution of b_0 as given by equation (D. 7). The constant K need not be explicitly evaluated, but is chosen to insure that b_0 has the desired rms value. The rms value of the quadrature voltage was made equal to the nominal pulse amlitude a_0 was chosen somewhat arbitrarily for the purpose of calculating error probabilities. This is a pessimistic assumption, for as seen from Table D. 1, the rms value of b_0 at pulse centers is actually about 19 percent less than the nominal pulse amplitude, a_0. On the other hand, the approximate distribution defined by equation D. 7 gives a result more optimistic than the exact distribution defined by equation D. 6. In addition, intersymbol interference has been neglected.

TABLE D.2

PROBABILITY DENSITY AND DISTRIBUTION FUNCTIONS FOR x AND y

x, y	$f_1(x)$	$F_1(x)$	$f_2(y)$	$F_2(y)$
0	0.25000	0.50000	0.21035	0.50000
0.1	0.24999	0.52500	0.21004	0.52102
0.2	0.24997	0.55000	0.20912	0.54199
0.3	0.24992	0.57499	0.20760	0.56283
0.4	0.24980	0.59998	0.20550	0.58349
0.5	0.24955	0.62495	0.20285	0.60391
0.6	0.24907	0.64988	0.19969	0.62404
0.7	0.24821	0.67475	0.19606	0.64383
0.8	0.24678	0.69951	0.19200	0.66324
0.9	0.24453	0.72408	0.18755	0.68222
1.0	0.24122	0.74838	0.18277	0.70074
1.1	0.23659	0.77228	0.17769	0.71876
1.2	0.23041	0.79564	0.17236	0.73627
1.3	0.22253	0.81830	0.16683	0.75323
1.4	0.21285	0.84009	0.16113	0.76963
1.5	0.20142	0.86082	0.15529	0.78545
1.6	0.18835	0.88032	0.14934	0.80068
1.7	0.17385	0.89844	0.14331	0.81531
1.8	0.15823	0.91505	0.13723	0.82934
1.9	0.14181	0.93006	0.13110	0.84276
2.0	0.12500	0.94340	0.12494	0.85556
2.1	0.10819	0.95506	0.11877	0.86775
2.2	0.09177	0.96505	0.11260	0.87931
2.3	0.07615	0.97344	0.10645	0.89027
2.4	0.06165	0.98032	0.10032	0.90061
2.5	0.04858	0.98582	0.09422	0.91033
2.6	0.03715	0.99009	0.08818	0.91945
2.7	0.02748	0.99331	0.08221	0.92797
2.8	0.01959	0.99564	0.07632	0.93590
2.9	0.01341	0.99728	0.07053	0.94324

TABLE D.2 (Continued)

x, y	$f_1(x)$	$F_1(x)$	$f_2(y)$	$F_2(y)$
3.0	0.00878	0.99838	0.06487	0.95001
3.1	0.00547	0.99908	0.05935	0.95622
3.2	0.00322	0.99951	0.05400	0.96188
3.3	0.00179	0.99975	0.04885	0.96702
3.4	0.00093	0.99988	0.04390	0.97166
3.5	0.00045	0.99995	0.03920	0.97581
3.6	0.00020	0.99998	0.03475	0.97951
3.7	0.00008	0.99999	0.03058	0.98277
3.8	0.00003	1.00000	0.02669	0.98563
3.9	0.00001	1.00000	0.02311	0.98812
4.0	0.00000	1.00000	0.01983	0.99026
4.1			0.01686	0.99210
4.2			0.01419	0.99365
4.3			0.01183	0.99494
4.4			0.00975	0.99602
4.5			0.00795	0.99690
4.6			0.00640	0.99762
4.7			0.00510	0.99819
4.8			0.00400	0.99864
4.9			0.00310	0.99900
5.0			0.00237	0.99927
5.1			0.00178	0.99948
5.2			0.00132	0.99963
5.3			0.00096	0.99974
5.4			0.00069	0.99983
5.5			0.00048	0.99988
5.6			0.00033	0.99992
5.7			0.00022	0.99995
5.8			0.00015	0.99997
5.9			0.00010	0.99998
6.0			0.00006	0.99999
6.1			0.00004	0.99999
6.2			0.00002	1.00000
6.3			0.00001	1.00000
6.4			0.00001	1.00000
6.5			0.00000	1.00000

D.2 THE ENVELOPE DISTRIBUTION

Having obtained the quadrature distribution, as previously described, an approximation to the envelope distribution is obtained as follows. The envelope e(t), is defined as:

$$e(t) = \sqrt{a^2(t) + b^2(t)} \tag{D.14}$$

Because a(t) and b(t) are Hilbert pairs, they are uncorrelated variables, but not necessarily statistically independent. When the pulse train has negligible intersymbol interference, however, a_0 and b_0 (the values at pulse center) are essentially independent. Also, under this condition, a_0^2 is a constant. Thus the normalized envelope is:

$$\frac{e}{a_0} = \sqrt{1 + b_0^2/a_0^2} \tag{D.15}$$

The probability that the normalized envelope exceeds some value, z, is:

$$Pr\left\{\frac{e}{a_0} > z\right\} = Pr\left\{\frac{b_0}{a_0} > \sqrt{z^2 - 1}\right\} \tag{D.16}$$

Using this relation and the distribution obtained for b_0/a_0, the probability that the normalized envelope at a pulse center exceeds a given level is obtained. This is given in Table D.3\.

TABLE D.3

AMPLITUDE DISTRIBUTION OF NORMALIZED ENVELOPE

x	Probability that $e/a_o > x$
1.0	1.0
1.65	0.1
2.40	0.01
2.88	0.001
3.20	0.0001
3.47	0.00001

This distribution described by Table D.3 is a pessimistic approximation to the envelope distribution at pulse centers as it has assumed that the rms value of the quadrature voltage equals the nominal peak pulse amplitude, a_o. The distribution given for the envelope at pulse edges is however, probably an optimistic estimate. The distribution given by Table D.3 is believed to be sufficiently accurate for all practical purposes.

The rms value of the envelope is given by:

$$e_{rms} = \sqrt{a^2_{rms} + b^2_{rms}}$$

Since $a^2_{rms} \approx b^2_{rms}$ then $e_{rms} = \sqrt{2}\, a_{rms}$

Since $a_{rms} = 0.923 a_o$ we have $e_{rms} = 1.31 a_o$.

If the "peak" envelope amplitude is defined as that which is exceeded less than 1 percent of the time, Table D.3 gives the ratio of "peak" amplitude to a_o as 2.4/1. Therefore, the ratio of "peak" to rms is 1.83/1, or 5.25 db.

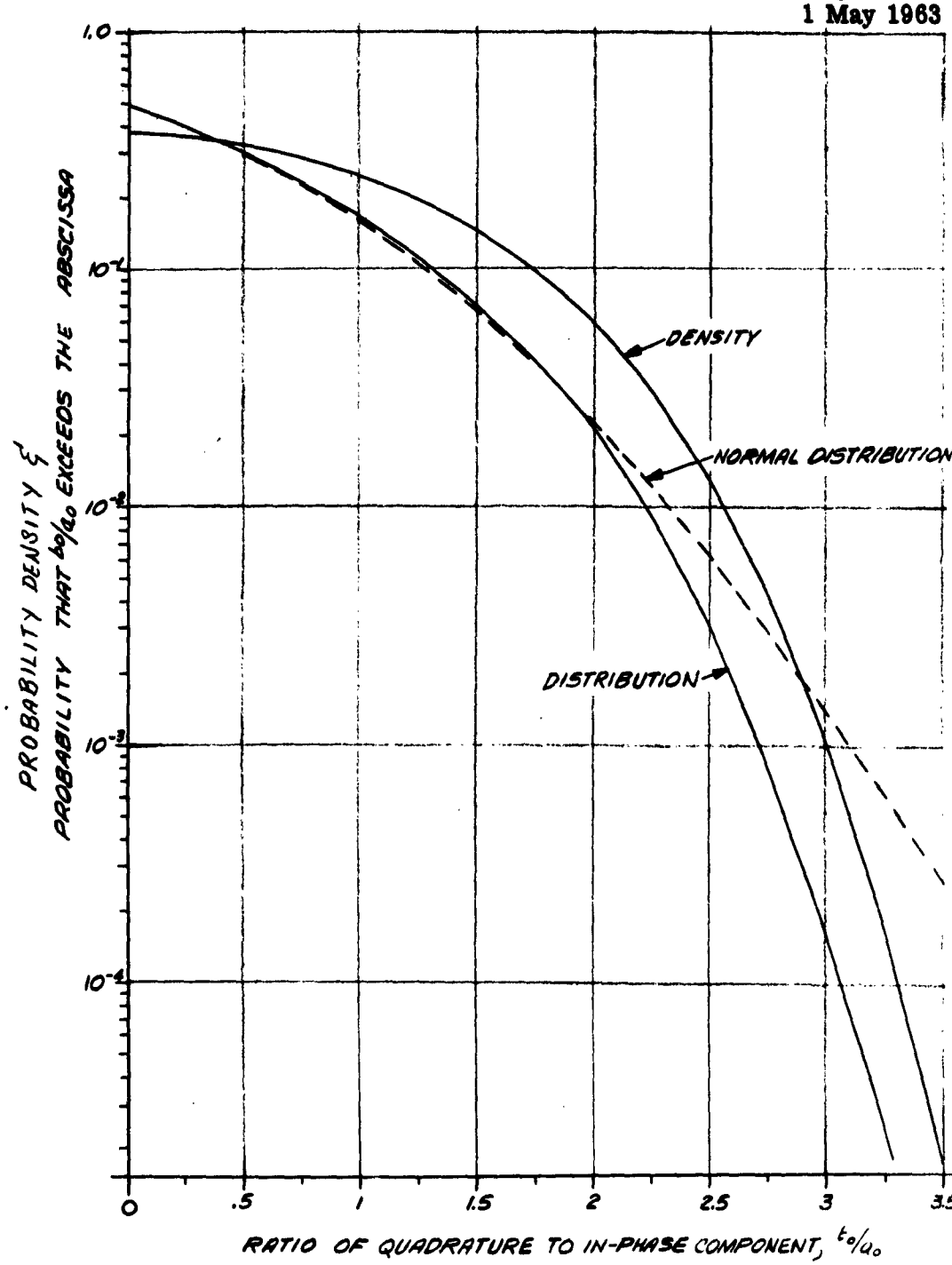

Figure D.1. Probability Density and Distribution For the Normalized Quadrature Voltage in a PCM-SSB Signal

APPENDIX E

THE ELEMENTS OF A FREQUENCY LOCATING SYSTEM

This appendix considers the operation of limiters, discriminators, and detectors, and their use in an AFC system for SSB signals. These devices are usually part of an FM demodulator and due to the wealth of experience which has accumulated for FM reception, can be taken for granted in that application. When the devices are used to process SSB signals, which have completely asymmetric spectra, it is worth reexamining the behavior of at least the idealized models of these devices.

E.1 LIMITERS

An "ideal" limiter is a device with an output of + 1 when the input signal is positive and - 1 when the input signal is negative. Thus, after limiting, only the location of zero crossings is preserved in the output. From the usual representation of a narrow band signal:

$$s(t) = R(t)\cos(\omega_0 t + \varphi(t)), \quad R > 0 \tag{E.1}$$

it is clear that zero crossings are determined solely by the total phase: $\varphi = \omega_0 t + \varphi(t)$. Also, all signals having the same phase function will become identical after ideal limiting. The question now arises as to the extent it is possible to convert the signal, s(t), to a purely phase modulated signal of the form: $\cos(\omega_0 t + \varphi(t))$. That is, to what extent can an ideal limiter be said to remove amplitude modulation and leave phase modulation unchanged? This question is answered as follows:

The limiter output is a function of Q, such that:

$$f(Q) = +1, \quad (4k-1)\frac{\pi}{2} \leq Q < (4k-3)\frac{\pi}{2}$$
$$= -1, \quad (4k-3)\frac{\pi}{2} \leq Q < (4k-1)\frac{\pi}{2} \qquad \text{(E.2)}$$

where: $k = 1, 2, 3 \ldots$

$$f(Q) = \sum_{k=1}^{\infty} a_{2k-1} \cos(2k-1)Q \qquad \text{(E.3)}$$

where:
$$a_{2k-1} = -(-1)^k \cdot \frac{4}{\pi} \cdot \frac{1}{(2k-1)}$$

The last relation is simply the Fourier series representation of the square wave, $F(Q)$. Except for a change in magnitude the first term in the summation is:

$$\cos Q \equiv \cos(\omega_0 t + \varphi(t)), \qquad \text{(E.4)}$$

The desired pure phase modulation. The remaining terms are pure phase modulations of multiples of the original carrier frequency. If the spectrum of the first term does not overlap the harmonic spectra, a simple filtering operation is sufficient to remove all but the desired pure phase modulation from the limiter output. In answer to the question raised, it appears that if the spectrum of $\cos\varphi(t)$ is essentially band limited, then for a sufficiently high carrier frequency all amplitude modulation can be removed with an ideal limiter and low-pass filter.

E.2 DISCRIMINATOR

An ideal discriminator is a device whose output voltage is proportional to the instantaneous frequency of any input signal having a constant envelope. Given an input signal, it is easily shown that by differentiation, and envelope

detection, the required property of a discriminator can be obtained. Thus

$$\frac{ds_i}{dt} = -\left(\omega_0 + \frac{d\varphi}{dt}\right) \sin\left(\omega_0 t + \varphi(t)\right) \qquad \text{(E.5)}$$

and for $\left|\frac{d\varphi}{dt}\right| < \omega_0$, the envelope of the derivative is just:

$$\left(\frac{ds_i}{dt}\right)_{env} = \omega_0 + \frac{d\varphi}{dt} = \omega_0 + \omega_i \qquad \text{(E.6)}$$

The requirement that the envelope be constant is important because if:

$$s_i = R(t) \cos\left(\omega_0 t + \varphi(t)\right) \qquad \text{(E.7)}$$

then $\frac{ds_i}{dt} = \dot{R} \cos\left(\omega_0 t + \varphi(t)\right) - \left(\omega_0 + \dot{\varphi}\right) R \sin\left(\omega_0 t + \varphi(t)\right)$

The envelope of this signal is:

$$\left(\frac{ds_i}{dt}\right)_{env} = \sqrt{(\dot{R})^2 + R^2(\omega_0 + \dot{\varphi})^2} \approx R(\omega_0 + \dot{\varphi}) \qquad \text{(E.8)}$$

This signal is clearly very different from the usually desired output, $\omega_0 + \dot{\varphi}$, unless R is constant.

From well known properties of Fourier transforms, a differentiation in time is equivalent to multiplying the signal spectrum by $j\omega$. Thus, the required operation is filtering, utilizing a filter whose amplitude response is proportional to frequency, with a 90° phase shift, over the band of significant frequency components. For proper discriminator operation the requirement of a 90° phase shift is unimportant, since this only has significant effect on the carrier, and is removed by subsequent envelope detection. Practical discriminators also make use of a balanced circuit for removal of the constant

term corresponding to the carrier frequency. The basic circuit element of an ideal discriminator is therefore, a filter having a transfer function which varies linearly with frequency over the band of interest. The band of interest is the band containing significant frequency components of the phase modulated carrier, and may have to be determined experimentally.

E.3 DETECTORS

For the purposes of the appendix an ideal envelope detector is a device with an output voltage that is a function of the "instantaneous" envelope of the input signal. Practical devices can be regarded as having a linear, or a square law relationship between input and output. It must be assumed that many carrier cycles are completed before the envelope changes significantly. A square law envelope detector can be represented mathematically as a squaring device followed by a low-pass filter. Thus for an input signal with envelope and phase variations, after squaring:

$$s^2 = R^2 \cos^2(\omega_0 t + \varphi(t))$$
$$= \tfrac{1}{2} R^2 (1 + \cos 2(\omega_0 t + \varphi(t)) \qquad \text{(E.9)}$$

Assuming that the spectrum of R^2 does not overlap that of $\cos 2(\omega_0 t + \varphi(t))$, after low-pass filtering only the term 1/2 R^2 will remain. The squaring operation generally consists of full wave rectification utilizing diodes, and using only a very small input signal in order to take advantage of the large curvature in diode characteristics near zero input. For a linear envelope detector, the same circuit can be used, but with a large signal input. Applications involving AFC circuits generally concern the mean detector output. For linear envelope detection the mean output is the mean envelope. For square law detection, the mean output has a simple interpretation in the frequency domain because of Parseval's formula (equation A. 12). Thus:

$$\overline{R^2} = \frac{1}{2\pi}\int_{-\infty}^{\infty} |R_p(\omega)|^2 d\omega \qquad \text{(E. 10)}$$

where: $|R_p(\omega)|^2$ is the power spectrum of R(t)

E.4 FREQUENCY LOCATION

Using a discriminator with or without limiting, and then either square law or linear envelope detection, four basic devices for frequency location are obtained. Two of these give a measure of location, which is difficult to interpret theoretically and will not be discussed here, although possibly experiment would show them to have special virtues. The other two combinations are: Limiter, discriminator, and linear envelope detection; and no limiter, discriminator, and square law envelope detection. The first combination develops an output proportional to the average instantaneous frequency. The second combination develops an output which can be interpreted as an operation on the power spectrum of the signal. The latter is analyzed as follows:

For a discriminator assume two filters having transfer functions: $D_1(\omega)$, and $D_2(\omega)$.

The signal is separately passed through each filter, and each output is squared and low-pass filtered, (i.e., square-law envelope detected). The difference of these outputs is then "averaged" by a low-pass filter and used to control the AFC system. The mean value of the difference voltage is calculated, by Parseval's formula, as:

$$\overline{e_o} = \frac{1}{2\pi}\int_{-\infty}^{\infty} |S(\omega)|^2 \left[\, |D_1(\omega)|^2 - |D_2(\omega)|^2 \right] d\omega \qquad \text{(E. 11)}$$

where: $|S(\omega)|^2$ is the signal power spectrum.

The equation clearly shows that the average voltage at the discriminator output corresponds to a weighted average of the signal power spectrum. A great variety of characteristics can be obtained by varying the characteristics of the amplitude response of the discriminator filters. Note that phase response is totally ignored. Because of the great flexibility of the formulation a circuit designer has an embarassing degree of freedom, for it is not clear what weighting should be applied to the various frequency components of the power spectrum. The basic goal is of course, that the discriminator output should be zero when the signal spectrum has been translated in frequency. This ensures that the carrier is within a specified narrow frequency range.

No attempt has been made in this analysis to determine an optimum frequency weighting function. However, the conventional linear discriminator response has been studied to gain some insight into the behavior of a typical system. Assuming the following symmetric linear forms for the filter amplitude responses:

$$\left.\begin{aligned} |D_1(\omega)| &= \tfrac{1}{2} + k(\omega-\omega_d) \\ |D_2(\omega)| &= \tfrac{1}{2} - k(\omega-\omega_d) \end{aligned}\right\} \; |\omega-\omega_d| < \frac{1}{2k} \text{ and } \omega > 0$$

$$\begin{aligned} |D_1(\omega)|^2 &= \tfrac{1}{4} + k^2(\omega-\omega_d)^2 + k(\omega-\omega_d) \\ |D_2(\omega)|^2 &= \tfrac{1}{4} + k^2(\omega-\omega_d)^2 - k(\omega-\omega_d) \\ |D_1(\omega)|^2 - |D_2(\omega)|^2 &= 2k(\omega-\omega_d) \end{aligned} \qquad \text{(E. 12)}$$

This result is substituted in equation (E. 11) and the mean discriminator output is:

$$\overline{e_o} = \frac{2k}{\pi} \int_0^\infty |S(\omega)|^2 (\omega-\omega_d)\, d\omega \qquad \text{(E. 13)}$$

The discriminator operation can thus be described as a calculation of the first moment of signal power spectrum, about the center frequency, W_d, of the discriminator. In an operating AFC system the signal spectrum is shifted until $\bar{e}_o$, hence the first moment, is zero. If the power spectrum is regarded as a distribution of mass, then the spectrum is shifted until the center of gravity, or centroid coincides with W_d. The centroid frequency is not generally the same as the carrier frequency; and the difference is the AFC frequency error. (To the extent that this difference is known and constant, it can, however, be compensated.)

The steady state frequency error can be calculated from equation (E. 13) as follows. The discriminator output $\bar{e}_o$ is zero, and the signal spectrum is shifted until the carrier is located at ω_1. Let $\omega = \omega_1 + \alpha$, then:

$$\int_{-\omega_1}^{\infty} |S(\omega_1+\alpha)|^2 (\omega_1+\alpha-\omega_d)\, d\alpha = 0 \qquad \text{(E. 14)}$$

For an upper sideband SSB signal, $S(\omega_1+\alpha)$ is zero except for $\alpha > 0$. Transposing terms in this equation, the frequency error is:

$$\omega_e = \omega_d - \omega_1 = \frac{\int_0^{\infty} |S'(\alpha)|^2 \alpha\, d\alpha}{\int_0^{\infty} |S'(\alpha)|^2 d\alpha} \qquad \text{(E. 15)}$$

where: $|S'(\alpha)|^2$ is the power spectrum, referred to baseband.

Note that the denominator is proportional to signal power, and that the ratio is independent of any multiplying constant associated with the power spectrum. Also, if the spectrum has a line component at the carrier frequency, this appears in equation (E. 15) as an impulse at $\alpha = 0$, and hence does not affect the numerator.

Supplemental Report

BIT-ERROR RATE IN SSB-PCM DEPENDING ON SIGNAL-TO-NOISE RATIO, PHASE JITTER IN RE-INSERTED CARRIER, AND QUADRATURE DISTORTION

BY

S. Weber

Contents

Abstract:

An SSB pulsed signal, plus noise, in the IF filter is mixed (multiplied) with the output of a phase-jittered oscillator. The product, after being passed through a low pass filter, is sampled at the bit-rate. Error rates at the LP filter output are determined and curves presented. These include the effect of fixed values of the quadrature component.

Conclusions

Consider Figure 4 where no quadrature is assumed to be present at the time of sampling. Plotted here are curves of error-rate versus signal-noise ratio in the IF, depending on the amount of phase jitter in the injected carrier (PLO). The signal-noise equivalent of the phase jitter on the injected carrier is also noted. At the time of sampling the desired in-phase component is either plus one or minus one in a binary system, or to put it another way, the in-phase component of carrier is in one of its two possible phases. Phase errors in the PLO, which acts like a phase reference in a coherent detection system, thus produce bit-errors. The error-rate curve farthest to the left is the case where no phase jitter exists, and errors arise due only to noise in the signal channel. The result is the well-known error-rate curve for coherent PSK detection. About one db to the right is a dashed curve denoted as "differential PSK". Intersections of the dashed curve with the error-rate curves determine points at which the signal-noise in the signal channel equals the equivalent signal-noise in the reference phase. The error-rate at such points are thus given by the well-known DPSK formula. Beyond this point, for a given phase-jitter, there is a sharp drop to a constant error-rate, irrespective of further increase in radiated power.

Now the curves of Figure 3 show how this limiting, constant error-rate is influenced by the presence of the quadrature component at the time of sampling. It is seen that the quadrature component has no effect until it comes within 15 db of the desired component. In the next 5 db, the error-rate approximately doubles. The quadrature level here is one-third the desired level. For further increases in quadrature level, the error-rate rises rapidly, increasing by a factor of ten, approximately, when the ratio of quadrature to in-phase components is one-half. Figures 1 and 2 each contain the same information as figure 3.

1. Introduction

Consider the following system used for the reception of transmitted marks and spaces.

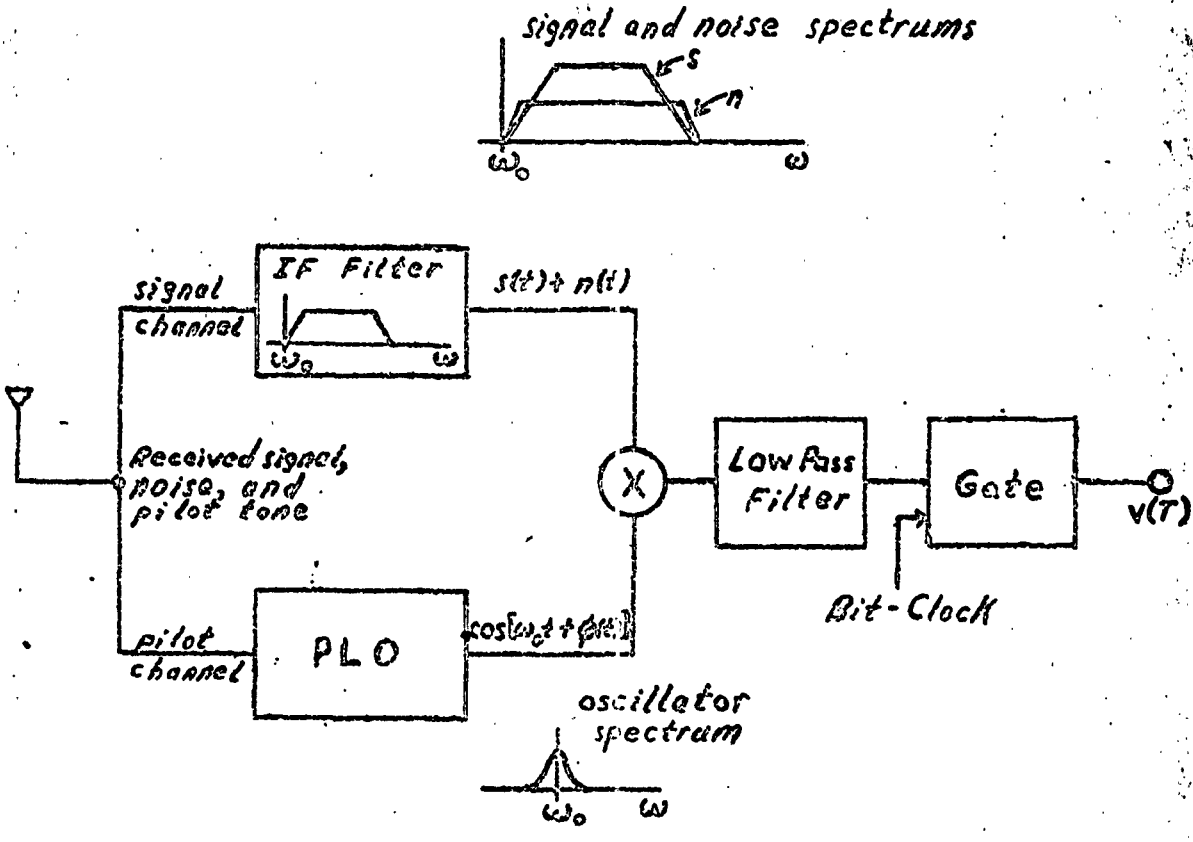

The received signal plus noise, and the pilot tone are fed into the IF filter and the phase-locked oscillator (PLO). The filter output is signal plus noise (the pilot tone having been rejected), and the oscillator output is the pilot frequency with a random phase perturbation due to the interference at the input to the PLO. These two outputs are passed to a mixer (multiplier) and then integrated in a low-pass (LP) filter. The LP filter output is fed into a gate which samples its input periodically. The gate output is then fed into a pulse regenerator which reconstitutes the transmitted bit-stream except for errors in decision. The problem considered here is to determine the probability of an incorrect decision.

2. Mathematical Formulation

Now let the signal at the IF filter output at time t be defined by

$$(1) \qquad S(t) = a(t)\cos(\omega_o t) + b(t)\sin(\omega_o t)$$

where $a(t)$ and $b(t)$ for the cases of a single transmitted mark and space are shown below. $b(t)$ is commonly referred to as the quadrature component or distortion generated by suppressing one sideband.

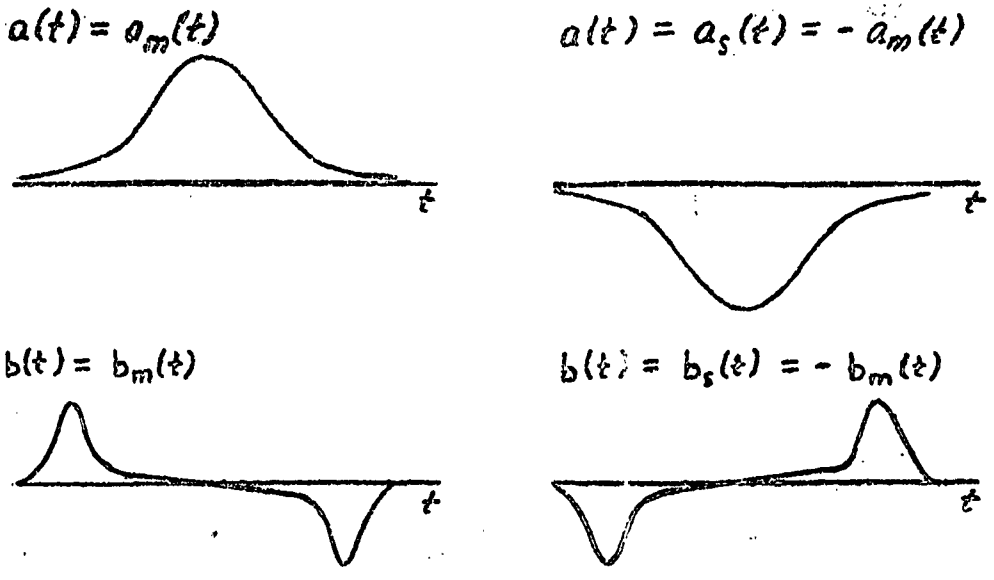

The polarities indicated for $b(t)$ are those for an upper sideband transmission. If the lower sideband is selected one need only invert the quadrature components shown. However, either choice does not affect the following work.

The ideal sampling time is at the peak of the $a(t)$ pulse at which time $b(t)$ is approximately zero (in fact exactly zero if $a(t)$ is symmetrical). Also sampling inaccuracies will cause one to miss the desired peak slightly, and thus even if $b(t)$ were exactly zero at the peak, one would sample some non-zero value of quadrature distortion.

Furthermore, the comparative amounts of desired and quadrature levels sampled depend on the accuracy with which the phase of the pilot tone has been mixed (multiplied) with the signal channel. An obvious example is a phase error of 90° which results in sampling of the quadrature component only. Thus SSB pulse transmission has inherent "noise" in it depending on the factors pointed out above. These are included in the analysis presented.

We represent the real noise at the IF filter output by

$$(2) \quad n(t) = x(t)\cos(\omega_0 t) + y(t)\sin(\omega_0 t),$$

where $x(t)$ and $y(t)$ are statistically independent gaussian random variables with zero means and unit variances, i.e.

$$(3) \quad P_1(x) = \frac{1}{\sqrt{2\pi}} e^{-\frac{1}{2}x^2}, \quad \bar{x} = 0, \quad \overline{x^2} = 1$$

$$(4) \quad P_2(y) = \frac{1}{\sqrt{2\pi}} e^{-\frac{1}{2}y^2}, \quad \bar{y} = 0, \quad \overline{y^2} = 1$$

where horizontal bars denote either time or ensemble averages, i.e. $x(t)$ and $y(t)$ are assumed to be members of ergodic stationary processes.

$n(t)$ is a single-sideband signal. Thus x(t) and y(t) constitute a Hilbert Transform pair.* This functional dependence of x(t) and y(t) can be shown not to contradict the fact that x(t) and y(t) are statistically independent.**

Let $\phi(t)$ be the phase jitter of the phase-locked oscillator, where $-\pi \leq \phi \leq \pi$ and ϕ is a random variable whose density will be specified later.

Now consider the quantity $[s(t) + n(t)] \cos [\omega_o t + \phi(t)]$, that is the LP filter input. We have from (1) and (2),

$$(5) \quad [s(t) + n(t)] \cos[\omega_o t + \phi(t)] = \frac{a(t) + x(t)}{2} \cos\phi(t) - \frac{b(t) + y(t)}{2} \sin\phi(t) + \frac{a(t) + x(t)}{2} \cos[2\omega_o t + \phi(t)] + \frac{b(t) + y(t)}{2} \sin[2\omega_o t + \phi(t)]$$

Then V(t), the LP filter output, is given by

$$(6) \quad V(t) = \frac{a(t) + x(t)}{2} \cos\phi(t) - \frac{b(t) + y(t)}{2} \sin\phi(t)$$

Then V(t) in the cases of transmitted marks and spaces is

$$(7) \quad V_m(t) = V(t)\Big]_{mark} = \frac{a_m(t) + x(t)}{2} \cos\phi(t) - \frac{b_m(t) + y(t)}{2} \sin\phi(t$$

$$(8) \quad V_s(t) = V(t)\Big]_{space} = \frac{a_s(t) + x(t)}{2} \cos\phi(t) - \frac{b_s(t) + y(t)}{2} \sin\phi(t$$

$$= -\frac{a_m(t) - x(t)}{2} \cos\phi(t) + \frac{b_m(t) - y(t)}{2} \sin\phi(t$$

* See References 1 and 2

** See Appendix 1

Now if $v(T) > 0$ ($v(T) < 0$) we must assume that a mark (space) was transmitted. Then the average error ϵ is given by

$$(9) \quad \epsilon = P_m \cdot P[v(T) < 0 | m] + P_s \cdot P[v(T) > 0 | s]$$
$$= \frac{1}{2}\left\{ P[v(T) < 0 | m] + P[v(T) > 0 | s] \right\}$$

where $P_m = \frac{1}{2}$ and $P_s = \frac{1}{2}$ are the a priori probabilities of a mark and space being transmitted.

Now since $a_s(t) = -a_m(t)$, $b_s(t) = -b_m(t)$, and since X, Y, and ϕ have even probability density functions then we have

$$(10) \quad P[v(T) < 0 | m] = P[v(T) > 0 | s]$$

Now define

$$(11) \quad a = a_m(T), \quad b = b_m(T), \quad V_m = v(T)$$

$$(12) \quad \phi = \phi(T), \quad x = X(T), \quad y = Y(T)$$

Then from (7), (9)-(12) we obtain

$$(13) \quad \epsilon = P[v(T) < 0 | m]$$
$$= P[V_m < 0]$$
$$= P[(a + x)\cos\phi - (b + y)\sin\phi < 0]$$

3. Equivalent Noise of Phase Jitter

Let us define the phase jitter ϕ on the inserted carrier to have the probability density $p(\phi)$. $p(\phi)$ will be assumed to be the result of the presence of a certain noise added on to the inserted carrier which produces a phase jitter equivalent to that at the output of a PLO. The actual jitter distribution has not as yet been solved due to difficulties in the analysis of the PLO. However, at total signal-to-interference ratios of 3 db or more at the input, the PLO takes on more and more of a linear transfer character. Under these conditions the PLO output carrier, though substantially constant in amplitude, will have a phase variation essentially as though a certain amount of noise were added to an ideal output. This amount of noise is referred to in this presentation as the equivalent noise corresponding to a given rms phase jitter. Figure 5 of this report provides a curve showing the correspondence between rms phase jitter and the equivalent signal-noise in the inserted carrier.

The probability density on phase jitter is thus given by

$$(14)\quad p(\phi) = \begin{cases} \frac{1}{2\pi} e^{-\frac{1}{2}\alpha^2} \left[1 + \sqrt{2\pi}\,\alpha \cos\phi\, e^{\frac{1}{2}\alpha^2 \cos^2\phi}\, \Phi(\alpha\cos\phi)\right], & |\phi| \le \pi \\ 0, & |\phi| > \pi \end{cases}$$

where and

$$(15)\quad \Phi(x) = \frac{1}{\sqrt{2\pi}} \int_{-\infty}^{x} e^{-\frac{1}{2}y^2}\, dy$$

At extremes we have

$$(16)\quad p(\phi)\Big]_{\alpha=0} = \begin{cases} \frac{1}{2\pi}, & |\phi| \le \pi \\ 0, & |\phi| > \pi \end{cases}$$

$$(17)\quad p(\phi)\Big]_{\alpha=\infty} = \delta(\phi)$$

Curves of $p(\phi)$ are shown on page 418 reference 3, where the value of Φ to be used in equation (9.58) and Figure 9.4 is $\Phi = 0$.

4. Determination of Error-Rates

We now determine the error rates in the noiseless and noise cases.

a. Noiseless Case

Here we have

$$x(t) = y(t) = 0 \tag{18}$$

Then from (13) we have

$$\begin{aligned} \epsilon &= P[a\cos\phi < b\sin\phi] \\ &= 1 - P[a\cos\phi \geq b\sin\phi] \\ &= 1 - P[-\pi + \phi_0 \leq \phi \leq \phi_0], \end{aligned} \tag{19}$$

*

where

$$\phi_0 = \tan^{-1}\left(\frac{a}{|b|}\right), \quad a > 0, \quad -\infty < b < \infty, \quad 0 < \phi_0 \leq \frac{\pi}{2} \tag{20}$$

Now it can be shown that**

$$P[-\pi + \phi_0 \leq \phi \leq \phi_0] = \Phi(\alpha \sin\phi_0) \tag{21}$$

where $P(\phi)$ is given in (14).

Then

$$\epsilon(\alpha, c) = 1 - \Phi(\alpha \sin\phi_0) = 1 - \Phi\left(\frac{\alpha}{\sqrt{1+c^2}}\right) \tag{22}$$

where

$$c = \frac{b}{a} \tag{23}$$

and where we have written $\epsilon(\alpha, c)$ rather than ϵ to show the parameters concerned.

* See Appendix 2

** See Appendix 3

Then

$$(24)\quad \epsilon(\alpha, c) = \epsilon\left(\frac{\alpha}{|c|}, \frac{1}{c}\right) = 1 - \Phi\left(\frac{\alpha}{\sqrt{1+c^2}}\right)$$

Thus if we plot $\epsilon(\alpha, c)$ vs. α with $|c| < 1$ as parameter, we can determine the value of $\epsilon(\alpha, c)$ for $|c| > 1$ from (24) since the curve for $\epsilon\left(\frac{\alpha}{|c|}, \frac{1}{c}\right)$ will have been plotted.

Curves of $\epsilon(\alpha, c)$ are shown in Figure 1 where ϵ is plotted vs. α with $|c|$ as parameter, in Figure 2 where α is plotted vs. $|c|$ with ϵ as parameter (i.e. curves of constant error rate), and in Figure 3 where $\epsilon(\alpha, c)$ is plotted vs. $\mathcal{C}$(db) with $\mathcal{A}$ (db) as parameter, where C and $\mathcal{A}$ are defined in (37) and (38).

b. Noise Case

Here we may show*

$$(25)\quad \epsilon(\alpha, a, b) = \int_{-\pi}^{\pi} p(\phi)\, \Phi(-a\cos\phi + b\sin\phi)\, d\phi$$

where $p(\phi)$ is given by (14), and where we have written $\epsilon(\alpha, a, b)$ rather than ϵ to show the parameters.

We can show**

$$(26)\quad \epsilon(\alpha, a, b) = \epsilon(\alpha, a, -b)$$

$$(27)\quad \epsilon(\alpha, a, b) = \frac{1}{2} - \frac{1}{\sqrt{2\pi}} \int_0^{\pi} \alpha\cos\phi\, e^{-\frac{1}{2}\alpha^2\sin^2\phi}\, \Phi(a\cos\phi - b\sin\phi)\, d\phi$$

$$= \Phi(\alpha) - \frac{1}{\sqrt{2\pi}} \int_0^{\pi/2} \alpha\cos\phi\, e^{-\frac{1}{2}\alpha^2\sin^2\phi} \left[\Phi(a\cos\phi - b\sin\phi) + \Phi(a\cos\phi + b\sin\phi)\right] d\phi$$

$$(28)\quad \epsilon(0, a, b) = \frac{1}{2}$$

$$(29)\quad \epsilon(\infty, a, b) = 1 - \Phi(a)$$

$$(30)\quad \epsilon(\alpha, 0, b) = \frac{1}{2}$$

$$(31)\quad \epsilon(\alpha, \infty, b) = 1 - \Phi(\alpha)$$

$$(32)\quad \epsilon(\alpha, \alpha, 0) = \frac{1}{2} e^{-\frac{1}{2}\alpha^2}$$

* See Appendix 4

** See Appendix 5

$$(33)\quad \epsilon(\alpha, a, \infty) = \frac{1}{2}$$

$$(34)\quad \lim_{a \to \infty} \epsilon(\alpha, a, ac) = 1 - \Phi\left(\frac{\alpha}{\sqrt{1+c^2}}\right) = \epsilon(\alpha, c) \qquad (c \neq 0)$$

Unfortunately it was not possible to perform the required integration in (25) or (27) to obtain $\epsilon(\alpha, a, b)$. However, much can be learned of the shape of $\epsilon(\alpha, a, b)$ curves from (28)-(34) and some numerical integrations for specific values of α, a, and b.

Now make the following definitions:

$$(35)\quad A\,(db) = 20 \log_{10}\left(\frac{a}{\sqrt{2}}\right)$$

$$(36)\quad B\,(db) = 20 \log_{10}\left(\frac{|b|}{\sqrt{2}}\right)$$

$$(37)\quad \Delta\,(db) = 20 \log_{10}\left(\frac{\alpha}{\sqrt{2}}\right)$$

$$(38)\quad C\,(db) = 20 \log_{10}|c| = B - A, \quad c = \frac{b}{a}$$

Figure 4 shows $\epsilon(\alpha, a, 0)$ vs. A with Δ as parameter. Included is the graph of (32). It is seen that the curves, for larger values of a, reach the limiting value of $1 - \Phi(\alpha)$ given by (31).

From (34) and (24) it is seen that Figures 1, 2, and 3 in addition to being curves representing (24) are also curves representing (34).

5. Determination of rms Phase Jitter, $\sqrt{\overline{\phi^2}}$

We now consider the rms value of ϕ i.e. $\sqrt{\overline{\phi^2}}$ where

$$(39)\quad \overline{\phi^2} = \int_{-\pi}^{\pi} \phi^2 P(\phi)\, d\phi ,$$

where $P(\phi)$ is given by (14). The most practical method of determining $\overline{\phi^2}$ appeared to be numerical integration, the results of which are shown in Figure 5. The integrations were performed using the result

$$(40)\quad \int_0^{\Theta} P(\phi)\, d\phi = \frac{\Theta}{2\pi} + \frac{1}{4}\,\mathrm{erf}\left(\frac{\alpha}{\sqrt{2}}\sin\Theta\right) + V(\alpha\sin\Theta, \alpha\cos\Theta) \quad , \quad -\pi \le \Theta \le \pi$$

where

$$(41)\quad \mathrm{erf}(x) = \frac{2}{\sqrt{\pi}}\int_0^x e^{-y^2}\, dy = 2\Phi(x\sqrt{2}) - 1$$

$$(42)\quad V(h,K) = \int_{x=0}^{x=h}\int_{y=0}^{y=\frac{K}{h}x} \frac{1}{2\pi} e^{-\frac{1}{2}(x^2+y^2)}\, dy\, dx$$

For the properties and tables of $V(h,K)$ see reference 6. (40) can be shown by the method used in Appendix 3.

The values of $\sqrt{\overline{\phi^2}}$ in degrees shown in Figures 1-4 were taken from Figure 5.

From (16), (17), and (39) we obtain the following limiting values of $\overline{\phi^2}$:

$$(43)\quad \overline{\phi^2}\Big]_{\alpha=0} = \int_{-\pi}^{\pi} \phi^2 \frac{1}{2\pi}\, d\phi = \frac{\pi^2}{3}$$

$$(44)\quad \phi^2\Big]_{\alpha=\infty} = \int_{-\pi}^{\pi} \phi^2\, \delta(\phi)\, d\phi = 0$$

APPENDIX I

Statistical Independence of Hilbert Noise Pairs

The Hilbert Transform of $f(t)$ is defined as*

$$(1\text{-}1) \qquad H_\tau [f(t)] = \frac{1}{\pi} \int_{t=-\infty}^{t=\infty} \frac{f(t)}{\tau - t}\, dt \equiv H_\tau f$$

Then from (2) we have*

$$(1\text{-}2) \qquad x(t) = H_t\, y$$

$$(1\text{-}3) \qquad y(t) = -H_t\, x$$

In view of (1-2) and (1-3) it might appear that $x(t)$ and $y(t)$ are dependent. However we may reason as follows.

From (1-2) and (1-3) we obtain the fact that $x(t)$ and $y(t)$ are uncorrelated at the same time instant, that is $E[x(t)y(t)] = 0$.** Since $x(t)$ and $y(t)$ are gaussian random variables then $x(t)$ and $y(t)$ are statistically independent. There is thus no contradiction between the facts that $x(t)$ and $y(t)$ are statistically independent random variables and a Hilbert Transform pair.

* See references 1 and 2

** See reference 2, page 55 and reference 4, page 6

APPENDIX 2

Proof that $P[a\cos\phi \geq b\sin\phi] = P[-\pi + \phi_0 \leq \phi \leq \phi_0]$

In the following we use the definition of ϕ_0 given in (20).

1. Let $a > 0,\ b \geq 0$

Then drawing the graphs of $a\cos\phi$ and $b\sin\phi$ it will be easily seen that

(2-1) $P[a\cos\phi \geq b\sin\phi] = P[-\pi + \phi_0 \leq \phi \leq \phi_0]$

2. Let $a > 0,\ b \leq 0$

Again from the graphs of $a\cos\phi$ and $b\sin\phi$ it will be easily seen that

(2-2) $$P[a\cos\phi \geq b\sin\phi] = P[-\phi_0 \leq \phi \leq \pi - \phi_0]$$

$$= \int_{\phi=-\phi_0}^{\phi=\pi-\phi_0} p(\phi)\,d\phi$$

$$= \int_{\theta=\phi_0}^{\theta=\phi_0-\pi} p(-\theta)\,(-d\theta) \qquad (\theta = -\phi)$$

$$= \int_{\theta=\phi_0-\pi}^{\theta=\phi_0} p(\theta)\,d\theta$$

$$= P[\phi_0 - \pi \leq \phi \leq \phi_0]$$

Thus from (2-1) and (2-2) we obtain

(2-3) $P[a\cos\phi \geq b\sin\phi] = P[\phi_0 - \pi \leq \phi \leq \phi_0]$ $\left(\begin{matrix} a > 0 \\ -\infty < b < \alpha \end{matrix}\right.$

APPENDIX 3

Proof that $P[-\pi + \phi_0 \le \phi \le \phi_0] = \Phi(\alpha \sin \phi_0)$

Let r and ϕ be two random variables having the joint probability density,

$$(3\text{-}1)\quad P(r,\phi) = \begin{cases} \frac{1}{2\pi N} e^{-\frac{1}{2}\alpha^2} \, r \, e^{-\frac{r^2 - 2\alpha\sqrt{N} r \cos\phi}{2N}} & \begin{pmatrix} 0 \le r < \infty \\ -\pi \le \phi \le \pi \end{pmatrix} \\ 0 \qquad (elsewhere) \end{cases}$$

where N is any positive quantity.*

Then for $-\pi \le \phi \le \pi$ we have

$$(3\text{-}2)\quad \int_0^\infty p(r,\phi)\,dr = \frac{1}{2\pi N} e^{-\frac{1}{2}\alpha^2} e^{\frac{1}{2}\alpha^2\cos^2\phi} \int_0^\infty r\, e^{-\frac{(r - \alpha\sqrt{N}\cos\phi)^2}{2N}} dr$$

$$= \frac{1}{2\pi N} e^{-\frac{1}{2}\alpha^2 \sin^2\phi} \int_{-\alpha\sqrt{N}\cos\phi}^{\infty} (u + \alpha\sqrt{N}\cos\phi)\, e^{-\frac{u^2}{2N}} du$$

$$= \frac{1}{2\pi} e^{-\frac{1}{2}\alpha^2} \left[1 + \sqrt{2\pi}\,\alpha \cos\phi\, e^{\frac{1}{2}\alpha^2\cos^2\phi}\, \Phi(\alpha\cos\phi) \right] \qquad (-\pi \le \phi \le \pi)$$

For $|\phi| > \pi$ we have from (3-1),

$$(3\text{-}3)\quad \int_0^\infty p(r,\phi)\,dr = 0 \qquad (|\phi| > \pi)$$

* See reference 5, page 399

From (14), (3-2), and (3-3) we obtain

$$(3\text{-}4) \qquad \int_0^\infty p(r,\phi)\,dr = p(\phi) \qquad (-\infty < \phi < \infty)$$

Now from (20) it is seen that $0 < \phi_0 \le \frac{\pi}{2}$ or

$-\pi < -\pi + \phi_0 < \phi_0 < \pi$. Then

$$(3\text{-}5) \quad P\left[-\pi + \phi_0 \le \phi \le \phi_0\right] = \int_{\phi=-\pi+\phi_0}^{\phi=\phi_0} p(\phi)\,d\phi$$

$$= \int_{\phi=-\pi+\phi_0}^{\phi=\phi_0} \int_{r=0}^{r=\infty} p(r,\phi)\,dr\,d\phi$$

where $p(r,\phi)$ is given by the first line of (3-1).

Now let

$$(3\text{-}6) \quad \begin{cases} r^2 = u^2 + v^2 \\ \phi = \tan^{-1}\left(\frac{v}{u}\right) \end{cases} \quad \text{or} \quad \begin{aligned} u &= r\cos\phi \\ v &= r\sin\phi \end{aligned} \qquad \begin{aligned} 0 &\le r < \infty \\ -\pi &\le \phi \le \pi \end{aligned}$$

Then

$$(3\text{-}7) \quad P\left[-\pi + \phi_0 \le \phi \le \phi_0\right]$$

$$= \int_{u=-\infty}^{u=\infty} \int_{v=-\infty}^{v=u\tan\phi_0} P[r = r(u,v),\ \phi = \phi(u,v)]\,\frac{dv\,du}{\sqrt{u^2+v^2}}$$

$$= \int_{u=-\infty}^{u=\infty} \int_{v=-\infty}^{v=u\tan\phi_0} \frac{\sqrt{u^2+v^2}}{2\pi N}\, e^{-\frac{1}{2}\alpha^2 - \frac{u^2+v^2-2\alpha\sqrt{N}u}{2N}}\,\frac{dv\,du}{\sqrt{u^2+v^2}}$$

$$= \int_{u=-\infty}^{u=\infty} \int_{v=-\infty}^{v=u\tan\phi_0} \frac{1}{2\pi N}\, e^{-\frac{1}{2N}\left[(u-\alpha\sqrt{N})^2 + v^2\right]}\,dv\,du$$

Now*

$$(3\text{-}8)\qquad \int_{u=-\infty}^{u=\infty}\int_{v=-\infty}^{v=mu+b} \frac{1}{2\pi\sigma_1\sigma_2}\, e^{-\frac{1}{2}\left[\left(\frac{u-\mu_1}{\sigma_1}\right)^2+\left(\frac{v-\mu_2}{\sigma_2}\right)^2\right]}\, dv\, du$$

$$= \Phi\left(\frac{m\mu_1-\mu_2+b}{\sqrt{m^2\sigma_1^2+\sigma_2^2}}\right) \qquad \begin{pmatrix} 0<\sigma_1,\ \sigma_2<\infty \\ -\infty<\mu_1,\mu_2,m,b<\infty \end{pmatrix}$$

Then

$$(3\text{-}9)\qquad P[-\pi+\phi_0 \le \phi \le \phi_0] = \Phi(\alpha \sin\phi_0)$$

* See Appendix 6

APPENDIX 4

Proof that $\epsilon(q,a,b) = \int_{\phi=-\pi}^{\phi=\pi} p(\phi)\, \Phi(-a\cos\phi + b\sin\phi)\, d\phi$

Define

$$(4\text{-}1) \qquad q = q(T) = x(T)\cos\phi(T) - y(T)\sin\phi(T) = x\cos\phi - y\sin\phi$$

Then from (7), (11), and (12) obtain

$$(4\text{-}2) \qquad V_m = V_m(T) = \tfrac{1}{2}(q + a\cos\phi - b\sin\phi)$$

Now consider ϕ fixed. Then by (3) and (4) we have

$$(4\text{-}3) \qquad \bar{q} = \bar{x}\cos\phi - \bar{y}\sin\phi = 0$$

$$(4\text{-}4) \qquad \overline{q^2} = \overline{x^2}\cos^2\phi - 2\bar{x}\bar{y}\cos\phi\sin\phi + \overline{y^2}\sin^2\phi = \cos^2\phi + \sin^2\phi = 1$$

For fixed ϕ, q is a normal random variable as seen from (4-1). Then the conditional density function of q, given ϕ, is by (4-3) and (4-4),

$$(4\text{-}5) \qquad p(q \mid \phi) = \frac{1}{\sqrt{2\pi}} e^{-\frac{1}{2}q^2}$$

Then by (4-2), (4-5), and (15) we obtain

$$(4\text{-}6) \qquad P[v(T) < 0 \mid m, \phi] = P[V_m < 0 \mid \phi]$$

$$= P[q < -a\cos\phi + b\sin\phi \mid \phi]$$

$$= \int_{q=-\infty}^{q=-a\cos\phi+b\sin\phi} p(q \mid \phi)\, dq$$

$$= \int_{-\infty}^{-a\cos\phi+b\sin\phi} \frac{1}{\sqrt{2\pi}} e^{-\frac{1}{2}q^2}\, dq$$

$$= \Phi(-a\cos\phi + b\sin\phi)$$

Now letting $p(\varrho, \phi)$ be the joint probability density function of ϕ we have from (13), (4=2) and (4=6),

$$(4\text{-}7)\quad \epsilon = \epsilon(\alpha, a, b)$$

$$= P[V_m < 0] = P[\varrho + a\cos\phi - b\sin\phi < 0]$$

$$= \int_{\phi=-\pi}^{\phi=\pi} \int_{\varrho=-\infty}^{\varrho=-a\cos\phi+b\sin\phi} p(\varrho, \phi)\, d\varrho\, d\phi$$

$$= \int_{\phi=-\pi}^{\phi=\pi} \int_{\varrho=-\infty}^{\varrho=-a\cos\phi+b\sin\phi} p(\varrho|\phi)\, p(\phi)\, d\varrho\, d\phi$$

$$= \int_{\phi=-\pi}^{\phi=\pi} p(\phi) \int_{\varrho=-\infty}^{\varrho=a\cos\phi+b\sin\phi} p(\varrho|\phi)\, d\varrho\, d\phi$$

$$= \int_{\phi=-\pi}^{\phi=\pi} p(\phi)\, P[V_m < 0 | \phi]\, d\phi$$

$$= \int_{\phi=-\pi}^{\phi=\pi} p(\phi)\, \Phi(-a\cos\phi + b\sin\phi)\, d\phi$$

APPENDIX 5

Proofs of (26)-(34)

Proof of (26)

We have by (25)

$$(5\text{-}1)\quad \epsilon(\alpha,a,b) = \int_{\phi=-\pi}^{\phi=\pi} p(\phi)\ \bar{\Phi}(-a\cos\phi + b\sin\phi)\,d\phi$$

$$= \int_{\theta=\pi}^{\theta=-\pi} p(-\theta)\ \bar{\Phi}(-a\cos\theta - b\sin\theta)(-d\theta) \quad (\theta=-\phi)$$

$$= \int_{\theta=-\pi}^{\theta=\pi} p(\theta)\ \bar{\Phi}(-a\cos\theta - b\sin\theta)\,d\theta$$

$$= \epsilon(\alpha, a, -b)$$

Proof of (27)

Let $\theta = \pi + \phi$. Then using (24) we obtain

$$(5\text{-}2)\quad \int_{-\pi}^{0} p(\phi)\ \bar{\Phi}(-a\cos\phi + b\sin\phi)\,d\phi$$

$$= \int_{0}^{\pi} p(\theta-\pi)\ \bar{\Phi}(a\cos\theta - b\sin\theta)\,d\theta$$

$$= \int_0^{\pi} \frac{e^{-\frac{1}{2}\alpha^2}}{2\pi}\left[1 - \sqrt{2\pi}\,\alpha\cos\theta\, e^{\frac{1}{2}\alpha^2\cos^2\theta}\ \bar{\Phi}(-\alpha\cos\theta)\right]\cdot$$

$$\bar{\Phi}(a\cos\theta - b\sin\theta)\,d\theta$$

$$= \int_0^{\pi} \frac{e^{-\frac{1}{2}\alpha^2}}{2\pi}\left[1 - \sqrt{2\pi}\,\alpha\cos\theta\, e^{\frac{1}{2}\alpha^2\cos^2\theta}\left\{1 - \bar{\Phi}(\alpha\cos\theta)\right\}\right]\cdot$$

$$\bar{\Phi}(a\cos\theta - b\sin\theta)\,d\theta$$

$$= \int_0^{\pi}\left[p(\theta) - \frac{\alpha}{\sqrt{2\pi}}\cos\theta\, e^{-\frac{1}{2}\alpha^2\sin^2\theta}\right]\bar{\Phi}(a\cos\theta - b\sin\theta)\,d\theta$$

$$= \int_0^{\pi} p(\phi)\ \bar{\Phi}(a\cos\phi - b\sin\phi)\,d\phi$$

$$- \frac{1}{\sqrt{2\pi}}\int_0^{\pi} \alpha\cos\phi\, e^{-\frac{1}{2}\alpha^2\sin^2\phi}\ \bar{\Phi}(a\cos\phi - b\sin\phi)\,d\phi$$

From (25) and (5-2) we have

$$\epsilon(\alpha,a,b) = \left[\int_{-\pi}^{0} + \int_{0}^{\pi}\right] p(\phi)\,\Phi(-a\cos\phi + b\sin\phi)\,d\phi$$

$$= \int_{0}^{\pi} p(\phi)\left[\Phi(a\cos\phi - b\sin\phi) + \Phi(-a\cos\phi + b\sin\phi)\right]d\phi$$

$$- \frac{1}{\sqrt{2\pi}}\int_{0}^{\pi} \alpha\cos\phi\, e^{-\frac{1}{2}\alpha^2\sin^2\phi}\,\Phi(a\cos\phi - b\sin\phi)\,d\phi$$

Now $\Phi(x) + \Phi(-x) = 1$ and $\int_{0}^{\pi} p(\phi)\,d\phi = \frac{1}{2}$. Then

$$(5\text{-}3)\quad \epsilon(\alpha,a,b) = \frac{1}{2} - \frac{1}{\sqrt{2\pi}}\int_{0}^{\pi} \alpha\cos\phi\, e^{-\frac{1}{2}\alpha^2\sin^2\phi}\,\Phi(a\cos\phi - b\sin\phi)\,d\phi$$

This proves the first part of (27). Continuing we have

$$(5\text{-}4)\quad \epsilon(\alpha,a,b) = \frac{1}{2} - \frac{1}{\sqrt{2\pi}}\left[\int_{0}^{\frac{\pi}{2}} + \int_{\frac{\pi}{2}}^{\pi}\right] \alpha\cos\phi\, e^{-\frac{1}{2}\alpha^2\sin^2\phi}\,\Phi(a\cos\phi - b\sin\phi)\,d\phi$$

Now let $\theta = \pi - \phi$. Then

$$(5\text{-}5)\quad \int_{\frac{\pi}{2}}^{\pi} \alpha\cos\phi\, e^{-\frac{1}{2}\alpha^2\sin^2\phi}\,\Phi(a\cos\phi - b\sin\phi)\,d\phi$$

$$= \int_{\frac{\pi}{2}}^{0} \alpha(-\cos\theta)\, e^{-\frac{1}{2}\alpha^2\sin^2\theta}\,\Phi(-a\cos\theta - b\sin\theta)\,(-d\theta)$$

$$= \int_{0}^{\frac{\pi}{2}} \alpha\cos\theta\, e^{-\frac{1}{2}\alpha^2\sin^2\theta}\left[1 - \Phi(a\cos\theta + b\sin\theta)\right]d\theta$$

Now let $x = \alpha\sin\theta$. Then

$$(5\text{-}6)\quad \int_{0}^{\frac{\pi}{2}} \alpha\cos\theta\, e^{-\frac{1}{2}\alpha^2\sin^2\theta}\,d\theta = \int_{0}^{\alpha} e^{-\frac{1}{2}x^2}\,dx$$

$$= \sqrt{2\pi}\left[\Phi(\alpha) - \frac{1}{2}\right]$$

Substituting (5-6) into (5-5) and the result into (5-4) we obtain

$$(5\text{-}7)\quad \epsilon(\alpha,a,b) = \Phi(\alpha) - \int_{0}^{\frac{\pi}{2}} \frac{\alpha\cos\phi}{\sqrt{2\pi}}\, e^{-\frac{\alpha^2}{2}\sin^2\phi}\left[\Phi(a\cos\phi - b\sin\phi) + \Phi(a\cos\phi + b\sin\phi)\right]d\phi$$

Proof of (28)

Letting $q=0$ in (27) we immediately obtain (28).

Proof of (29)

From (17) and (25) we obtain

$$(5\text{-}8)\quad \epsilon(\infty, a, b) = \int_{-\pi}^{\pi} \delta(\phi)\, \bar{\Phi}(-a\cos\phi + b\sin\phi)\, d\phi$$
$$= \bar{\Phi}(-a) = 1 - \bar{\Phi}(a)$$

Proof of (30)

From (25) we have

$$(5\text{-}9)\quad \epsilon(\alpha, 0, b) = \int_{-\pi}^{\pi} P(\phi)\, \bar{\Phi}(b\sin\phi)\, d\phi$$
$$= \int_{\pi}^{-\pi} P(-\theta)\, \bar{\Phi}(-b\sin\theta)\, (-d\theta) \qquad (\theta = -\phi)$$
$$= \int_{-\pi}^{\pi} P(\theta)\, [1 - \bar{\Phi}(b\sin\theta)]\, d\theta$$
$$= \int_{-\pi}^{\pi} P(\phi)\, d\phi - \int_{-\pi}^{\pi} P(\phi)\, \bar{\Phi}(b\sin\phi)\, d\phi$$
$$= 1 - \epsilon(\alpha, 0, b)$$

Then

$$(5\text{-}10)\quad \epsilon(\alpha, 0, b) = \tfrac{1}{2}$$

Proof of (31)

From (27) and (5-6) we obtain

$$(5\text{-}11)\quad \epsilon(\alpha, \infty, b) = \bar{\Phi}(\alpha) - \frac{1}{\sqrt{2\pi}} \int_0^{\frac{\pi}{2}} \alpha\cos\phi\, e^{-\frac{1}{2}\alpha^2\sin^2\phi}\, (2)\, d\phi$$
$$= \bar{\Phi}(\alpha) - 2\left[\bar{\Phi}(\alpha) - \tfrac{1}{2}\right]$$
$$= 1 - \bar{\Phi}(\alpha)$$

Proof of (32)

From (25) and (14) and we obtain

$$(5\text{-}12)\quad \epsilon(\alpha,\alpha,0) = \int_{-\pi}^{\pi} \frac{1}{2\pi} e^{-\frac{1}{2}\alpha^2}\left[1+\sqrt{2\pi}\,\alpha\cos\phi\, e^{\frac{1}{2}\alpha^2\cos^2\phi}\,\Phi(\alpha\cos\phi)\right]\cdot \Phi(-\alpha\cos\phi)\,d\phi$$

$$= \left[\int_{-\pi}^{0} + \int_{0}^{\pi}\right]\frac{1}{2\pi} e^{-\frac{1}{2}\alpha^2}\left[\Phi(-\alpha\cos\phi) + \sqrt{2\pi}\,\alpha\cos\phi\, e^{\frac{1}{2}\alpha^2\cos^2\phi}\,\Phi(\alpha\cos\phi)\,\Phi(-\alpha\cos\phi)\right]d\phi$$

Now let $\theta = \pi + \phi$. Then

$$(5\text{-}13)\quad \int_{-\pi}^{0}\left[\Phi(-\alpha\cos\phi) + \sqrt{2\pi}\,\alpha\cos\phi\, e^{\frac{1}{2}\alpha^2\cos^2\phi}\,\Phi(\alpha\cos\phi)\,\Phi(-\alpha\cos\phi)\right]d\phi$$

$$= \int_{0}^{\pi}\left[\Phi(\alpha\cos\theta) - \sqrt{2\pi}\,\alpha\cos\theta\, e^{\frac{1}{2}\alpha^2\cos^2\theta}\,\Phi(-\alpha\cos\theta)\,\Phi(\alpha\cos\theta)\right]d\theta$$

$$= \int_{0}^{\pi}\left[\Phi(\alpha\cos\phi) - \sqrt{2\pi}\,\alpha\cos\phi\, e^{\frac{1}{2}\alpha^2\cos^2\phi}\,\Phi(\alpha\cos\phi)\,\Phi(-\alpha\cos\phi)\right]d\phi$$

Substituting (5-13) into (5-12) and using the fact that $\Phi(\alpha\cos\phi)+\Phi(-\alpha\cos\phi)=1$ we obtain

$$(5\text{-}14)\qquad \epsilon(\alpha,\alpha,0) = \tfrac{1}{2}\, e^{-\frac{1}{2}\alpha^2}$$

Proof of (33)

From the second form of (27) we obtain

$$\epsilon(\alpha,a,\infty) = \Phi(\alpha) - \frac{1}{\sqrt{2\pi}}\int_{0}^{\frac{\pi}{2}} \alpha\cos\phi\, e^{-\frac{1}{2}\alpha^2\sin^2\phi}\cdot \left[\Phi(-\infty)+\Phi(\infty)\right]d\phi$$

$$= \Phi(\alpha) - \frac{1}{\sqrt{2\pi}}\int_{0}^{\frac{\pi}{2}} \alpha\cos\phi\, e^{-\frac{1}{2}\alpha^2\sin^2\phi}\,d\phi$$

$$= \frac{1}{2}\ ,$$

by (5-6).

Proof of (34)

From the second form of (27) we have for $b = ac$, $a > 0$, $c > 0$,

(5-16) $$\epsilon(\alpha, a, ac) = \Phi(\alpha) - \frac{1}{\sqrt{2\pi}} \int_0^{\frac{\pi}{2}} \alpha \cos\phi \, e^{-\frac{1}{2}\alpha^2 \sin^2\phi} \cdot$$

$$\Phi(a\cos\phi + ac\sin\phi)\, d\phi$$

$$- \frac{1}{\sqrt{2\pi}} \left[\int_0^{\tan^{-1}\left(\frac{1}{c}\right)} + \int_{\tan^{-1}\left(\frac{1}{c}\right)}^{\frac{\pi}{2}} \right] \alpha \cos\phi \, e^{-\frac{1}{2}\alpha^2 \sin^2\phi} \cdot$$

$$\Phi(a\cos\phi - ac\sin\phi)\, d\phi$$

$$= \Phi(\alpha) - \frac{1}{\sqrt{2\pi}} \int_0^{\frac{\pi}{2}} \alpha \cos\phi \, e^{-\frac{1}{2}\alpha^2 \sin^2\phi} \, \Phi[\alpha(\cos\phi + c\sin\phi)]\, d\phi$$

$$- \frac{1}{\sqrt{2\pi}} \int_0^{\tan^{-1}\left(\frac{1}{c}\right)} \alpha \cos\phi \, e^{-\frac{1}{2}\alpha^2 \sin^2\phi} \, \Phi[a\cos\phi(1 - c\tan\phi)]\, d\phi$$

$$- \frac{1}{\sqrt{2\pi}} \int_{\tan^{-1}\left(\frac{1}{c}\right)}^{\frac{\pi}{2}} \alpha \cos\phi \, e^{-\frac{1}{2}\alpha^2 \sin^2\phi} \, \Phi[-a\cos\phi(c\tan\phi - 1)]\, d\phi$$

Then

$$(5\text{-}17)\quad \lim_{a\to\infty} \epsilon(\alpha, a, ac)$$

$$= \Phi(\alpha) - \frac{1}{\sqrt{2\pi}}\int_0^{\frac{\pi}{2}} \alpha\cos\phi\, e^{-\frac{1}{2}\alpha^2\sin^2\phi}\, \Phi(\infty)\, d\phi$$

$$- \frac{1}{\sqrt{2\pi}}\int_0^{\tan^{-1}\left(\frac{1}{c}\right)} \alpha\cos\phi\, e^{-\frac{1}{2}\alpha^2\sin^2\phi}\, \Phi(\infty)\, d\phi$$

$$- \frac{1}{\sqrt{2\pi}}\int_{\tan^{-1}\left(\frac{1}{c}\right)}^{\frac{\pi}{2}} \alpha\cos\phi\, e^{-\frac{1}{2}\alpha^2\sin^2\phi}\, \Phi(-\infty)\, d\phi$$

$$= \Phi(\alpha) - \frac{1}{\sqrt{2\pi}}\int_0^{\alpha} e^{-\frac{1}{2}x^2}\, dx - \frac{1}{\sqrt{2\pi}}\int_0^{\frac{\alpha}{\sqrt{1+c^2}}} e^{-\frac{1}{2}x^2}\, dx \quad (x=\alpha\sin\phi)$$

$$= \Phi(\alpha) - \left[\Phi(\alpha) - \tfrac{1}{2}\right] - \left[\Phi\left(\frac{\alpha}{\sqrt{1+c^2}}\right) - \tfrac{1}{2}\right]$$

$$= 1 - \Phi\left(\frac{\alpha}{\sqrt{1+c^2}}\right) \qquad (c > 0)$$

From (26) and (5-17) we obtain for $b = ac$, $a > 0$, $c < 0$,

$$(5\text{-}18)\quad \lim_{a\to\infty} \epsilon(\alpha, a, ac) = \lim_{a\to\infty} \epsilon(\alpha, a, -ac)$$

$$= \lim_{a\to\infty} \epsilon(\alpha, a, a|c|) = 1 - \Phi\left(\frac{\alpha}{\sqrt{1+c^2}}\right) \qquad (c<0)$$

Then from (5-17), (5-18), and (24) we obtain

$$(5\text{-}19)\quad \lim_{a\to\infty} \epsilon(\alpha, a, ac) = 1 - \Phi\left(\frac{\alpha}{\sqrt{1+c^2}}\right) = \epsilon(\alpha, c) \qquad (c \neq 0)$$

APPENDIX 6

Proof of (3-8)

Let

$$(6\text{-}1)\quad I = \int_{x=-\infty}^{x=\infty} \int_{y=-\infty}^{y=mx+b} P(x,y)\, dy\, dx$$

$$(6\text{-}2)\quad P(X,Y) = \frac{1}{2\pi\sigma_1\sigma_2} e^{-\frac{1}{2}\left[\left(\frac{x-\mu_1}{\sigma_1}\right)^2 + \left(\frac{y-\mu_2}{\sigma_2}\right)^2\right]}$$

where $0 < \sigma_1, \sigma_2 < \infty, \quad -\infty < \mu_1, \mu_2, m, b < \infty.$

Let

$$(6\text{-}3)\quad \begin{cases} x' = \dfrac{x-\mu_1}{\sigma_1} \\ y' = \dfrac{y-\mu_2}{\sigma_2} \end{cases}$$

Define

$$(6\text{-}4)\quad q(x',y') = P(x,y)$$

Then

$$(6\text{-}5)\quad q(x',y') = \frac{1}{2\pi\sigma_1\sigma_2} e^{-\frac{1}{2}(x'^2 + y'^2)}$$

Also from (6-3) we have

$$(6\text{-}6)\quad dx\, dy = \sigma_1\sigma_2\, dx'\, dy'$$

Now under (6-2) the line $y = mx + b$ becomes $y' = m'x' + b'$ i.e.

$$(6\text{-}7)\quad y = mx + b \longrightarrow y' = m'x' + b'$$

where

$$(6\text{-}8)\quad m' = \frac{m\sigma_1}{\sigma_2}$$

$$(6\text{-}9)\quad b' = \frac{m\mu_1 - \mu_2 + b}{\sigma_2}$$

Thus substituting (6-5) - (6-7) into (6-3) we obtain

$$(6\text{-}10)\qquad I = \int_{x'=-\infty}^{x'=\infty} \int_{y'=-\infty}^{y'=m'x'+b'} \frac{1}{2\pi} e^{-\frac{1}{2}(x'^2+y'^2)}\, dy'\, dx'$$

Now we rotate axes through an angle $\theta = \tan^{-1}\left(-\frac{1}{m'}\right)$, $-\pi \le \theta \le 0$, i.e. a clockwise rotation through an angle $|\theta|$.

Thus let

$$(6\text{-}11)\qquad \sin\theta = -\frac{1}{\sqrt{m'^2+1}}\,,\quad \cos\theta = \frac{m'}{\sqrt{m'^2+1}} \qquad (-\pi \le \theta \le 0)$$

Let

$$(6\text{-}12)\qquad \begin{cases} x'' = x'\cos\theta + y'\sin\theta = \dfrac{m'x' - y'}{\sqrt{m'^2+1}} \\[2ex] y'' = -x'\sin\theta + y'\cos\theta = \dfrac{x' + m'y'}{\sqrt{m'^2+1}} \end{cases}$$

or

$$(6\text{-}13)\qquad \begin{cases} x' = x''\cos\theta - y''\sin\theta = \dfrac{m'x'' + y''}{\sqrt{m'^2+1}} \\[2ex] y' = x''\sin\theta + y''\cos\theta = \dfrac{-x'' + m'y''}{\sqrt{m'^2+1}} \end{cases}$$

From (6-12) or (6-13) we have

$$(6\text{-}14) \qquad x'^2 + y'^2 = x''^2 + y''^2$$

Also from (6-12),

$$(6\text{-}15) \qquad dx'\,dy' = \begin{vmatrix} \frac{\partial x'}{\partial x''} & \frac{\partial x'}{\partial y''} \\ \frac{\partial y'}{\partial x''} & \frac{\partial y'}{\partial y''} \end{vmatrix} dx''\,dy'' = dx''dy''$$

Under (6-12) or (6-13) the line $y' = m'x' + b'$ becomes $x'' = b''$, i.e.

$$(6\text{-}16) \qquad y' = m'x' + b' \longrightarrow x'' = b''$$

where

$$(6\text{-}17) \qquad b'' = -\frac{b'}{\sqrt{1 + m'^2}}$$

From (6-10), (6-14) & (6-17) we obtain

$$(6\text{-}18) \qquad I = \int_{y''=-\infty}^{y''=\infty} \int_{x''=b''}^{x''=\infty} \frac{1}{2\pi} e^{-\frac{1}{2}(x''^2 + y''^2)}\, dy''\,dx''$$

$$= 1 - \Phi(b'') = \Phi(-b'') = \Phi\left(\frac{b'}{\sqrt{1 + m'^2}}\right)$$

$$= \Phi\left(\frac{m\mu_1 - \mu_2 + b}{\sqrt{m^2\sigma_1^2 + \sigma_2^2}}\right) \qquad \begin{pmatrix} 0 < \sigma_1, \sigma_2 < \infty \\ -\infty < \mu_1, \mu_2, m, b < \infty \end{pmatrix}$$

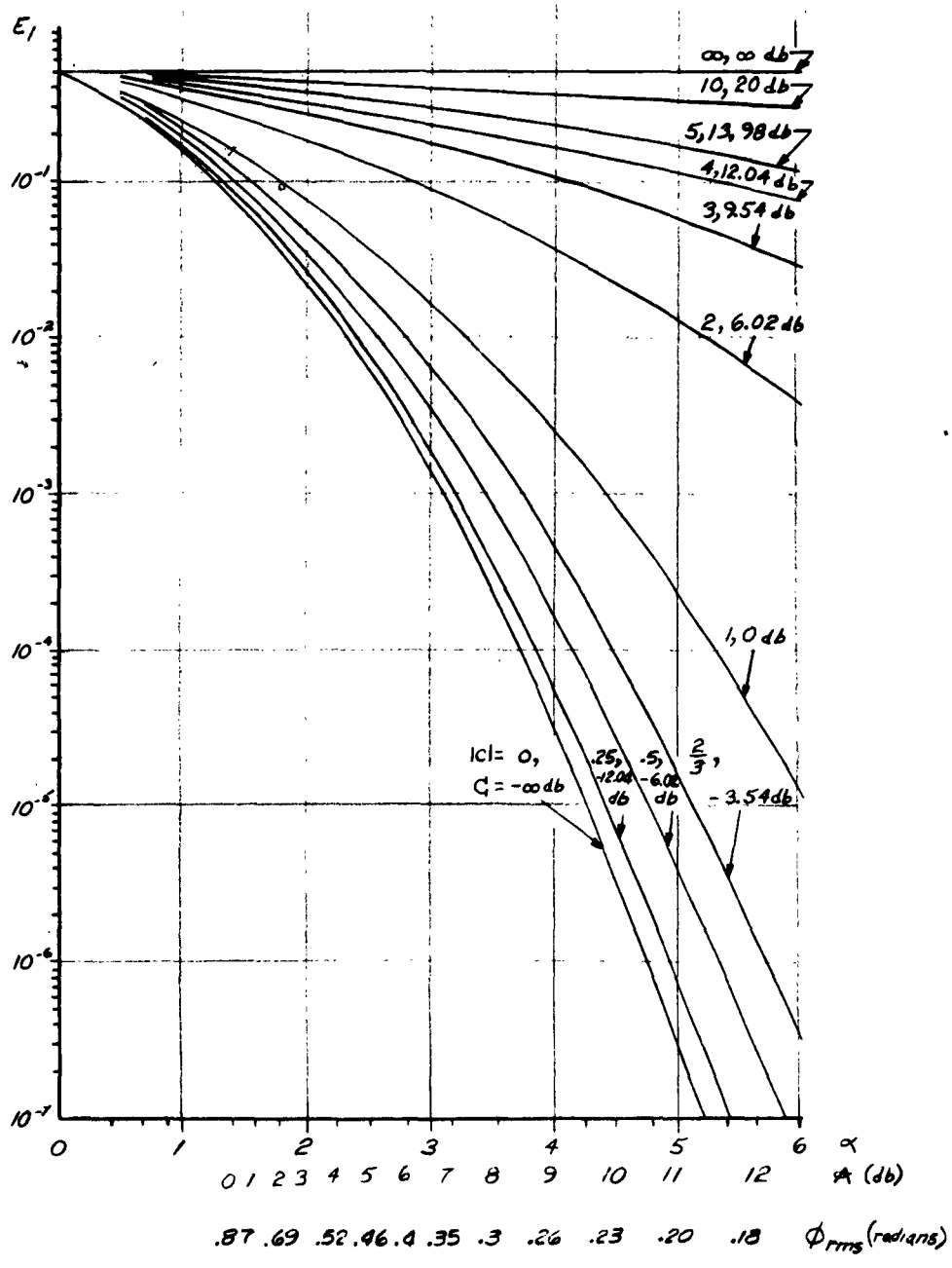

Figure 1. SSB Error-Rate vs. Inserted Carrier Phase Jitter with Quadrature Distortion as Parameter

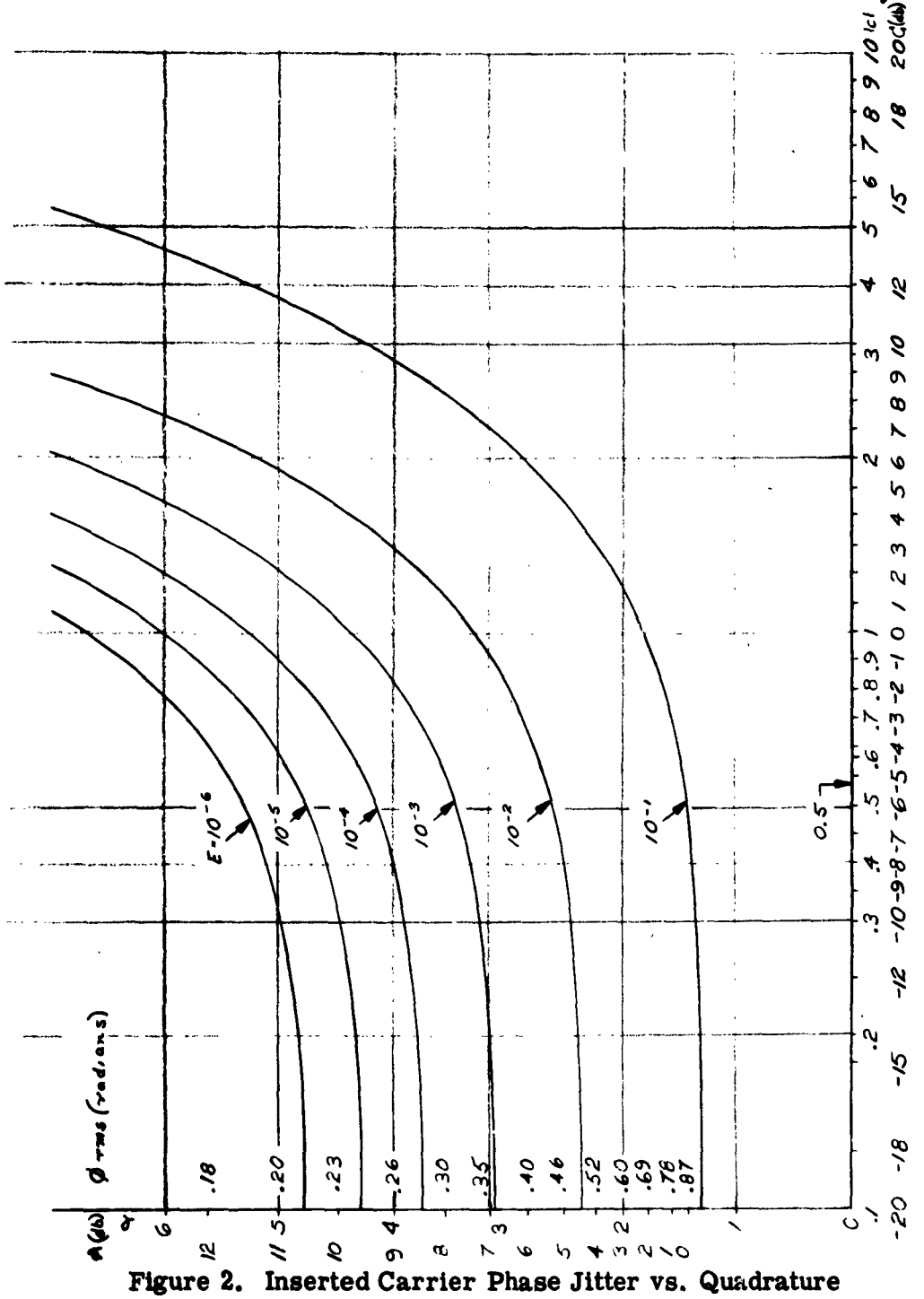

Figure 2. Inserted Carrier Phase Jitter vs. Quadrature Distortion with SSB Error Rate as Parameter

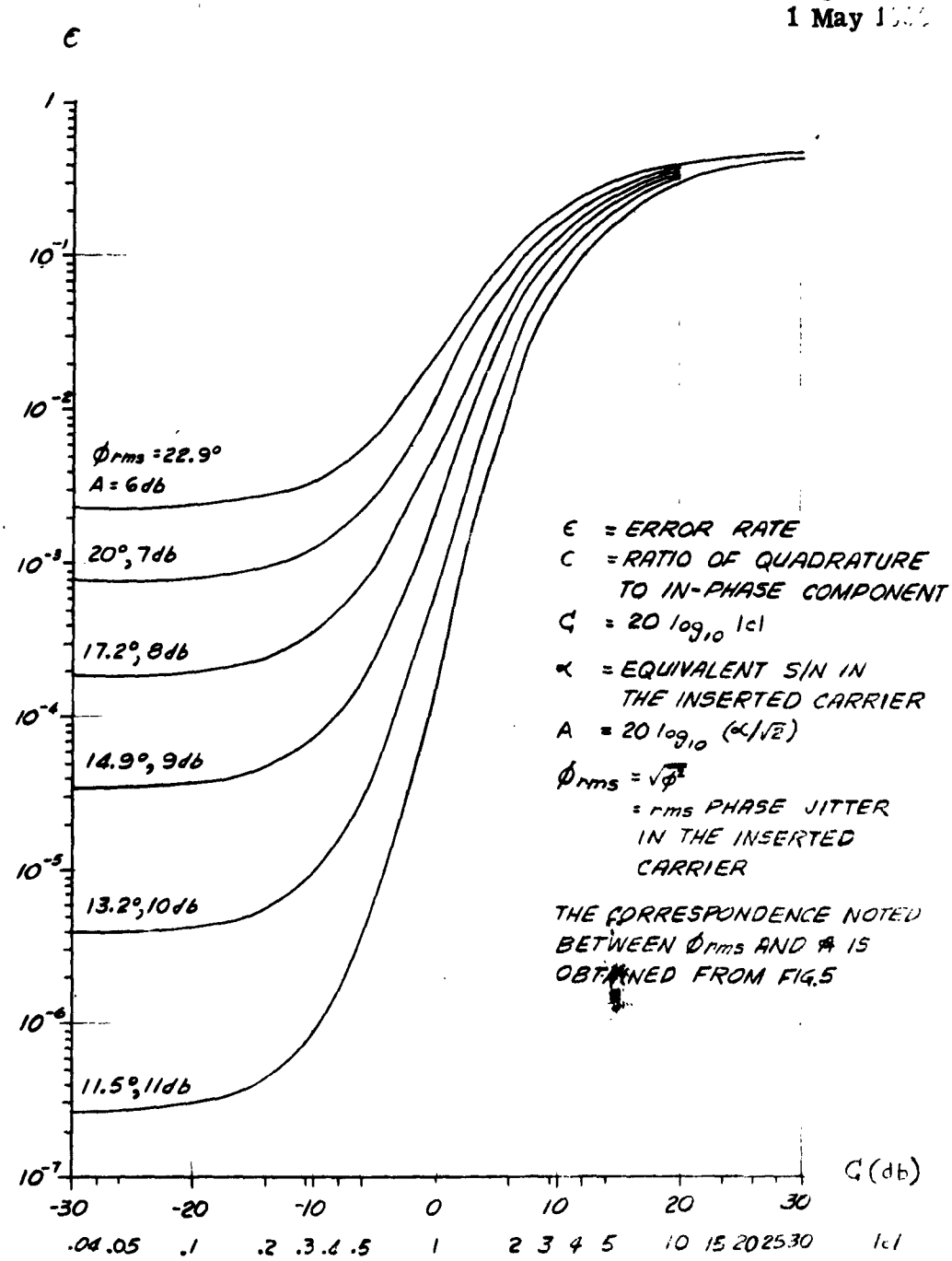

Figure 3. SSB Error-Rate vs. Quadrature Distortion with Inserted Carrier Phase Jitter as Parameter

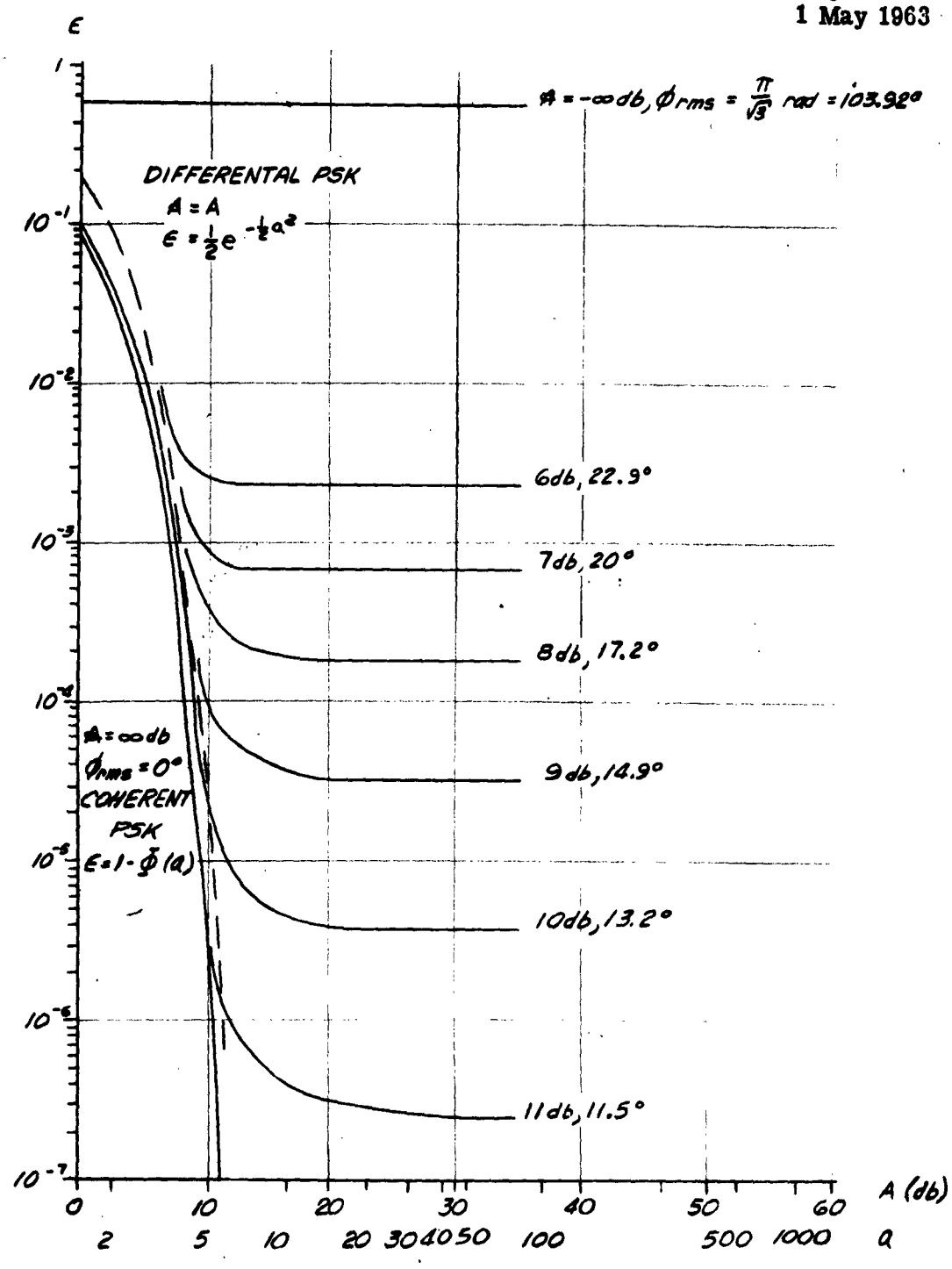

Figure 4. SSB Error-Rate vs. S/N in Signal Channel with Inserted Carrier Phase Jitter as Parameter, Assuming Zero Quadrature Component

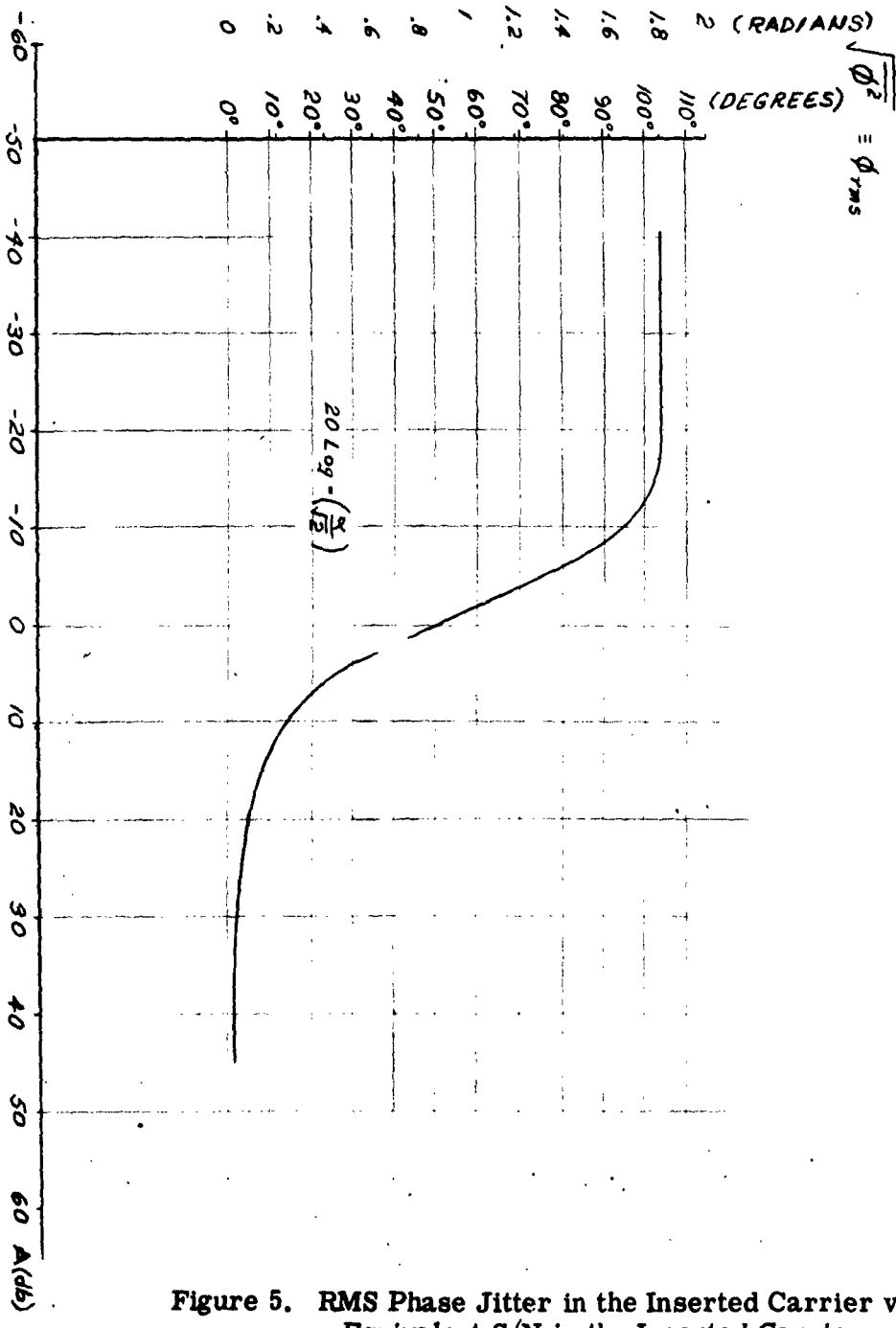

Figure 5. RMS Phase Jitter in the Inserted Carrier vs. Equivalent S/N in the Inserted Carrier

REFERENCES

1. Powers, K. H., "The Compatability Problem In Single-Sideband Transmission," Proceedings of the IRE, August 1960, pages 1431-1435.

2. Dugundji, J., "Envelopes and Pre-Envelopes of Real Waveforms," IRE Transactions on Information Theory, March 1958, pages 53-57.

3. Middleton, D., "An Introduction To Statistical Communication Theory," McGraw-Hill, 1960.

4. Deutsch, R., "Nonlinear Transformations of Random Processes," Prentice-Hall, 1962.

5. Schwartz, M., "Information Transmission, Modulation, and Noise," McGraw-Hill, 1959.

6. National Bureau of Standards, "Tables of the Bivariate Normal Distribution Function and Related Functions," Applied Mathematics Series, No. 50, 1959.

BIBLIOGRAPHY

1. "The Computation of SSB Peak Power" - Squires, Bedrosian, Proc. IRE Jan. 1960, pg. 123.

2. "Communication Efficiency Comparison of Several Communication Systems" - Sanders, Proc. IRE April 1960, pg. 575.

3. "Combined AM & PM for a one-sided spectrum" - Taylor, Proc. IRE May 1960, pg. 953.

4. "Noise Spectrum of Phase-Locked Oscillators" - Strandberg, Proc. IRE June 1960, pg. 1168.

5. "Increasing the Dynamic Tracking Range of Phase-Locked Loop" - Weaver, Proc. IRE May 1960, pg. 952.

6. "The Compatibility Problem in SSB Transmission" - Powers, Proc. IRE Aug. 1960, pg. 1431.

7. "Noise in Oscillators" - Edson, Proc. IRE Aug. 1960, pg. 1454
   " " " Mullen " " " " " 1467
   " " " Golay " " " " " 1473

8. "Poisson, Shannon & the Ham" - Basly, Costas Proc. IRE, Aug. 1960, pg. 1495.

9. "The Compatibility Problem in SSB" - Kahn, Proc. IRE Aug. 1960, pg. 1504.

10. "High Selectivity with Constant Phase Over the Pass Band" - Rihaczek, Proc. IRE Oct. 1960, pg. 1756.

11. "Automatic Phase Control Theory & Design" - Rey, Proc. IRE, Oct. 1960, pg. 1760.

12. Correction to "A New Look at the Phase-Locked Oscillator" - McAllen, Proc. IRE Oct. 1960, pg. 1771.

13. "Interrelation and Combination of Various Types of Modulation" - Meewezen, Proc. IRE Nov. 1960, pg. 1824.

14. "Traffic Efficiencies in Congested Band Radio Systems" - Weber, Costàs, Proc. IRE Nov. 1960, pg. 1910.

15. "Regenerative Fractional Frequency Generators" - Plotkin, Lumpkin, Proc. IRE Dec. 1960, pg. 1988.

16. "Evaluation of Modulation Methods for Tange Telemetry" - Rudin, IRE Convention Board - 1960, Part 5, pg. 17.

17. "Detection Levels & Error Rates in PCM Telemetry" - Balakrishnan, Abrams, IRE Convention Record - 1960, Part 5, pg. 37.

18. "Optimized SSB Transmitter Loading by Multichannel Freq. Division Data" - Brennan, Daly, Goldberg, IRE Convention Record - 1960, Part 5, pg. 188.

19. "Electromagnetic Interference and Vulnerability Reduction" - J. J. Egli, IRE Convention Record - 1960, Part 8, pg. 48.

20. "Phase Stability of Oscillators" - Sann, Proc. IRE Feb. 1961, pg. 527.

21. "Correction to "APC Theory & Design" - Rey, Proc. IRE March 1961, pg. 590.

22. "SSB Communication" - Makris, Proc. IRE March, 1961, pg. 632.

23. "A Note on Instantaneous Spectrum" - Rothschild, Proc. IRE March 1961, pg. 649.

24. "Dynamic Response of Rihaczek's Constant Phase Non-Linear Filter", Proc. IRE April 1961, pg. 822.

25. "A Method for Generating Signals of Arbitrary Yet Frequency - Independent Phase Differences" - Nilssen, Proc. IRE May 1961, pg. 964.

26. "Results of a Long Range Clock Synchronization Experiment" - Redes, Winkler, Bichart, Proc. IRE June 1961, pg. 1028.

27. "A Superposition Property of Angle Modulation" - Goodman, Proc.IRE June 1961, pg. 1084.

28. "A Mechanism for Direct Adjacent Channel Interference" - Ruthroff, Proc. IRE June 1961, pg. 1091.

29. "Discussion of Combined AM & PM for a One-Sided Spectrum" - Golden, et al, Proc. IRE June 1961, pg. 1094.

30. "Pull-in Frequency of the Phase-Controlled Oscillator" - Goldstein & Byrne, Proc. IRE July 1961, pg. 1209.

31. "Receivers with Zero IF" - Rubin, Proc. IRE Aug. 1961, pg. 1327.

32. "Compatible SSB" - Kahn, Proc. IRE Oct. 1961, pg. 1503.

33. "The Linearized Transfer Function of a Phase-Locked Loop Containing an IF Amplifier" - Lowhorn, Weaver, Proc. IRE Nov. 1961, pg. 1704.

34. "A Static Electronic Frequency Changer" - Griffith, Ulmer, IRE Convention Record 1961, Part 5, pag. 342.

35. "Voice Modulated SSB and DSB Peak to Average Envelope Power Ratios" - Griffiths, IRE Convention Record 1961, Part 8, pg. 84.

36. "Analysis of Multiple Tone Clipping" - Styers, IRE Convention Record 1961, Part 8, pg. 134.

37. "The Dwindling HF Spectrum" - Jacobs, Martin, IRE Convention Record - 1961, Part 8, pg. 179.

38. "Performance of a 640 Mile, 24-channel UHF-SSB System" - Nichols, Trans. PGCS, March 1960, pg. 26.

39. "Combined Digital Phase & AM Systems" - Cahn, PGCS, Sept. 1960, pg. 150.

40. "FM & SSB Radiotelephone Tests on a VHF Ionoscatter Link During Multipath Conditions" - Koch, Harding, Jansen, PGCS, Sept. 1960, pg. 183.

41. "Military Radio Communications Equipment Cost-Design Relationships" - Ports, et al. PGCS, Dec. 1960, pg. 203.

42. "Distortion of Angle - Modulated Systems in Misaligned Linear Filters" Galejs PGCS, Dec. 1960, pg. 228.

43. "Performance of Combined AM & PM Systems" - Hancock, Lucky, PGCS, Dec. 1960.

44. "Precision Frequency Control for Military Applications" - Gerber, Hand, PGMIL, Oct. 1960, pg. 424.

45. "Multichannel Radio Communication Within the Army" - L. G. Fobes, PGMIL, Oct. 1960, pg. 505.

46. "Energy Spectra of FM System with Low β, Hi-Deviation Ratio, and MG Which Approaches Carrier Frequency" - Simmons, PGSET, March 1960, pg. 17.

47. "Threshold Improvement in an FM Subcarrier System" - Martin PGSET, March 1960, pg. 25.

48. "The Case of FM-AM vs. FM-PM Telemetry" - Rauch, PGSET, June 1960, pg. 81.

49. "The Effect of Different Types of Video Filters on PDM-FM and PCM-FM Radio Telemetry" - Nichols, Bublitz, PGSET, June 1960, pg. 85.

50. "Considerations on Synch. for PCM Telemetry" - Rauch, PGSET, Sept.-Dec. 1960, pg. 94.

51. "PCM/FM Telemetry Signal Analysis and Bandwidth Effects" - Ormsby, PGSET, Sept.-Dec. 1960, pg. 129.

52. "A Comparison of Wideband and Narrowband Mobile Circuits at 150 Mc" - Nylund, PGVC, May 1960, pg. 69.

53. "Can SSB Provide More Usable Channels in the Land Mobile Service?"- Korolenko, Shepherd PGVC, Aug. 1960, pg. 47.

54. "Study by RMA-RTMA - TR 8. 9 (1877-A-1) 1946 Mobile Vehicular Systems - Geographical Pattern of Frequency Assignments for Mobile Systems Near 150 Mc."

55. "Adjacent Channel and the Courier Curse" - Smith PGVC, June 1957.

56. "Application of SSB For Mobile Communication" - Firestone, Magnuski, PGVC-11, 1948, pg. 48.

57. "The Gaussian Curse - XMTR Noise Limits Spectrum Utilization" - Shepherd, Smith, PGVC-10, April 1948, pg. 27.

58. "Channel Spacing Considerations in the 154-174 MC Band" - Strauss, PGVC, June 1952, pg. 44.

59. "Choosing the Optimum Type of Modulation - A Comparison of Several Systems of Comm." - Kelly, PGCS-6, June 1958, pg. 14.

60. "Poisson, Channon, and the Radio Amateur" - Costas, Proc. IRE Dec. 1959, pg. 2058.

61. "Receivers With Zero IF" - Greene & Lyons, Proc. IRE Feb. 1959, pg. 335.

62. "Progress and Problems in U.S. Army Communications" - Lacy, Proc. IRE May 1959, pg. 650.

63. "A Critical Analysis of Some Communications Systems Derived from AM" - Nupp, Proc. IRE May 1959, pg. 697.

64. "A New Look at The Phase-Locked Oscillator" - McAllen, Proc. IRE June 1959, pg. 1137.

65. "FM Multiplex Spectrum and Interference" - Arguimbau, Proc.IRE Aug. 1959, pg. 1372.

66. "Combined AM & PM For a One-Sided Spectrum" - Chakrabarti, Proc. IRE Sept. 1959, pg. 1663.

67. "Short-Time Stability of a Quartz-Crystal Oscillator as Measured With and Ammonia - Maser" - Morgan & Barnes, Proc.IRE Oct.1959, pg. 1782.

68. "Crystal Noise Effects on Zero IF Receiver" - Andrews & Bazydlo, Proc. IRE Nov. 1959, pg. 2018.

69. "Experience With SSB Mobile Equipment" - Richardson, Eness, Dronsuth, Proc. IRE June 1957, pg. 823.

70. "On The Use of Ferrites For Microwave SSB Modulators" - Khoury, Proc. IRE Oct. 1957, pg. 1418.

71. "DSB vs. SSB Systems" - Costas, Proc. IRE April 1957, pg. 534.

72. "SSB Performance As a Function of Carrier Strength" - Shepherd, Proc. IRE April 1957, pg. 541.

73. "A Simplified Method for Designing Wideband High Precision 90° Phase Networks" - Lerner, R.M., MIT Lincoln Lab Group Report 36-40, Aug. 7, 1959.

74. "Wideband Phase Shift Networks" - R. B. Dome, Electronics, Dec. 1946, pg. 112.

75. "The Serrodyne Frequency Translator" - R.C. Cummings, Proc.IRE, Feb. 1957.

76. "A Microwave SSB Modulator" - H. G. Pascalar, MIT Lincoln Lab Group Report No. 8, April 22, 1958.

77. "Design of a Broadband Microwave SSB Generator" - J. P. Dougherty, RCA TR-62-564-2, (GE&D #998690, Co. Private).

78. "Properties of Some Wideband Phase - Splitting Networks" - D.G.C. Luck, Proc. IRE, Feb. 1949.

79. "Realization of a Constant Phase Difference" - S. Darlington, B.S.T.J. Jan. 1950.

80. "Synthesis of Wideband Two-Phase Networks" - H. J. Orchard, Wireless Engineer, March 1950.

81. "Cascade Connection of 90-Degree Phase Shift Networks" - O. G. Villard Jr., Proc. IRE, March 1952.

82. "Standardization of the Transient Response of Television Transmitters" - Kell & Fredendall, RCA Review, March 1949.

83. "Phase and Amplitude Equalizer for Television Use" - Goodale and Kennedy RCA Review, March 1949.

84. "Selective Sideband Transmission in Television" - Kell and Fredendall, RCA Review, April 1940.

85. "Selective Sideband vs. Double Sideband Transmission of Telegraph and Facsimile Signals" - Smith, Trevor, Carter, RCA Review, Oct. 1938.

86. "Certain Topics in Telegraph Transmission Theory" - H. Nyquist, BTL Mono. #B-331, August 1928.

87. "An AM Vestigial Sideband Data Transmission Set Using Synchronous Detection for Serial Transmission Up to 3,000 Bits per Second" - Becker, Davey, Saltzberg, Communication and Electronics, May 1962.

88. "Theoretical Fundamentals of Pulse Transmission" - Sunde, BSTJ, May 1954, July 1954.

89. "Ideal Binary Pulse Transmission by AM And FM" - Sunde, BSTJ, Nov. 1959.

90. "Pulse Transmission by AM, FM and PM In the Presence of Phase Distortion" - Sunde, BSTJ, March 1961.

91. "Sage Data Terminals" - Soffel, Spack, AIEE Trans. Pt. 1 (Communication and Electronics) vol. 77, 1958 (Jan. 1959 section).

92. "Digital Data Fundamentals and the Two Level Vestigial Sideband System for Voice Bandwidth Circuits" - Hollis, WESCON Conv. Record, Vol. 4, Part 5, 1960.

93. "Synchronous Communications" - Costas, Proc. IRE, Dec. 1956.

94. "Phase Reversal Data Transmission System for Switched and Private Telephone Line Applications"- Hopner, IBM Journal of Research and Development, April 1961.

95. "The L-s Coaxial System - TV Terminals" - Rieke, Graham, BSTJ, July 1953.

96. "Theory of AFC Synchronization" - Gruen Proc. IRE, August 1953.

97. "Data System Tests Using Simulated Transmission Impairments" - Andrews, Communication and Electronics, Vol. 80, 1961 (Jan 1962 section).

98. "Capabilities of the Telephone Network for Data Transmission" - Alexander, Gryb, Nast, BSTJ, May 1960.

99. "Design and Performance of Phase-Lock Circuits Capable of Near-Optimum Performance Over a Wide Range of Input Signal and Noise Levels" - Jaffe, Rechtin, Trans. PGIT, March 1955.

100. "Frequency Economy in Mobile Radio Bands" - Bullington, BSTJ, Jan. 1953.

101. "Intermodulation Interference in Radio Systems" - Babcock, BSTJ, Jan. 1953.

102. "Reduction of Bandwidth Requirements for Radio Relay Systems" - Mack, Meyerhoff, Jacoby, Levine, IRE Conv. Record, Part 8, 1958.

103. "Practical Considerations in the Design of Minimum Bandwidth Digital FM Systems Using Gaussian Filtering" - Glomb, Trans. PGCS, Dec. 1959.

104. "Gaussian Response Filter Design" - Dishal, Electrical Communication, Vo. 36, No. 1, 1959.

105. "A Simple Wideband 90^{O} Phase Splitter for Speech or Music" - L. V. Kriger, AFCRL 930, Oct. 1961, AD 271757.

106. "Radio Propagation Variations at VHF and UHF" - K. Bullington, Proc. IRE, Jan. 1950.

107. "Study of I-F Transformers for SSB Operation" - I11. Inst. of Tech., Feb. 1, 1960 to Oct. 31, 1962 FINAL Report.

108. "Ferroelectric Ceramic Filters, IF Transformers, And Networks" - Koneval, Curran. Report #23, DA-36-039-sc-87275, Clevite Corp., 30 June 1962. AD-282835.

109. "Phase-Lock Loop Frequency Acquisition Study" - Frazier, Page, Trans. PGSET, Sept. 1962.

110. "Comparison of Split Channel FM & SSB For Land Mobile Services" - A. A. MacDonald, PGVC, Dec. 1956.

DISTRIBUTION LIST

OASD (RUE), Rm 3E1065 ATTN: Technical Library The Pentagon Washington 25, D. C.	1
Chief of Research and Development OCS, Department of the Army Washington 25, D. C.	1
Commanding General U. S. Army Materiel Command ATTN: R&D Directorate Washington 25, D. C.	1
Commanding General U. S. Army Electronics Command ATTN: AMSEL-AD Fort Monmouth, N.J.	3
Commander, Armed Services Technical Information Agency ATTN: TISIA Arlington Hall Station Arlington 12, Virginia	10
Commanding General USA Combat Developments Command ATTN: CDCMR-E Fort Belvoir, Virginia	1
Commanding Officer USA Communication and Electronics Combat Development Agency Fort Huachuca, Arizona	1
Commanding General U. S. Army Electronics Research and Development Activity ATTN: Technical Library Fort Huachuca, Arizona	1
Chief, U. S. Army Security Agency Arlington Hall Station Arlington 12, Virginia	2

Deputy President
U. S. Army Security Agency Board
Arlington Hall Station
Arlington 12, Virginia 1

Commanding Officer
Diamond Ordnance Fuze Laboratories
ATTN: Library, Rm. 211, Bldg. 92
Washington 25, D. C. 1

Director, U. S. Naval Research Laboratory
ATTN: Code 2027
Washington 25, D. C. 1

Commanding Officer and Director
U. S. Navy Electronics Laboratory
San Diego 52, California 1

Aeronautical Systems Division
ATTN: ASAPRL
Wright-Patterson Air Force Base, Ohio 1

Air Force Cambridge Research Laboratories
ATTN: CRZC
L. G. Hanscom Field
Bedford, Massachusetts 1

Air Force Cambridge Research Laboratories
ATTN: CRXL-R
L. G. Hanscom Field
Bedford, Massachusetts 1

Hq. Electronic Systems Division
ATTN: ESAT
L. G. Hanscom Field
Bedford, Massachusetts 1

AFSC Scientific/Technical Liaison Office
U. S. Naval Air Development Center
Johnsville, Pennsylvania 1

Commanding Officer
U. S. Army Electronics Materiel Support Agency
ATTN: SELMS-ADJ
Fort Monmouth, New Jersey 1

Director, Fort Monmouth Office
USA Communication and Electronics
Combat Development Agency
Fort Monmouth, New Jersey 1

Corps of Engineers Liaison Office
U. S. Army Electronics Research & Development
Laboratory
Fort Monmouth, New Jersey 1

Marine Corps Liaison Office
U. S. Army Electronics Research &
Development Laboratory
Fort Monmouth, New Jersey 1

AFSC Scientific/Technical Liaison Office
U. S. Army Electronics Research &
Development Laboratory
Fort Monmouth, New Jersey 1

Commanding Officer
U. S. Army Electronics Research & Development
Laboratory
ATTN: Logistics Division, MARKED FOR James Bailey
Fort Monmouth, New Jersey 8

Commanding Officer
U. S. Army Electronics Research & Development
Laboratory
ATTN: Director of Research/Engineering
Fort Monmouth, New Jersey 1

Commanding Officer
U. S. Army Electronics Research & Development
Laboratory
ATTN: Technical Documents Center
Fort Monmouth, New Jersey 1

Commanding Officer
U. S. Army Electronics Research & Development Laboratory
ATTN: SELRA-NR-5
Fort Monmouth, New Jersey 1

Commanding Officer
U. S. Army Electronics Research & Development Laboratory
ATTN: Technical Information Division
Fort Monmouth, New Jersey 3